arXiv:1604.05250v2 [math.NA] 11 Jun 2016

The Numerical Approximation of Functional Differential Equations

Daniele Venturi
Department of Applied Mathematics and Statistics
University of California, Santa Cruz

April 20, 2016

Abstract

The fundamental importance of functional differential equations has been recognized in many areas of mathematical physics, such as fluid dynamics (Hopf characteristic functional equations), quantum field theory (Schwinger-Dyson equations) and statistical physics (equations for generating functionals and effective action methods). However, no effective numerical method has yet been developed to compute their solution. The purpose of this manuscript is to fill this gap, and provide a new perspective on the problem of numerical approximation of nonlinear functionals and functional differential equations. The proposed methods will be described and demonstrated through various examples.

Contents

1 Introduction **3**

2 Examples of Functional Differential Equations **6**
2.1 Variational Form of PDEs . . . 6
2.2 Schwinger-Dyson Equations . . . 6
2.3 Probability Density Functional Equations . . . 7
2.4 Hopf Characteristic Functional Equations . . . 11
2.5 Moment Generating Functional Equations . . . 13
2.6 Conjugate Flow Action Functionals . . . 14
2.7 Minimum Action Methods and Optimal Control . . . 15

3 Derivation of Functional Differential Equations **15**
3.1 The Generating Functional Approach . . . 16
3.2 The Method of Continuum Limits . . . 16
3.3 From Functional Equations to PDEs: Finite-Dimensional Series Expansions . . . 17
3.3.1 From Functional Equations Multivariate PDEs . . . 19
3.3.2 From Functional Equations to Systems of PDEs . . . 19

4 Approximation of Functionals **20**
4.1 Closed Functional Representations . . . 21
4.2 Functional Interpolation Methods . . . 22
4.2.1 Interpolation Nodes in Function Spaces . . . 24

4.2.2 Polynomial Interpolation of Nonlinear Functionals . . . 26
4.2.3 Porter Interpolants . . . 28
4.2.4 Prenter Interpolants . . . 34
4.2.5 Khlobystov Interpolants . . . 35
4.3 Functional Approximation on Cylindrical Sets . . . 39
4.3.1 Functional HDMR . . . 40
4.3.2 Functional SSE . . . 41
4.3.3 The Distance Between two Functionals . . . 42
4.3.4 Functional SSE: Alternating Least Squares Formulation . . . 43
4.3.5 Functional SSE - Alternating Galerkin Formulation . . . 44
4.3.6 Functional Derivatives of SSE . . . 47
4.4 Generalized Lagrangian Interpolation . . . 48
4.4.1 Optimal Interpolation Nodes . . . 51
4.5 The Cluster Expansion . . . 53
4.6 Functional Approximation Based on Random Processes . . . 55

5 Approximation of Functional Differential Equations 57
5.1 The Method of Weighted Residuals . . . 59
5.1.1 Functional Collocation Methods . . . 59
5.1.2 Functional Galerkin Methods . . . 60
5.1.3 Functional Least Squares . . . 60
5.1.4 An Example: The Hopf-Burgers Equation . . . 60
5.2 Alternating Direction Algorithms . . . 61
5.2.1 Alternating Least-Squares Method . . . 62
5.2.2 Alternating Galerkin Method . . . 62
5.3 Finite Elements in Function Spaces . . . 63

6 Numerical Results: Functionals 63
6.1 Linear functionals . . . 64
6.1.1 Polynomial Functional Interpolation . . . 64
6.1.2 Functional SSE Approach . . . 66
6.2 Quadratic Functionals . . . 67
6.2.1 Polynomial Functional Interpolation . . . 68
6.2.2 Functional SSE Approach . . . 68
6.3 Hopf Characteristic Functionals . . . 69
6.3.1 Effective Dimension . . . 72
6.3.2 Polynomial Functional Interpolation . . . 73
6.3.3 Functional SSE Approach . . . 75
6.3.4 Functional Derivatives . . . 77
6.4 Sine Functional . . . 79
6.4.1 Functional Derivatives . . . 82

7 Numerical Results: Functional Differential Equations 84
7.1 Time Discretization . . . 85
7.2 Functional SSE Approach . . . 86
7.2.1 Alternating Least-Squares Method . . . 87
7.2.2 Alternating Galerkin Method . . . 87
7.3 Summary of the Algorithm . . . 92

7.4 Simulation Results 93

A Functional Fourier Transforms **95**

B Functional Derivatives **96**

C Evaluation of Functional Integrals **99**
C.1 Functional Integrals Involving SSE 100

---

1 Introduction

Why should we be interested in computing the solution to a functional differential equation? Anyone actively working in statistical fluid mechanics, quantum field theory, statistical physics, or stochastic partial differential equations (SPDEs) would have an immediate answer to that question: the dynamics of nonlinear infinite-dimensional systems can be formulated in an exact and beautifully elegant way in terms of functional differential equations, in most cases linear ones. For example, in the context of fluid dynamics, the Hopf characteristic functional equation

$$\frac{\partial \Phi}{\partial t} = \sum_{k=1}^{3} \int_V \theta_k(\boldsymbol{x}) \left(i \sum_{j=1}^{3} \frac{\partial}{\partial x_j} \frac{\delta^2 \Phi}{\delta \theta_k(\boldsymbol{x}) \delta \theta_j(\boldsymbol{x})} + \nu \nabla^2 \frac{\delta \Phi}{\delta \theta_k(\boldsymbol{x})} - i \frac{\partial \Pi}{\partial x_k} \right) dV \tag{1}$$

was deemed by Monin and Yaglom [116] (Ch. 10) to be "the most compact formulation of the general turbulence problem", which is the problem of determining the statistical properties of the velocity and pressure fields of Navier-Stokes equations given statistical information on the initial state. This is of great conceptual importance: one single equation can describe all statistical features of turbulence[1], and there is no need to refer again to the Navier-Stokes equations.

Similarly, in quantum mechanics, the Schwinger-Dyson functional equation describes the exact dynamics of the Green functions of a field theory, and it allows for the propagation of field interactions, either in a perturbative setting (weak coupling regime) or in a strong coupling regime [191, 186]. The usage of functional differential equations grew very rapidly during the sixties, when it became clear that techniques developed for quantum field theory by Dyson, Feynman, and Schwinger could be applied, at least formally, to other branches of mathematical physics. The seminal work of Martin, Siggia, and Rose [109] became a landmark on this subject when it revealed the possibility of applying quantum field theoretic methods, such as functional integrals and diagrammatic expansions [135, 76, 134, 77], to classical physics. Relevant fields of application of these techniques can be found in non-equilibrium statistical mechanics [76, 135, 134, 77, 46, 93, 170, 171], stochastic dynamical systems [66, 178, 89], and turbulence theory [54, 110, 47, 26, 58, 39, 2, 97, 115, 116, 149, 150, 153, 118, 69].

An open question that has persisted over the years, perhaps since the very first appearance of functional differential equations is: *How do we solve them?* In the early years, from the sixties to the eighties, researches were of course investigating analytical methods, e.g., based on functional power series [149, 150, 153, 152, 116, 181, 161], functional integrals [88, 43, 137], transforms with respect to appropriate measures ([116], p. 802), or diagrammatic techniques. More recently, Waclawczyc and Oberlack [182] proposed a Lie group analysis of the Hopf-Burgers equation, which represents a step forward toward developing new analytical solution methods. However, the lack of significant quantitative results in areas

[1] In the book [164], Stanišić refers to Eq. (1) as the "only exact formulation in the entire field of turbulence" (Ch. 12, p. 233).

other than quantum field theory has raised serious doubts about the effectiveness of analytical perturbation methods to solve functional equations. For example, U. Frish ([54], p. 215) states that diagrammatic methods for the Navier-Stokes-Hopf equation "have led repeatedly to false hopes in the theory of turbulence. A caricature of this situation would be to state that either they produced wrong results or that, when the results were right, they could be obtained by much simpler methods."

If functional equations are so important, why do they not have a prominent role in computational mathematics? There are several possible answers to this question. First of all, functional differential equations are infinite-dimensional, in the sense that they are, in principle, equivalent to an infinite-dimensional system of PDEs or PDEs in an infinite number of variables. This may have understandably discouraged some researchers to even attempt a numerical discretization. Most schemes proposed so far are based on truncations of hierarchies of PDEs, for example from power series expansions [149, 150, 153, 152, 116], cumulant approximations [54], Bogoliubov-Born-Green-Kirkwood-Yvon (BBGKY) hierarchies [117, 30], or Lundgren-Monin-Novikov hierarchies [183, 53, 103, 69, 154], or functional integral techniques [88, 43, 137]. Dealing with systems of infinitely many PDEs can indeed be discouraging, but nowadays it is quite common, e.g., in stochastic simulations of SPDEs through polynomial chaos or probabilistic collocation methods [189, 184, 180, 44]. Another reason functional differential equations have not yet been studied numerically may be due to a lack of awareness of their existence within the computational mathematics community. Also, there is no universal agreement across scientific disciplines as to even the basic definition of a functional differential equation. For example, most applied mathematics literature refers to functional differential equations as ordinary differential equations with memory or delay terms [62, 188, 6]. In the pure mathematics community, functional equations have been studied in the context of approximate homeomorphism (the Ulam stability problem) [147, 146], or more generally within problems where the unknown is a function, e.g., Cauchy or d'Alambert functional equations [157]. Physics literature, on the other hand, clearly identifies functional differential equations as those equations whose unknown is a functional (i.e., a nonlinear operator) and that involve partial derivatives with respect to independent variables (e.g., space and time), as well as derivatives with respect to functions (functional derivatives).

These kinds of equations are usually far more challenging than the functional equations studied by the pure mathematics community, and indeed there are very few general theorems on the existence and the uniqueness of their solution [50, 62, 188]. In this paper we take the physicist viewpoint and consider linear functional differential equations[2] in the form

$$\frac{\partial F([\boldsymbol{\theta}],t)}{\partial t} = L([\boldsymbol{\theta}],t)F([\boldsymbol{\theta}],t) \qquad F([\boldsymbol{\theta}],0) = F_0([\boldsymbol{\theta}]), \tag{2}$$

where $F([\boldsymbol{\theta}],t)$ is the solution functional (time-dependent nonlinear operator on the space of test functions $\boldsymbol{\theta}$), F_0 is a given initial condition, and $L([\boldsymbol{\theta}],t)$ is a linear operator on the space of functionals. As we will see, such an operator may involve functional derivatives with respect to $\boldsymbol{\theta}(\widehat{\boldsymbol{x}})$ as well as partial derivatives with respect to independent variables. For example, $L([\boldsymbol{\theta}],t)$ could define the right hand side of equation (1). We remark that the class of equations (2) is very broad as it encompasses functional equations describing many interesting systems, including statistical properties nonlinear SODEs and SPDEs, e.g., Hopf characteristic functional equations [68, 118, 116, 89] or equations for probability density functionals [58, 13, 39]), Green functions of quantum field theories [191, 74, 135, 77, 76, 93], Euler-Lagrange equations arising in generalized principles of least action [174], and turbulence [39, 2, 129, 150, 115, 116, 118, 69].

To the best of our knowledge, no effective numerical method has yet been developed to compute the solution to functional differential equations, and very little has been done for functional differential equations

[2]The linearity assumption implies that there exists a superimposition principle. In particular, if we have available the evolution of the solution functional for different initial conditions then we can simply sum up the various functionals to determine the solution corresponding to a linear combination of initial conditions.

in general. These equations, however, are of fundamental importance in many areas of physics and mathematics. The main objective of this paper is to fill this gap, and develop new classes of numerical methods to approximate the solution to functional differential equations. This is a very challenging, beautiful, and rather unexplored area of computational mathematics. Within this research effort, we identify the following tasks:

1. **Approximation of Functionals and Functional Derivatives**

   Approximation theory for nonlinear functionals is strongly connected to approximation theory for nonlinear operators [71, 169, 12]. A nonlinear functional $F([\theta])$ is, in fact, a particular type of nonlinear operator from a space of functions into a vector space, e.g., $\mathbb{R}$ or $\mathbb{C}$. Thus, the process of approximating nonlinear functionals is basically the same as approximating nonlinear operators. This topic has been extensively studied for obvious reasons (see, e.g., [169, 155, 124, 156, 161, 56, 143, 15, 107, 83]). We will present different approaches to approximate nonlinear functionals. In particular we will discuss collocation methods in spaces of functions, polynomial functional representations, separated series expansions, and expansions based on stochastic processes. Within the collocation setting we will study Lagrange interpolation in Hilbert and Banach spaces [143, 141, 15, 3]. This allows us to construct representations of functionals and functional derivatives based on interpolation nodes in spaces of functions. Also, we will address fundamental questions related to the optimal choice of such interpolation nodes, leading to the best possible approximation. For example: What is the equivalent of Fekete points [19] in a space of infinite dimension? How do we construct interpolants in function spaces with minimal Lebesgue constant? We will also discuss separated series expansion based on cylindrical representations of functionals, and show how such new approximation methods outperform classical methods in terms of accuracy and computational efficiency.

2. **Approximation of Functional Differential Equations**

   A functional differential equation can be seen as an operator equation whose unknown is a nonlinear operator, i.e., a nonlinear functional. The goal of approximation theory for functional differential equations is therefore to determine an approximation of such a nonlinear operator, e.g., its time evolution given an initial state. We will discuss new classes of methods that extend classical Galerkin, least-squares, and collocation techniques to functional equations. These methods are based on suitable representations of the solution functional, e.g., in terms of polynomial interpolants or separated series expansions.

This paper is organized as follows: In Section 2 we provide examples of functional differential equations and show how they arise in the context of well-known physical theories. In Section 4 we address the problem of approximating functionals and functional derivatives. In particular, we discuss Lagrange interpolation in spaces of infinite dimensions (function spaces), series expansions in terms of polynomial functionals, and separated series expansions. Section 5 deals with the numerical approximation of functional differential equations. Specifically, we introduce infinite-dimensional extensions of least squares, Galerkin, and collocation methods. Finally, in Sections 6 and 7 we present numerical results of functional approximation and approximation of functional differential equations, respectively.

2 Examples of Functional Differential Equations

In this section we provide simple examples of functional differential equations and, more importantly, we show how they arise in the context of well-known mathematical theories.

2.1 Variational Form of PDEs

Perhaps, the most well-known example of a functional equation is the variational (weak) form of a partial differential equation. In this setting, the functional equation is quite simple as it involves a linear functional in a test function space. To show how such equation looks like, consider a nonlinear scalar PDE in the form

$$N(u) = 0, \tag{3}$$

where N is a nonlinear differential operator subject to appropriate initial and boundary conditions. For example,

$$N(u) = \frac{\partial u}{\partial t} - u\frac{\partial u}{\partial x} - \frac{\partial^2 u}{\partial x^2}, \qquad u(x,0) = u_0(x), \qquad u(0,t) = u(L,t). \tag{4}$$

By introducing a bilinear form $(\cdot,\cdot)$, it is straightforward to define the following linear functional corresponding to (3)

$$F([\theta]) = (N(u), \theta)\,, \qquad \forall \theta \in D(F), \tag{5}$$

where $D(F)$ is a space of test functions (domain of the functional F). A weak solution to (3) satisfies the *algebraic* functional equation

$$F([\theta]) = 0. \tag{6}$$

This equation yields the well-known method of *weighed residuals* for PDEs [49], from which classical Galerkin, collocation, least-squares and finite volumes schemes can be derived (see [80], p.18). As we will see in Section 4, to identify the functional F in this case it is sufficient to test it relative to a set of linearly independent functions θ_i ($i = 1, 2, ...$), e.g., an orthonormal basis of $D(F)$.

2.2 Schwinger-Dyson Equations

The functional integral approach to classical statistical dynamics [76, 135, 77, 93] allows us derive formally exact evolution equations for phase space functions such as the mean and the correlation function of the solution to SODEs and SPDEs. The standard approach relies on a *generating functional* Z. For stochastic dynamical systems in the form

$$\frac{d\boldsymbol{\psi}(t)}{dt} = \boldsymbol{\Lambda}(\boldsymbol{\psi}(t), t) + \boldsymbol{f}(t;\omega), \tag{7}$$

Z can be explicitly written as a functional integral (see [135, 76, 191, 4, 165])

$$Z([\boldsymbol{\xi},\boldsymbol{\eta}]) = Z_0 \int \mathcal{D}[\boldsymbol{\psi}]\mathcal{D}[\boldsymbol{\chi}] A([\boldsymbol{\psi},\boldsymbol{\chi}]) \exp\left(\int_0^t d\tau(\boldsymbol{\xi}(\tau)\cdot\boldsymbol{\psi}(\tau) + \boldsymbol{\eta}(\tau)\cdot\boldsymbol{\chi}(\tau))\right), \tag{8}$$

where Z_0 is a normalization constant and

$$A([\boldsymbol{\psi},\boldsymbol{\chi}]) = C([\boldsymbol{\chi}]) \exp\left(-\frac{1}{2}\int_0^t d\tau \nabla\cdot\boldsymbol{\Lambda}(\boldsymbol{\psi}(\tau),\tau) - i\int_0^t d\tau \boldsymbol{\chi}(\tau)\cdot\left[\frac{d\boldsymbol{\psi}(\tau)}{dt} - \boldsymbol{\Lambda}(\boldsymbol{\psi}(\tau),\tau)\right]\right). \tag{9}$$

Here $C([\boldsymbol{\chi}])$ denotes the (known) characteristic functional of the external random noise $\boldsymbol{f}(t;\omega)$. Clearly, if we have available the solution to the stochastic dynamical system (7) then we can construct the functional $Z([\boldsymbol{\xi},\boldsymbol{\eta}])$, and from it compute any statistical property we may be interested in. On the other hand, it is

straightforward to show that $Z([\boldsymbol{\xi}, \boldsymbol{\eta}])$ satisfies a coupled system of *linear* functional differential equations, known as *Schwinger-Dyson equations* in quantum field theory [74]. The equations are in the form

$$\frac{\partial}{\partial \tau}\left(\frac{1}{i}\frac{\delta Z}{\delta \xi_k(\tau)}\right) = \eta_k(\tau) Z + \Lambda_k\left(\frac{1}{i}\frac{\delta}{\delta \boldsymbol{\xi}(\tau)}, \tau\right) Z - i D_k\left(\left[\frac{1}{i}\frac{\delta}{\delta \boldsymbol{\eta}(\tau)}\right], \tau\right) Z, \tag{10}$$

$$\frac{\partial}{\partial \tau}\left(\frac{1}{i}\frac{\delta Z}{\delta \eta_k(\tau)}\right) = -\xi_k(\tau) Z + i\frac{\delta}{\delta \eta_j(\tau^+)}\frac{\partial \Lambda_k}{\partial \psi_j}\left(\frac{1}{i}\frac{\delta}{\delta \boldsymbol{\xi}(\tau)}, \tau\right) Z, \tag{11}$$

where

$$D_i([\boldsymbol{\chi}], \tau) = \frac{\delta}{\delta \chi_i(\tau)} \ln C[\boldsymbol{\chi}]. \tag{12}$$

The quantities $\delta/\delta\xi_k$ and $\delta/\delta\eta_k$ are first-order functional derivative operators, defined in Appendix B. By solving (10)-(11) we can identify $Z([\boldsymbol{\xi}, \boldsymbol{\eta}])$ without any knowledge of the stochastic process $\boldsymbol{\psi}(t; \omega)$. By generalizing (8), it is possible to derive a functional integral formalism to classical statistical dynamics yielding Schwinger-Dyson equations for generating functionals associated with SPDEs (see, e.g., [76, 109]). In particular, if the SPDE admits an action functional $S[\phi]$ (see [174, 47, 59, 55, 190, 46, 4]), then the construction of the generating functional as well as the derivation of the corresponding Schwinger-Dyson equations are standard.

In this setting, the Schwinger-Dyson functional differential equations provide a non-perturbative formulation of the problem of computing the statistical properties of nonlinear random systems, including stochastic ODEs and stochastic PDEs.

Schwinger-Dyson Equations In Quantum Field Theory In the context of quantum theory, Schwinger-Dyson equations govern the dynamics of the Green functions of the theory and they characterize the propagation field interactions [191, 186]. Such functional equations can be used in a perturbative setting (weak coupling regime), but they show their true strength in the non-perturbative setting (strong coupling). Let us we briefly recall how Schwinger-Dyson equations are are derived in quantum field theory. To this end, consider a scalar field theory, e.g., the φ^4 theory [4], described by the action functional $A([\phi])$. The generating functional is

$$Z([\eta]) = \int \mathcal{D}[\phi] e^{iA([\phi]) + i(\eta, \phi)}, \tag{13}$$

where $(,)$ is an inner product between the source field η (test field) and ϕ. By using standard methods (see, e.g., [74]), we obtain the following Schwinger-Dyson equation

$$\frac{\delta A[\phi]}{\delta \phi(\boldsymbol{x})}\left[-i\frac{\delta}{\delta \eta(\boldsymbol{x})}\right] Z[\eta] + \eta(\boldsymbol{x}) Z[\eta] = 0. \tag{14}$$

Solution methods for the Schwinger-Dyson equations were proposed based on truncated series expansions [132, 11] or renormalized expansions of the generating functional $Z([\eta])$ (see [87] and [4], p. 385).

2.3 Probability Density Functional Equations

In statistical mechanics, a system of N particles can be described by the joint probability density function $f(x_1, ..., x_n, v_1, ...v_n, t)$ where (x_i, v_i) denotes the position and the velocity of the i-th particle. Similarly, the phase space associated with any finite-dimensional approximation of the solution to a stochastic PDE can be described by the joint probability density function of the corresponding phase variables, e.g., the Fourier or collocation coefficients of the series expansion of the solution. Early formulations in this direction are

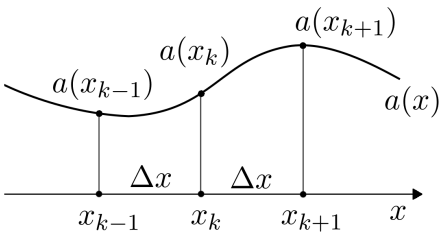

Figure 1: Sketch of the variables $a(x_k)$ representing the random field $u(x,t;\omega)$ at x_k. When we send Δx to zero, the number of variables $ax(_k)$ goes to infinity and the joint probability density function becomes a probability density functional (see equation (16)).

due to Edwards [42], Herring [63], and Montgomery [117]. Consider a scalar random field $u(x,t;\omega)$. The full statistical information of $u(x,t;\omega)$ at time t is encoded in the probability density functional[3]

$$P([a(x)],t) = \langle \delta\left[a(x) - u(x,t;\omega)\right]\rangle\,, \tag{16}$$

where $\delta[\cdot]$ denotes a *Dirac delta functional* (see Appendix A), and the average $\langle\cdot\rangle$ is a Lebesgue-Stieltjes integral over the probability functional of $u(x,t;\omega)$.

Any well-defined nonlinear stochastic PDE for the scalar random field $u(x,t;\omega)$ can be rewritten as *linear functional differential equation* for $P([a(x)],t)$. Such an equation can be obtained by taking an appropriate continuum limit of a finite-dimensional joint probability density equation [178, 176]. In practice, we can replace the discrete set of variables $\{a_1 = a(x_1), a_2 = a(x_2), ..., a_n = a(x_n)\}$ in the joint PDF equation by a continuous set denoted by $[a(x)]$. Partial derivatives with respect to $a_i = a(x_i)$ are then replaced by functional derivatives with respect to $a(x)$, etc. To illustrate this procedure in a simple and intuitive way consider Figure 1. Let $p(a_1, ..., a_n, t)$ be the joint PDF of $\{u(x_1,t;\omega), ..., i(x_n,t;\omega)\}$. Assume that Δx is small enough to allow for numerical differentiation by using finite differences. In this hypothesis we have, for example,

$$\begin{aligned}&\frac{a(x_{k+1}) - 2a(x_k) + a(x_{k-1)}}{\Delta x^2}\left\langle \prod_{k=1}^{n} \delta\left(a(x_k) - u(x_k,t;\omega)\right)\right\rangle = \\ &\left\langle \frac{u(x_{k+1},t;\omega) - 2u(x_k,t;\omega) + u(x_{k-1},t;\omega)}{\Delta x^2} \prod_{j=1}^{n} \delta\left(a(x_j) - u(x_j,t;\omega)\right)\right\rangle.\end{aligned} \tag{17}$$

This yields,

$$\frac{\tilde{\partial}^2 a(x_k)}{\tilde{\partial} x^2}\left\langle \prod_{k=1}^{n} \delta\left(a(x_k) - u(x_k,t;\omega)\right)\right\rangle = \left\langle \frac{\tilde{\partial}^2 u(x_k,t;\omega)}{\tilde{\partial} x^2} \prod_{j=1}^{n} \delta\left(a(x_j) - u(x_j,t;\omega)\right)\right\rangle, \tag{18}$$

where $\tilde{\partial}^2/\tilde{\partial}x^2$ here denotes a numerical differentiation operator, i.e., an approximation of the second-order derivative operator by using finite differences. Other schemes such as pseudospectral collocation can be

[3] The probability density functional $P([a(x)],t)$ allows us to compute moments, cumulants and joint PDFs by using functional integration. For example,

$$p(b_1,b_2,t) = \int \delta(b_1 - a(x_1))\delta(b_2 - a(x_2))P([a(x)],t)\mathcal{D}[a(x)]. \tag{15}$$

Computing functional integrals often requires a careful definition of the integration measure as it may be possible to run into convergence issues (see [13], §2.2.4).

obviously used as well. By extending these arguments to higher-order derivatives, we obtain the expression

$$\frac{\tilde{\partial}^s a(x_k)}{\tilde{\partial} x^s}\left\langle \prod_{k=1}^{n} \delta\left(a(x_k) - u(x_k,t;\omega)\right)\right\rangle = \left\langle \frac{\tilde{\partial}^s u(x_k,t;\omega)}{\tilde{\partial} x^s} \prod_{j=1}^{n} \delta\left(a(x_j) - u(x_j,t;\omega)\right)\right\rangle, \quad s = 1,2,... \tag{19}$$

Now we have all elements to derive (at least formally) probability density functional equations corresponding to arbitrary PDEs. To this end, let us first consider a simple problem, i.e., the 1D diffusion equation on the real line

$$\frac{\partial u(x,t;\omega)}{\partial t} = \frac{\partial^2 u(x,t;\omega)}{\partial x^2}, \qquad u(x,0;\omega) = u_0(x;\omega) \quad \text{(random)}. \tag{20}$$

In a collocation setting, the semi-discrete form of (20) is

$$\frac{du(x_i,t;\omega)}{dt} = \frac{\tilde{\partial}^2 u(x_i,t;\omega)}{\tilde{\partial} x^2}, \qquad u(x_i,0;\omega) = u_0(x_i;\omega) \qquad i = 1,...,n. \tag{21}$$

Here n is the number of collocation points and $\tilde{\partial}^2 u(x_i,t;\omega)/\tilde{\partial} x^2$ denotes a numerical approximation of the second-order derivative, e.g., by using finite differences or pseudospectral collocation methods [64]. The joint probability density function of the state vector $u(x_i,t;\omega)$ $(i = 1,...,n)$ satisfies the equation [178, 176, 179]

$$\frac{\partial p}{\partial t} = -\sum_{k=1}^{n} \frac{\partial}{\partial a_k}\left\langle \frac{\tilde{\partial}^2 u(x_i,t;\omega)}{\tilde{\partial} x^2} \prod_{j=1}^{n} \delta\left(a_j - u(x_j,t;\omega)\right)\right\rangle \tag{22}$$

$$= -\sum_{k=1}^{n} \frac{\partial}{\partial a_k}\left(\frac{\tilde{\partial}^2 a(x_i)}{\tilde{\partial} x^2} p\right), \tag{23}$$

where $p = p(a_1,...,a_n,t)$. The last equality easily follows from (18). By taking the continuum limit, i.e., by sending Δx to zero (and correspondingly n to infinity), we obtain the following functional differential equation for the probability density functional of the solution to equation (20)

$$\frac{\partial P([a(x)],t)}{\partial t} = -\int_{-\infty}^{\infty} \frac{\delta}{\delta a(x)}\left(\frac{\partial^2 a(x)}{\partial x^2} P([a(x)],t)\right) dx. \tag{24}$$

The quantity $\delta/\delta a(x)$ appearing at the right hand side is the first-order functional derivative operator with respect to $a(x)$ (see Appendix B). The initial condition for $P([a(x)],t)$ is obtained by computing the probability density functional of $u_0(x;\omega)$ in (20).

Remark: The functional differential equation (24) is linear in $P([a(x)],t)$, but it involves singular terms. Such terms arise from the continuum limit that takes (23) into (24). Specifically, when we send Δx to zero we have that x_k approaches x_{k+1} (see Figure 1). Correspondingly the PDF of $u(x_k;t,\omega)$ tends to the PDF of $u(x_{k+1};t,\omega)$. In this situation, the joint PDF of $u(x_k;t,\omega)$ and $u(x_{k+1};t,\omega)$ tends to a Dirac delta function as $x_k \to x_{k+1}$ (see [103], p. 970). From a formal mathematical viewpoint, consider the following term appearing in the integral (23)

$$\begin{aligned}\frac{\delta}{\delta a(x)}\left(\frac{\partial^2 a(x)}{\partial x^2}\right) &= \frac{\delta}{\delta a(x)}\int_{-\infty}^{\infty} a(y)\delta''(x-y)dy, \\ &= \int_{-\infty}^{\infty} \delta(x-y)\delta''(x-y)dy.\end{aligned} \tag{25}$$

	Covariance	Inverse Covariance
Matérn (2D) $(r^2 = x^2 + y^2)$	$\sigma^2 r B_1\left(\frac{r}{a}\right)$	$\frac{1}{4\pi\sigma^2 a^2}\left(\frac{\delta(r)}{\pi r} - 2a^2\nabla^2\frac{\delta(r)}{\pi r} + a^4\nabla^4\frac{\delta(r)}{\pi r}\right)$
Exponential (3D) $(r^2 = x^2 + y^2 + z^2)$	$\sigma^2 \exp\left(-\frac{r}{a}\right)$	$\frac{1}{8\pi\sigma^2 a^3}\left(\frac{\delta(r)}{\pi r} - 2a^2\nabla^2\frac{\delta(r)}{\pi r} + a^4\nabla^4\frac{\delta(r)}{\pi r}\right)$

Table 1: Convolution inverses of well-known covariance functions [131]. Here B_1 denotes the modified Bessel function of the first kind. It is seen that the convolution inverse of smooth functions are rough functions involving Laplacians and bi-harmonic operators applied to Dirac deltas.

The last integral is equivalent to the second derivative of the Dirac delta function at zero. This singularity can also be seen from a purely discrete viewpoint. To this end, substitute the (second-order) finite-difference approximation to the second-order derivative into (23). This yields the equation

$$\frac{\partial p}{\partial t} = -\sum_{k=1}^{n} \frac{a(x_{k+1}) - 2a(x_k) + a(x_{k-1})}{\Delta x^2}\frac{\partial p}{\partial a_k} - \frac{2}{\Delta x^2}p. \tag{26}$$

It is clear that when Δx goes to zero (continuum limit), the term $2p/\Delta x^2$ generates the singularity that corresponds to equation (25).

More complex probability density functional equations have been derived and studied in the context turbulent flows, e.g., by Dopazo and O'Brien [39] and Rosen [149, 153, 150]. The functional Fourier transform of the probability density functional is known as Hopf characteristic functional (see Section 2.4). Hopf functionals are usually easier to compute than probability density functionals. As an example, consider the classical Gaussian probability functional

$$P[a(x)] \sim \exp\left[-\frac{1}{2}\int_a^b\int_a^b C^{-1}(x,y)\left[a(x) - \mu(x)\right]\left[a(y) - \mu(y)\right]dxdy\right], \tag{27}$$

where $C^{-1}(x,y)$ is the inverse covariance function of $u(x;\omega)$. Such inverse covariance may be obtained by solving the Fredholm integral equation of the first kind

$$\int_a^b C(x,y)C^{-1}(y,z)dy = \delta(x-z). \tag{28}$$

If $C(x,y)$ is smooth then its differential inverse $C^{-1}(y,z)$ must have serious singularities in order for the integral in (28) to yield a Dirac delta function (see Table 1). If $C(x,y)$ is homogeneous, i.e., if $C(x,y) = C(x-y)$, and the integration in (28) is extended over all space, then $C^{-1}(y,z)$ is called *convolution inverse* [67, 119]. This method was pioneered by Hirschman and Widder [65] in the late forties. Relevant cases of convolution inverses are summarized in Table 1, where we see that the convolution inverse of smooth correlations are actually *rough* functions involving Laplacians and bi-harmonic operators applied to Dirac delta functions. However, such rough functions appear within integrals in (27), and therefore we expect some regularization - i.e. the probability functional of a Gaussian random field may be a relatively smooth object. In general, one should proceed with great caution when dealing with probability density functionals[4]

[4]Even in finite (low) dimension the joint PDF of a nonlinear system can be a very complex function. For example, it is known that the time-asymptotic PDF of Lorenz-84 [20] or the Lorenz-96 [79] lies on fractal attractors. Even in periodically forced two-dimensional systems one may have attractors with fractal structure and chaotic phase similarities [18, 177, 175].

Field Equation	Functional Differential Equation
$\frac{\partial u}{\partial t} + u\frac{\partial u}{\partial x} = \nu\frac{\partial^2 u}{\partial x^2}$	$\frac{\partial M}{\partial t} = \int_a^b \theta(x)\left(\nu\frac{\partial^2}{\partial x^2}\frac{\delta M}{\delta\theta(x)} - \frac{1}{2}\frac{\partial}{\partial x}\frac{\delta^2 M}{\delta\theta(x)^2}\right)dx.$
$\frac{\partial \boldsymbol{u}}{\partial t} + (\boldsymbol{u}\cdot\nabla)\boldsymbol{u} = -\nabla p + \nu\Delta\boldsymbol{u}$	$\frac{\partial \Phi}{\partial t} = \sum_{k=1}^{3}\int_V \theta_k(\boldsymbol{x})\left(i\sum_{j=1}^{3}\frac{\partial}{\partial x_j}\frac{\delta^2\Phi}{\delta\theta_k(\boldsymbol{x})\delta\theta_j(\boldsymbol{x})} + \nu\nabla^2\frac{\delta\Phi}{\delta\theta_k(\boldsymbol{x})} - i\frac{\partial\Pi}{\partial x_k}\right)dV$
$\frac{\partial u}{\partial t} = \nu\frac{\partial^2 u}{\partial x^2}$	$\frac{\partial P}{\partial t} = -\int_{-\infty}^{\infty}\frac{\delta}{\delta a(x)}\left(\frac{\partial^2 a(x)}{\partial x^2}P\right)dx$
$(\Box\phi + \mu)\phi + \frac{\lambda}{6}\phi^3 = 0$	$\frac{\delta A[\phi]}{\delta\phi(\boldsymbol{x})}\left[-i\frac{\delta}{\delta\eta(\boldsymbol{x})}\right]Z[\eta] + \eta(\boldsymbol{x})Z[\eta] = 0$

Table 2: Examples of functional differential equations. In this table, M denotes the moment generating functional, Φ is the Hopf characteristic functional, P is the probability density functional, and Z is the generating functional of a quantum field theory (ϕ^4-theory).

and corresponding functional differential equations. In fact, we have seen that the continuum limit of the semi-discrete form of PDEs (even linear ones!) can yield singular probability density functional equations, which are very difficult to solve. Such functional equations, however, represent an excellent starting point to obtain effective approximations to quantities of interest. To this end, we can follow (by analogy) the route taken in classical statistical mechanics in which we start with a rigorous differential equation, e.g. the Liouville equation, and make approximations in order to derive an equation which is approximate, lower-dimensional and computable, e.g., the Boltzmann equation. Such *coarse-graining* process of functional differential equations is discussed by McComb [110] in the context of fluid turbulence.

2.4 Hopf Characteristic Functional Equations

The Hopf characteristic functional of a random field is the functional Fourier transform of the probability density functional (see [151, 178] and Appendix A). To introduce this mathematical object in a simple way, let us consider an integrable random function $u(x;\omega)$ on an interval $x \in [a,b]$. The Hopf functional associated with $u(x;\omega)$ is defined as

$$\Phi([\theta(x)]) = \left\langle \exp\left[i\int_a^b u(x;\omega)\theta(x)dx\right]\right\rangle, \tag{29}$$

where $\theta(x)$ is a deterministic function (test function), i is the imaginary unit and the average is defined as a Lebesgue-Stieltjes integral over the probability functional of $u(x;\omega)$. Equation (29) assigns to each function $\theta(x)$ a complex number $\Phi([\theta(x)])$ (see Figure 2). Similarly to the probability density functional, the Hopf characteristic functional (29) encodes the *full statistical information* of the random function $u(x;\omega)$, including multi-point moments, joint characteristic functions and probability density functions (see [115, 116]). If we consider instead of a random function $u(x;\omega)$ a random vector field $\boldsymbol{u}(\boldsymbol{x},t;\omega)$, e.g., the

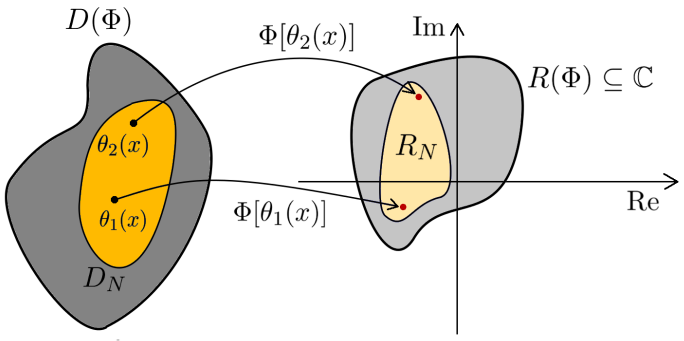

Figure 2: Sketch of the mapping at the basis of the Hopf functional. The domain of the functional Φ, denoted as $D(\Phi)$ is a suitable of space of functions while the range of Φ, denoted as $R(\Phi)$, is a subset of the complex plane $\mathbb{C}$. The approximation space D_N is a subset of $D(\Phi)$, which is mapped into R_N.

solution to the Navier-Stokes equations, then we define[5]

$$\Phi([\boldsymbol{\theta}(\boldsymbol{x})], t) = \left\langle \exp\left[i \int_V \boldsymbol{u}(\boldsymbol{x}, t; \omega) \cdot \boldsymbol{\theta}(\boldsymbol{x}) dV \right] \right\rangle, \tag{31}$$

where V is a spatial domain and the test function $\boldsymbol{\theta}(\boldsymbol{x})$ is vector valued. By the Riemann-Lebesgue lemma we have that

$$\Phi([\boldsymbol{\theta}(\boldsymbol{x})], t) \to 0 \quad \text{as} \quad \|\boldsymbol{\theta}(\boldsymbol{x})\| \to \infty, \tag{32}$$

with a rate that depends on the regularity of the underlying probability density functional.

Let us now provide simple examples of Hopf functional differential equations. In principle, such equations can be derived for rather general classes of PDEs, e.g. wave equations or Maxwell's equations subject to random boundary or random initial states. The procedure is usually simpler than the one to obtain probability density functional equations, but essentially equivalent. The two types of equations are indeed related by functional Fourier transforms. In any case, this allows us to determine the statistical properties of the solution linear and nonlinear PDEs by solving linear functional differential equations (e.g., Hopf or probability density functional equations). In other words, we can to condense the entire statistical problem in *one single linear functional differential equation*. All possible information of statistical nature may be obtained from such equation and there is no need to refer again to the original system.

1. **Burgers-Hopf Equation** Consider the Burgers equation

$$\frac{\partial u}{\partial t} + u \frac{\partial u}{\partial x} = \nu \frac{\partial^2 u}{\partial x^2} \qquad x \in [a, b], \tag{33}$$

and let the initial condition be random. By differentiating the Hopf functional

$$\Phi([\theta(x)], t) = \left\langle \exp\left[i \int_a^b \theta(x) u(x, t; \omega) dx \right] \right\rangle \tag{34}$$

[5] Lewis and Kraichnan [97, 151] introduced a space-time generalization of (31), namely

$$\Phi([\boldsymbol{\theta}(\boldsymbol{x}, t)]) = \left\langle \exp\left[i \int_V \int_T \boldsymbol{u}(\boldsymbol{x}, t; \omega) \cdot \boldsymbol{\theta}(\boldsymbol{x}, t) dV dt \right] \right\rangle. \tag{30}$$

This functional allows us to determine joint multi-point statistics of the random field $\boldsymbol{u}(\boldsymbol{x}, t; \omega)$ at different times.

it is straightforward to obtain the following Burgers-Hopf functional differential equation (see [116, 1])

$$\frac{\partial \Phi}{\partial t} = \int_a^b \theta(x) \left(\frac{i}{2} \frac{\partial}{\partial x} \frac{\delta^2 \Phi}{\delta \theta(x)^2} + \nu \frac{\partial^2}{\partial x^2} \frac{\delta \Phi}{\delta \theta(x)} \right) dx. \tag{35}$$

2. **Navier-Stokes-Hopf Equation** The problem of determining the evolution of the Hopf characteristic functional for the Navier-Stokes equations

$$\frac{\partial \boldsymbol{u}}{\partial t} + (\boldsymbol{u} \cdot \nabla)\boldsymbol{u} = -\nabla p + \nu \Delta \boldsymbol{u}, \qquad \nabla \cdot \boldsymbol{u} = 0 \tag{36}$$

was deemed by Monin and Yaglom as the most compact formulation of the *turbulence problem*, which is the problem of determining the statistical properties of the velocity and pressure field given statistical information on the initial condition. The Hopf functional differential equation corresponding to the Navier-Stokes equations is derived in in [116] Ch. 10 (see also [13], §3.1.4), and it is hereafter summarized for convenience

$$\frac{\partial \Phi}{\partial t} = \sum_{k=1}^{3} \int_V \theta_k(\boldsymbol{x}) \left(i \sum_{j=1}^{3} \frac{\partial}{\partial x_j} \frac{\delta^2 \Phi}{\delta \theta_k(\boldsymbol{x}) \delta \theta_j(\boldsymbol{x})} + \nu \nabla^2 \frac{\delta \Phi}{\delta \theta_k(\boldsymbol{x})} - i \frac{\partial \Pi}{\partial x_k} \right) dV, \tag{37}$$

$$\nabla^2 \Pi = \sum_{k,j=1}^{3} \frac{\partial^2}{\partial x_k \partial x_j} \frac{\delta^2 \Phi}{\delta \theta_k(\boldsymbol{x}) \delta \theta_j(\boldsymbol{x})}. \tag{38}$$

Functional formulations of non-isothermal turbulent reactive flow have been also considered, leading to more complicated Hopf equations [39]. As we will see in Section 3.3, Hopf equations are equivalent to PDEs in an infinite number of variables or to infinite-dimensional systems of coupled PDEs, e.g., the Monin-Lundgren-Novikov hierarchy [69, 117, 183, 103]. It is interesting to note that the structure of the Hopf equation somehow resembles the weak form of a PDE. However, there is a remarkable difference: in the Hopf case both the solution (Hopf functional) as well as its functional derivatives depend on the test function. In other words, the test function appears in the functional equation a *nonlinear way*. In addition the equation involves functional derivatives which are usually not present in classical PDEs.

Hopf Functionals Versus Probability Density Functionals We have seen that Hopf equations and probability density functional equations are related by a functional Fourier transform. Therefore, from a purely mathematical viewpoint they are completely equivalent. However, from the viewpoint of approximation theory they are not equivalent at all. Hopf functionals may be hard to resolve due to high-frequencies related to the complex exponential. On the other hand, probability density functionals may easily degenerate to functional distributions such as functional Dirac deltas. The statistical properties of a random field can be equivalently computed by using the Hopf functional or the probability density functional. In the first case, we simply need to take functional derivatives and evaluate them at $\theta(x) = 0$ (see Appendix (B)). In the second case, we need to compute functional integrals, i.e., integrals in an infinite number of variables. This requires requires a careful definition of the integration measure as it may be possible to run into convergence issues (see [13], §2.2.4).

2.5 Moment Generating Functional Equations

In probability theory and statistics, the moment-generating function of a random variable is an alternative specification of its probability distribution. Thus, it provides the basis of an alternative route to analytical

results compared to working directly with probability density functions or cumulative distribution functions. The infinite-dimensional extension of the moment generating function associated with the random function $u(x,t;\omega)$ is

$$M([\theta(x)],t) = \left\langle \exp\left[\int_a^b u(x,t;\omega)\theta(x)dx\right]\right\rangle, \tag{39}$$

where, similarly to (29), $\langle\cdot\rangle$ is a Lebesgue-Stieltjes integral with respect to the probability measure of $u(x,t;\omega)$. The moment generating functional is the "two-sided" functional Laplace transform of the probability density functional. On the other hand, the Hopf characteristic functional is the functional Fourier transform of the probability density functional. Such transforms differ only by the imaginary unit at the exponent. Such little difference, however, has big important consequences. First of all, the moment generating functional is real valued. Also, it does not exhibit the high-frequency problem discussed at the end of the previous Section, and therefore it easier to compute than the Hopf functional. However, M is unbounded and it goes to infinity (usually pretty fast) as the norm of θ increases. Also, M may not exist at all, as the functional Laplace transform of a probability functional may not converge. By contrast, the characteristic functional Φ always exists - it is the integral of a bounded functional on a space of finite measure. For example, if $u(x;\omega)$ is a Cauchy random field then $M([\theta])$ does not exist, while $\Phi([\theta])$ does exist. The technique to derive evolution equations for M based on functional differentiation is exactly the same as the one for the Hopf functional. For example,

$$\frac{\partial M}{\partial t} = \int_a^b \theta(x)\left(\nu\frac{\partial^2}{\partial x^2}\frac{\delta M}{\delta\theta(x)} - \frac{1}{2}\frac{\partial}{\partial x}\frac{\delta^2 M}{\delta\theta(x)^2}\right)dx \tag{40}$$

is the functional differential equation for the moment generating functional of the solution to the Burgers equation (33).

2.6 Conjugate Flow Action Functionals

In a recent paper [174], we have shown how to construct an action functional for a non-potential field theory by using methods of differential geometry and nonlinear functional analysis [172, 123]. The key idea is to represent the governing equations of the field theory relative to a diffeomorphic flow of curvilinear coordinates which is assumed to be functionally dependent on a field that satisfies the field equations, i.e., their solution. Such flow evolves in space and time similarly to a physical fluid flow of classical mechanics and it can be selected in order to symmetrize the Gâteaux derivative of the field equations relative to suitable local bilinear forms. This is equivalent to requiring that the governing equations of the field theory can be derived from a principle of stationary action on a functional flow, which we called the *conjugate flow of the theory*. The determining equations of the conjugate flow are functional differential equations. In particular, for a second-order nonlinear scalar field theory

$$f\left(u; u_{,\mu}; u_{,\mu\nu}; \widehat{x}^{\mu}_{,\nu}; \widehat{x}^{\mu}_{,\nu\lambda}\right) = 0, \tag{41}$$

we obtain

$$R^{\mu\nu}_{,\nu} + R^{\mu\nu}\Gamma^{\lambda}_{\lambda\nu} = Z^{\nu}, \tag{42}$$

where the comma denotes differentiation with respect to the independent variable σ^{ν}, $\Gamma^{\lambda}_{\lambda\nu}$ is the Christoffel symbol of the second kind and

$$Z^{\nu} = \frac{\partial f}{\partial u_{,\nu}} + \frac{\partial f}{\partial \widehat{x}^{\mu}_{,\nu}}\frac{\delta\widehat{x}^{\mu}}{\delta u} + \left(\frac{\partial f}{\partial \widehat{x}^{\mu}_{,\nu\rho}} + \frac{\partial f}{\partial \widehat{x}^{\mu}_{,\rho\nu}}\right)\left(\frac{\partial}{\partial\sigma^{\rho}}\frac{\delta\widehat{x}^{\mu}}{\delta u} + \frac{\delta^2\widehat{x}^{\mu}}{\delta u^2}\frac{\partial u}{\partial\sigma^{\rho}}\right), \tag{43}$$

$$R^{\rho\nu} = \frac{\partial f}{\partial u_{,\nu\rho}} + \frac{\partial f}{\partial \widehat{x}^{\mu}_{,\rho\nu}}\frac{\delta\widehat{x}^{\mu}}{\delta u}. \tag{44}$$

Given a solution u to the field equation (41), the system of functional differential equations (42) allows us to identify the *conjugate flow* $\widehat{x}^\mu(\sigma^\nu;[u])$, i.e., the functional relation between the flow $\widehat{x}^\mu$ and the solution field u for which the PDE (41) can be derived from a *principle of least action* (see [174] for further details). The identification of transformation groups leaving the conjugate flow action functional invariant could lead to the discovery of new conservation laws in fluid dynamics and other disciplines.

2.7 Minimum Action Methods and Optimal Control

Consider a nonlinear PDE perturbed by space-time additive random noise of small amplitude ϵ

$$\frac{\partial \boldsymbol{u}}{\partial t} + \boldsymbol{G}(\boldsymbol{u}) = \sqrt{\epsilon}\boldsymbol{f}(\boldsymbol{x}, t; \omega). \tag{45}$$

Define the set trajectories connecting two arbitrary states $\{\boldsymbol{u}_1, \boldsymbol{u}_2\}$

$$B = \{\boldsymbol{u}(\boldsymbol{x}, t; \omega) | \quad \boldsymbol{u}(\boldsymbol{x}, 0; \omega) = \boldsymbol{u}_1, \quad \boldsymbol{u}(\boldsymbol{x}, T; \omega) = \boldsymbol{u}_2\} \tag{46}$$

If $\boldsymbol{f}$ is white noise, then the Freidlin-Wentzell theory gives us the following large deviation principle

$$\lim_{\epsilon \to 0^+} \epsilon \mathrm{Pr}(\boldsymbol{u} \in B) = \inf_{\boldsymbol{u} \in B} \frac{1}{2} \int_0^T \left\| \frac{\partial \boldsymbol{u}}{\partial t} + \boldsymbol{G}(\boldsymbol{u}) \right\|_{L_2}^2 dt \tag{47}$$

where $\mathrm{Pr}(A)$ denotes the probability of the event A, $\|\cdot\|_{L_2}^2$ indicates the L_2 norm in space. The large deviation principle is equivalent to minimum action principle

$$\min_{\substack{\boldsymbol{u}(0,\boldsymbol{x};\omega)=\boldsymbol{u}_1 \\ \boldsymbol{u}(T,\boldsymbol{x};\omega)=\boldsymbol{u}_2}} S_T([\boldsymbol{u}]), \qquad S_T([\boldsymbol{u}]) = \frac{1}{2} \int_0^T \left\| \frac{\partial \boldsymbol{u}}{\partial t} + \boldsymbol{G}(\boldsymbol{u}) \right\|_{L_2}^2 dt. \tag{48}$$

The minimizer of (48) is called *minimum action path*, and it satisfies the functional differential equation

$$\frac{\delta S_T([\boldsymbol{u}])}{\delta \boldsymbol{u}(\boldsymbol{x}, t)} = 0 \quad \boldsymbol{u} \in B. \tag{49}$$

A method to solve (49) is based on a direct discretization of $S_T(\boldsymbol{u})$ [41]. Other optimization problems, e.g., arising in the calculus of variations [57] or *optimal control* theory [100], can be formulated in a similar setting and they can be solved by using functional approximation. The stationarity condition of a cost functional relative to variations of a control is a functional differential equation in the form (49).

3 Derivation of Functional Differential Equations

In this Section we briefly discuss how to derive functional differential equations. Clearly this depends on the specific system under consideration, and indeed there are different methods that can be used for different systems. Hereafter, we describe two of them which are broad enough to include many applications of interest. The first approach relies on generating functionals. The second approach is based on (formal) infinite-dimensional limits of multivariate PDEs (method of continuum limits). At the end of the Section we also discuss in what sense functional equations are equivalent to infinite dimensional systems of PDEs, or PDEs in an infinite number of variables.

3.1 The Generating Functional Approach

The seminal work of Martin, Siggia and Rose [109] opened the possibility to apply quantum field theoretic methods, such as Feynman diagrams and Schwinger-Dyson equations, to classical and statistical physics. The key idea is to construct a generating functional (action functional) based on the equations of motion and then apply a Heisenberg operator theory which parallels the Schwinger formalism of quantum field theory. This allows us to obtain closed equations for quantities of interest such as the correlation functions and response functions (averaged Green's functions). For a through description of the method see the excellent review paper of Jensen [76].

3.2 The Method of Continuum Limits

We have seen in Section 2 how to derive probability density functional equations and Hopf functional equations as continuum limits of joint PDF equations and joint characteristic function equations, respectively. Such procedure is rather formal but easy to follow and effective in many cases. More importantly, it can be applied to many different linear and nonlinear PDEs. To show this, let us consider the Burgers equation

$$\frac{\partial u}{\partial t} + \frac{1}{2}\frac{\partial u^2}{\partial x} = \nu \frac{\partial^2 u}{\partial x^2} \tag{50}$$

with a random initial condition $u(x,0;\omega) = u_0(x;\omega)$. In a collocation setting, the solution to (50) can be written as

$$u(x,t;\omega) = \sum_{k=1}^{n} u_k(t;\omega) l_k(x), \tag{51}$$

where $u_k(t;\omega) = u(x_k,t;\omega)$ is the solution at the point x_k while $l_j(x)$ are suitable basis functions, e.g., Lagrange characteristic polynomials through Gauss quadrature points. Substituting (51) into (50) and setting the residual at collocation points equal to zero yields the system

$$\frac{du_k}{dt} + \frac{1}{2}\sum_{j=1}^{n} D_{kj}^{(1)} u_j^2 = \nu \sum_{j=1}^{n} D_{kj}^{(2)} u_j \qquad k = 1, ..., n \tag{52}$$

where $D_{kj}^{(1)}$ and $D_{kj}^{(2)}$ are first- and second-order differentiation matrices, respectively. The joint characteristic function of $\{u_1, ..., u_n\}$ is

$$\phi(\theta_1, ..., \theta_n, t) = \left\langle \exp\left[i \sum_{j=1}^{n} \theta_j u_j(t;\omega) \right] \right\rangle \tag{53}$$

and it satisfies the evolution equation

$$\begin{aligned} \frac{\partial \phi}{\partial t} =& -\frac{i}{2}\sum_{k,j=1}^{n} \theta_k D_{kj}^{(1)} \left\langle u_j^2 \exp\left[i \sum_{j=1}^{n} \theta_j u_j) \right] \right\rangle + \nu i \sum_{k,j=1}^{n} \theta_k D_{kj}^{(2)} \left\langle u_j \exp\left[i \sum_{j=1}^{n} \theta_j u_j) \right] \right\rangle \\ =& \frac{i}{2}\sum_{k,j=1}^{n} \theta_k D_{kj}^{(1)} \frac{\partial^2 \phi}{\partial \theta_j^2} + \nu \sum_{k,j=1}^{n} \theta_k D_{kj}^{(2)} \frac{\partial \phi}{\partial \theta_j}. \end{aligned} \tag{54}$$

By taking the continuum limit of this equation, i.e., by sending n to infinity, we formally obtain

$$\frac{\partial \Phi}{\partial t} = \int_a^b \theta(x) \left[\frac{i}{2}\frac{\partial}{\partial x}\frac{\delta^2 \Phi([\theta])}{\delta \theta(x)^2} + \nu \frac{\partial^2}{\partial x^2}\frac{\delta \Phi([\theta])}{\delta \theta(x)} \right] dx \tag{55}$$

which coincides with (35). The continuum-limit argument just invoked is completely formal and can be used for other finite-dimensional equations (see [182]). In particular, it can be used for the joint probability density function equation (23), leading to the functional differential equation (24). In the next Section we discuss the inverse operation, i.e., how to transform functional differential equations into PDEs with a finite number of variables. This allows us to to establish important relation between functional derivatives and partial derivatives.

3.3 From Functional Equations to PDEs: Finite-Dimensional Series Expansions

The restriction of functionals and functional differential equations to finite-dimensional function spaces yields multivariate fields and multivariate PDEs, respectively. Such PDEs can be obtained directly by using the finite dimensional theory, i.e., functional equations on finite-dimensional function spaces are *in toto* equivalent to multivariate PDEs. To show this, let us consider the finite-dimensional function space

$$D_N = \text{span}\{\varphi_1(x), ..., \varphi_N(x)\}, \tag{56}$$

where $\varphi_1, ..., \varphi_N$ are orthonormal. Let us represent the test function $\theta(x)$ relative to such orthonormal basis

$$\theta(x) = \sum_{k=1}^{N} a_k \varphi_k(x). \tag{57}$$

Restricting the domain of the Hopf functional (29) to the finite-dimensional space (56) (see Figure 2) yields the joint characteristic function

$$\phi(a_1, ..., a_N) = \left\langle e^{i(a_1 U_1(\omega) + \cdots + a_N U_N(\omega))} \right\rangle, \qquad U_k(\omega) = \int_a^b u(x;\omega)\varphi_k(x)dx. \tag{58}$$

Note that the linear combination of $U_k(\omega)$ yields a finite-dimensional approximation of $u(x, \omega)$, i.e.,

$$\widehat{u}(x;\omega) = \sum_{k=1}^{N} U_k(\omega)\varphi_k(x). \tag{59}$$

Based on this expansion, the mean field and the correlation function of $\widehat{u}(x, \omega)$ can be easily expressed as

$$\langle \widehat{u}(x,\omega) \rangle = \sum_{k=1}^{N} \langle U_k(\omega) \rangle \varphi_k(x) = \sum_{k=1}^{N} \frac{1}{i} \left. \frac{\partial \phi}{\partial a_k} \right|_0 \varphi_k(x), \tag{60}$$

$$\langle \widehat{u}(x,\omega)\widehat{u}(y;\omega) \rangle = \sum_{k,j=1}^{N} \langle U_k(\omega)U_j(\omega) \rangle \varphi_k(x)\varphi_j(x) = -\sum_{k,j=1}^{N} \left. \frac{\partial^2 \phi}{\partial a_k \partial a_j} \right|_0 \varphi_k(x)\varphi_j(x). \tag{61}$$

Similar equations hold for higher-order moments. At this point, we observe that by restricting the functional derivatives of the Hopf functional to the space (56) we obtain

$$\left. \frac{\delta \Phi(\theta)}{\delta \theta(x)} \right|_{\theta \in D_N} = i \left\langle u(x) e^{i(a_1 U_1(\omega) + \cdots + a_N U_N(\omega))} \right\rangle, \tag{62}$$

$$\left. \frac{\delta^2 \Phi(\theta)}{\delta \theta(x) \delta \theta(y)} \right|_{\theta \in D_N} = -\left\langle u(x)u(y) e^{i(a_1 U_1(\omega) + \cdots + a_N U_N(\omega))} \right\rangle. \tag{63}$$

Therefore the following relations hold true

$$\frac{\partial \phi}{\partial a_k} = \int_a^b \varphi_k(x) \left. \frac{\delta \Phi(\theta)}{\delta \theta(x)} \right|_{\theta \in D_N} dx, \tag{64}$$

$$\frac{\partial^2 \phi}{\partial a_k \partial a_j} = \int_a^b \int_a^b \varphi_k(x) \varphi_j(y) \left. \frac{\delta^2 \Phi(\theta)}{\delta \theta(x) \delta \theta(y)} \right|_{\theta \in D_N} dxdy. \tag{65}$$

This means that *the partial derivative of the characteristic function is nothing but the projection of the Hopf functional derivative onto* D_N. Clearly, if the random function $u(x;\omega)$ is itself in D_N then we have $u(x;\omega) = \widehat{u}(x;\omega)$ (see Eq. (59)) and the following inverse formulas hold true

$$\left. \frac{\delta \Phi([\theta])}{\delta \theta(x)} \right|_{\theta, u \in D_N} = \sum_{k=1}^N \varphi_k(x) \frac{\partial \phi}{\partial a_k}, \tag{66}$$

$$\left. \frac{\delta^2 \Phi([\theta])}{\delta \theta(x) \delta \theta(y)} \right|_{\theta, u \in D_N} = \sum_{j,k=1}^N \varphi_k(x) \varphi_j(y) \frac{\partial \phi}{\partial a_j \partial a_k}. \tag{67}$$

Note that this also means that we can compute the mean field and two-point correlation function of the solution to the diffusion equation as in (60)-(61).

Generalizations Equations (66)-(67) hold for functionals that are way more general than Hopf functionals. To show this, let us consider a simple example. Let

$$F([\theta]) = \sin\left(\int_a^b K_1(x) \theta(x) dx \right) \tag{68}$$

where $K_1(x)$ is a given kernel. Evaluating F in D_N yields the multi-dimensional function

$$f(a_1, ..., a_N) = \sin\left(\sum_{i=1}^N a_i \int_a^b K_1(x) \varphi_i(x) dx \right). \tag{69}$$

Evaluating the functional derivative of F in D_N yields

$$\left. \frac{\delta F}{\delta \theta(x)} \right|_{\theta \in D_N} = \cos\left(\sum_{i=1}^N a_i \int_a^b K_1(x) \varphi_i(x) dx \right) K_1(x). \tag{70}$$

From (69) and (70) we immediately obtain

$$\frac{\partial f}{\partial a_k} = \int_a^b \left. \frac{\delta F}{\delta \theta(x)} \right|_{\theta \in D_N} \varphi_j(x) dx, \tag{71}$$

i.e., the gradient of f is the projection of the functional derivative restricted to D_N onto (56). On the other hand, if $K_1(x)$ is in D_N then

$$\left. \frac{\delta F}{\delta \theta(x)} \right|_{\theta \in D_N} = \sum_{k=1}^N \frac{\partial f}{\partial a_k} \varphi_k(x). \tag{72}$$

This explains the meaning of the functional derivative in both finite- and infinite-dimensional ($N \to \infty$) settings.

3.3.1 From Functional Equations Multivariate PDEs

Evaluating the Hopf functional differential equation in the finite-dimensional space D_N yields a characteristic function equation that can be obtained more directly by using simpler methods, e.g., by differentiating the characteristic function. To show this, let us consider again the 1D diffusion equation with a random initial condition as a prototype problem. We have seen that Hopf characteristic functional equation is

$$\frac{\partial \Phi}{\partial t} = \int_a^b \theta(x) \frac{\partial^2}{\partial x^2} \left[\frac{\delta \Phi}{\delta \theta(x)} \right] dx. \tag{73}$$

Now, let θ be in the finite-dimensional function space D_N. Evaluating the Hopf functional for $\theta \in D_N$ yields the multivariate characteristic function

$$\phi(a_1, ..., a_N, t) = \Phi([\theta], t) \qquad \theta \in D_N. \tag{74}$$

A substitution of (66) and (74) into (73) yields

$$\frac{\partial \phi}{\partial t} = \sum_{k,j=1}^{N} a_k \frac{\partial \phi}{\partial a_j} H_{kj}, \qquad H_{kj} = \int_a^b \varphi_k(x) \frac{\partial^2 \varphi_j(x)}{\partial x^2} dx. \tag{75}$$

This is an equation for the joint characteristic function of the coefficients $\{U_k(\omega)\}_{k=1,...,N}$ defined in (58)). Such equation can be obtained directly by using the semidiscrete (Galerkin) form of the diffusion equation

$$\frac{du_j(t;\omega)}{dt} = \sum_{k=1}^{N} u_k(t;\omega) \int_a^b \varphi_k(x) \frac{\partial^2 \varphi_j(x)}{\partial x^2} dx \qquad j = 1, ..., N. \tag{76}$$

Indeed, by differentiating the joint characteristic function of $\{u_1, ..., u_N\}$ we obtain

$$\frac{\partial \phi}{\partial t} = \sum_{k=1}^{N} i \left\langle \frac{du_k}{dt} a_k \exp \left[i \sum_{j=1}^{N} u_k(t;\omega) a_k \right] \right\rangle = \sum_{k,j=1}^{N} a_k H_{kj} \frac{\partial \phi}{\partial a_j}, \tag{77}$$

which coincides with (75).

3.3.2 From Functional Equations to Systems of PDEs

We have mentioned that functional differential equations are equivalent to PDEs in an infinite number of variables or infinite systems of PDEs. We provided an example of the first type of equivalence in Section 3.3.1. Hereafter we discuss the connection between functional differential equations and systems of PDEs. To this end, we restrict our attention to the simple Hopf equation (73). First of all, we notice that evaluating the Hopf functional at $\theta(x) = \alpha \delta(y - x)$ yields the one-point characteristic function of $u(y, t; \omega)$

$$\Phi([\theta], t) = \left\langle e^{i\alpha \int_a^b u(x,t;\omega)\delta(y-x)dx} \right\rangle = \left\langle e^{i\alpha u(y,t;\omega)} \right\rangle. \tag{78}$$

Similarly, if we consider

$$\theta(x) \in \text{span}\{\delta(y_1 - x), ..., \delta(y_N - x)\} \tag{79}$$

then we have that $\Phi([\theta], t)$ coincides with the joint characteristic function of $\{u(y_k, t; \omega)\}_{k=1,..,N}$. Now, let us see what happens to the Hopf equation when we evaluate it at $\theta(x) = \alpha_1 \delta(y_1 - x)$. We have

$$\frac{\partial \phi(\alpha_1, y_1, t)}{\partial t} = \alpha_1 \int_a^b \delta(y_1 - x) \frac{\partial^2}{\partial x^2} \left[\frac{\delta \Phi}{\delta \theta(x)} \right]_{\theta = \alpha_1 \delta(y_1 - x)} dx,$$
$$= i\alpha_1 \left\langle \frac{\partial^2 u(y_1, t; \omega)}{\partial y^2} e^{i\alpha u(y_1, t; \omega)} \right\rangle. \tag{80}$$

This equation can also be obtained directly by differentiating the one-point characteristic function $\phi(\alpha, y, t)$ with respect to time and then using the diffusion equation. Note that the term at the right hand side of (80) cannot be easily expressed in terms of the one-point characteristic function. However, if we use the two-point function we have

$$\left[\frac{\partial^3 \phi(\alpha_1, \alpha_2, y_1, y_2, t)}{\partial \alpha_2 \partial y_2^2} \right]_{\substack{\alpha_2 = 0 \\ y_2 = y_1}} = \left\langle \frac{\partial^2 u(y, t; \omega)}{\partial y^2} e^{i\alpha u(y, t; \omega)} \right\rangle. \tag{81}$$

Therefore, we obtain

$$\frac{\partial \phi(\alpha_1, y_1, t)}{\partial t} = i\alpha_1 \left[\frac{\partial^3 \phi(\alpha_1, \alpha_2, y_1, y_2, t)}{\partial \alpha_2 \partial y_2^2} \right]_{\substack{\alpha_2 = 0 \\ y_2 = y_1}} \tag{82}$$

At this point we need an evolution equation for the two point characteristic function $\phi(\alpha_1, \alpha_2, y_1, y_2, t)$. Such equation may be obtained from (73) by using the test function $\theta(x) = \alpha_1 \delta(y_1 - x) + \alpha_2 \delta(y_2 - x)$. If we perform the calculation we find that such evolution depends on the three-point characteristic function. If we keep get on going we obtain *an infinite hierarchy* of finite-dimensional characteristic function PDEs. Taking the Fourier transform of such hierarchy yields the well-known Bogoliubov-Born-Green-Kirkwood-Yvon (BBGKY) hierarchy of probability density function equations [117, 30]. Other functional equations yield other types of hierarchies of PDEs, which should be studied on a case-by-case basis.

4 Approximation of Functionals

Approximation theory for nonlinear functionals is strongly related to approximation theory of nonlinear operators [71, 169, 12]. A nonlinear functional $F([\theta])$ is in fact a particular type of nonlinear operator from a space of functions $D(F)$ (the domain of the functional F) into a vector space, e.g., $\mathbb{R}$ or $\mathbb{C}$. Thus, the question of approximating nonlinear functionals is basically the same as approximating nonlinear operators. This topic has been studied extensively by different scientific communities (see, e.g., [169, 155, 124, 161, 56, 143, 15, 107, 83]) for obvious reasons. Let us first provide simple examples of nonlinear functionals.

Example 1 Consider

$$F([\theta]) = \int_0^1 x^3 e^{-\theta(x)} dx, \qquad \theta \in D(F) = C^{(0)}([0, 1]), \tag{83}$$

where $C^{(0)}([0, 1])$ is the space of continuous functions in $[0, 1]$. Representing $F([\theta])$ by means of a functional approximant means that we are looking for an operator that provides the value of *all* integrals in the form (83), for arbitrary continuous functions in $[0, 1]$. This challenging problem includes cases in which $F([\theta])$ admits an analytical solution, e.g., $F([x])$ or $F([\sin(x)])$, as well as cases where no analytical solution is available, e.g., $F([x^2])$.

Example 2 (Homogeneous polynomial functionals of order n). Consider

$$P_n([\theta]) = \underbrace{\int_0^1 \cdots \int_0^1}_{n \text{ times}} K_n(x_1, ..., x_n)\theta(x_1) \cdots \theta(x_n) dx_1 \cdots dx_n, \tag{84}$$

where K_n are given kernel functions.

The fundamental question we would like to address in this Section is how to represent $F([\theta])$ in terms of simpler functionals (operators) with known structure. This is the first step in the process of developing numerical methods for functional differential equations. Perhaps, the most classical and widely used approach to represent nonlinear functionals relies on functional power series[6]. The method was originally developed by Volterra [181], and it represents the counterpart of power series expansions in the theory of functions. In practice, the functional of interest is represented in terms of a series of integral operators involving increasing powers of the test function and kernels that need to be determined. The canonical form of the power series expansion is

$$F([\theta]) = \sum_{k=0}^{\infty} P_k([\theta]), \quad \text{where} \quad P_k([\theta]) = \int_{-\infty}^{\infty} \cdots \int_{-\infty}^{\infty} K_k(x_1, ..., x_k)\theta(x_1) \cdots \theta(x_k) dx_1 \cdots dx_k. \tag{85}$$

Functional power series are known to have bad approximation properties and other issues. For example, they often do not preserve important properties of the functional, e.g., positive definiteness or normalization in the case of Hopf functionals.

4.1 Closed Functional Representations

Consider the initial value problem

$$\frac{\partial u}{\partial t} = \nu \frac{\partial^2 u}{\partial x^2}, \qquad u(x, 0; \omega) = u_0(x; \omega), \qquad x \in \mathbb{R}, \tag{86}$$

where u_0 is a random function. The functional differential equation governing the Hopf characteristic functional of the solution to (86) is

$$\frac{\partial \Phi}{\partial t} = \nu \int_{-\infty}^{\infty} \theta(x) \frac{\partial^2}{\partial x^2} \left(\frac{\delta \Phi}{\delta \theta(x)} \right) dx, \qquad \Phi([\theta(x)], t) = \Phi_0[\theta(x)]. \tag{87}$$

In order to solve this equation, we need a representation of $\Phi([\theta(x)], t)$ that is sufficient to determine the first-order functional derivative $\delta\Phi/\delta\theta(x)$. We shall call such representation a *closed functional representation*. To explain why, it useful to establish a parallel between the representation functionals and the representation of functions. Specifically, let us consider a polynomial interpolant of the solution to (86) on a set of nodes $\{x_1, ..., x_N\}$. Given the field values $u(x_j, t; \omega)$ $(j = 1, ..., N)$ at whatever time t, we can easily compute such interpolant and, correspondingly, the first- and second-order derivatives at x_j. This means that the function values at the nodes are *sufficient* to represent both $u(x, t; \omega)$ as well as its derivatives. This allows us to discretize and solve (86), e.g., by setting the residual equal to zero at the collocation nodes. According to the definition given above, $\{x_j, u(x_j, t; \omega)\}$ $(j = 1, ..., N)$ is a *closed* (finite-dimensional) representation of $u(x, t; \omega)$. The question of accuracy of such representation is a different matter, and it is ultimately related to the number of collocation points and their location. As we shall see in Section 4.2, the main

[6]Functional power series have been widely used in the theory of turbulence to obtain moment and cumulant expansions (see [54, 116, 150]).

ideas of collocation in finite-dimensional spaces can be extended to functionals, i.e., collocation in infinite-dimensional spaces. In this case, the collocation nodes are functions in Hilbert or Banach spaces. One of the simplest ways to establish a closed functional representation is to restrict the domain of the functional to a finite-dimensional function space spanned by the basis $\{\varphi_1(x), ..., \varphi_N(x)\}$, i.e.,

$$D_N = \text{span}\{\varphi_1(x), ..., \varphi_N(x)\}. \tag{88}$$

In this way, any element in D_N can be represented as[7]

$$\theta(x) = \sum_{k=1}^{N} a_k \varphi_k(x). \tag{90}$$

Possible choices of $\varphi_k(x)$ are:

1. *Lagrange Characteristic Polynomials*. Given a set of nodes N nodes $\{x_j\}$ in $[a, b]$, for example Gauss-Chebyshev-Lobatto nodes, we set

$$\varphi_j(x) = \prod_{\substack{i=1 \\ i \neq j}}^{N} \frac{(x - x_i)}{(x_i - x_j)}. \tag{91}$$

2. *Jacobi Polynomials*. Another set of basis functions in D_N could be the set of Jacobi polynomials $J_j^{(\alpha,\beta)}(x)$, i.e.

$$\varphi_j(x) = J_j^{(\alpha,\beta)}(x). \tag{92}$$

3. *Trigonometric Polynomials*. If we are dealing with continuous periodic functions in $[0, 2\pi]$, then a convenient choice for $\varphi_k(x)$ may be the set of (nodal) trigonometric polynomials [64]

$$\varphi_j(x) = \frac{1}{N} \sin\left(N \frac{x - x_j}{2}\right) \cot\left(\frac{x - x_j}{2}\right). \tag{93}$$

For each specific choice of the basis set $\{\varphi_1(x), ..., \varphi_N(x)\}$, the test function (90) lies on a *parametric manifold* of dimension N, i.e., on a hyperplane. A substitution of (90) into, e.g., the Hopf functional (29) yields a complex-valued multivariate function, i.e., the joint characteristic function $\phi(a_1, ..., a_N)$ in N real variables $(a_1, ..., a_N)$. Such multivariate function can be seen as a N-dimensional parametrization of the mapping Φ shown in Figure 2, i.e., a parametrization of the nonlinear transformation $D_N \to \Phi(D_N)$.

4.2 Functional Interpolation Methods

Suppose we are given a functional $F([\theta(x)])$ in some function space $D(F)$. In this Section we discuss how to construct an approximation of $F([\theta])$ in terms of a *functional interpolant* $\Pi([\theta])$, i.e., a functional that interpolates $F([\theta])$ at at a given set of nodes $\{\theta_1(x), ..., \theta_m(x)\} \in D(F)$

$$F([\theta_j]) = \Pi([\theta_j]) \qquad j = 1, ..., m. \tag{94}$$

[7]The space of test functions in higher-dimensional domains can be defined similarly, e.g.,

$$\theta(\boldsymbol{x}) = \sum_{k=1}^{N} a_k \varphi_k(\boldsymbol{x}), \qquad \boldsymbol{x} \in \mathbb{R}^3. \tag{89}$$

Differently from interpolation methods in spaces of finite dimension (e.g., d-dimensional Euclidean spaces), interpolation here is in a space of functions, i.e., the *interpolation nodes* $\theta_k(x)$ are functions in a Hilbert or a Banach space. Over the years, the problem of constructing a functional interpolant through a selected set of nodes in Hilbert or Banach spaces has been considered by several authors and convergence results were established in rather general cases (see, e.g., [107, 82, 143, 138, 78, 3, 85, 83, 139, 169]).

Before discussing the functional interpolation problem in detail, let us provide some geometric intuition on what functional interpolation is and what kind of representations we should expect. To this end, let us first recall recall that a hyperplane in a d-dimensional space is defined uniquely by d interpolation nodes, each node being a vector of $\mathbb{R}^d$. If we send d to infinity then the hyperplane intuitively becomes a linear functional, which is therefore defined uniquely by an infinite number of ∞-dimensional nodes, i.e., an *infinite number of functions*. This suggests that if we consider any finite number of nodes in a function space, say $\{\theta_1(x), ..., \theta_m(x)\}$, then we cannot even represent *linear functionals* in an exact way, i.e., functionals in the form

$$P_1([\theta]) = \int_a^b K_1(x_1)\theta(x_1)dx_1, \tag{95}$$

where $K_1(x)$ is a given function. In summary, functional interpolation with a finite number of nodes is, in general, not sufficient to represent even linear functionals[8]! The same conclusion obviously holds for nonlinear functionals, with the aggravating factor that the number of test functions theoretically required for the exact representation grows dramatically. For example, quadratic and cubic forms in d-dimensions are identified by by d^2 and d^3 interpolation nodes, respectively, where each node is vector of $\mathbb{R}^d$. When we send d to infinity, we intuitively obtain homogeneous polynomial functionals of second- and third-order, respectively. These functionals are in the form

$$P_2([\theta]) = \int_a^b \int_a^b K_2(x_1, x_2)\theta(x_1)\theta(x_2)dx_1dx_2, \tag{96}$$

$$P_3([\theta]) = \int_a^b \int_a^b \int_a^b K_3(x_1, x_2, x_3)\theta(x_1)\theta(x_2)\theta(x_3)dx_1dx_2dx_3. \tag{97}$$

Thus, to represent P_2 and P_3 exactly we need ∞^2 and ∞^3 nodes in a function space. Why ∞^2 and ∞^3? Consider $P_2([\theta])$ and assume that the kernel function $K_2(x_1, x_2)$ is in a separable Hilbert space. Represent K_2 relative to any complete orthonormal basis $\{\varphi_k\}_{k=1,...,\infty}$

$$K_2(x_1, x_2) = \sum_{i,j=1}^{\infty} a_{ij}\varphi_i(x_1)\varphi_j(x_2). \tag{98}$$

A substitution of (98) into (96) yields

$$P_2([\theta]) = \sum_{i,j=1}^{\infty} a_{ij} \int_a^b \varphi_i(x)\theta(x)dx \int_a^b \varphi_j(x)\theta(x)dx. \tag{99}$$

Without loss of generality we can assume that K_2 is symmetric, i.e., that a_{ij} is a symmetric matrix. To represent $P_2([\theta])$ exactly by means of a functional interpolant we need enough nodes $\{\theta_p(x)\}$ to determine each a_{ij} in (98) uniquely. Clearly, the choice $\theta_p(x) = \varphi_p(x)$ (p = 1,..., ∞) is not sufficient for this purpose, since it allows us to determine only the diagonal entries a_{pp}. Therefore we need to construct a larger set of collocation nodes, e.g., the set $\theta_p(x) = \varphi_{p_i}(x) + \varphi_{p_j}(x)$, where $p_i \geq p_j$ and $p_i \in \{1, ..., \infty\}$. This is the ∞^2 number of functions we have mentioned above. Similarly, to identify $P_3([\theta])$ through functional

[8]We recall that the variational form of nonlinear PDEs is defined by linear functionals on test function spaces. In this setting, classical Galerkin methods to solve PDEs (see Section 2.1) are basically identification problems for linear functionals.

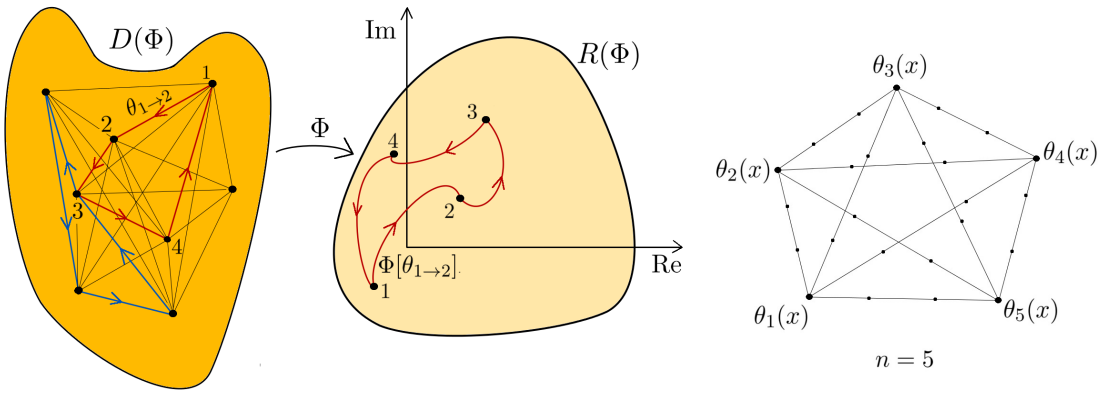

Figure 3: Network of test functions: A closed path in the function space $D(\Phi)$ made of four lines (e.g., the red polygon) is mapped through the functional Φ into a closed curve in the complex plane. Vertex and edges of the network are elements of $S_2^{(m)}$. We also show a complete graph with $n = 5$ nodes, where each edge is discretized with $p = 4$ points.

interpolation we need ∞^3 nodes, e.g., in the form $\theta_p(x) = \varphi_{p_i}(x) + \varphi_{p_j}(x) + \varphi_{p_k}(x)$, where $p_i \geq p_j \geq p_k$ and $p_k \in \{1, ..., \infty\}$. As we shall see later in this Section, determining a polynomial interpolant of an unknown functional $F([\theta])$, i.e., determining the kernels $K_j(x_1, ..., x_j)$ in (85) from input-output relations is a *linear problem* that involves very large dimensions.

4.2.1 Interpolation Nodes in Function Spaces

Let $F([\theta])$ be a continuous functional with domain $D(F)$. Within $D(F)$ we define the spaces of functions

$$S_q^{(m)} = \left\{\theta(x) \in D(F) \mid \theta(x) = a_{i_1}\varphi_{i_1}(x) + \cdots + a_{i_q}\varphi_{i_q}(x)\right\}. \tag{100}$$

where $i_j \in \{1, ..., m\}$, $a_{i_j} \in \mathbb{R}$ and $\{\varphi_1(x), ..., \varphi_m(x)\} \in D(F)$. The elements of $S_1^{(m)}$, $S_2^{(m)}$ and $S_3^{(m)}$ are in the form

$$\begin{aligned} S_1^{(m)}: &\quad \theta(x) = a_{i_1}\varphi_{i_1}(x), \\ S_2^{(m)}: &\quad \theta(x) = a_{i_1}\varphi_{i_1}(x) + a_{i_2}\varphi_{i_2}(x), \\ S_3^{(m)}: &\quad \theta(x) = a_{i_1}\varphi_{i_1}(x) + a_{i_2}\varphi_{i_2}(x) + a_{i_3}\varphi_{i_3}(x). \end{aligned}$$

Clearly, if $\theta_1 \in S_j^{(m)}$ and $\theta_2 \in S_q^{(m)}$, then $(\theta_1 + \theta_2) \in S_{j+q}^{(m)}$ (if $q + j < m$). Also, note that the sequence of spaces $S_j^{(m)}$, $j = 1, 2, ...$ is *hierarchical* in the sense that the following embedding hold true

$$S_1^{(m)} \subset S_2^{(m)} \subset \cdots \subset S_m^{(m)} \subset D(F). \tag{101}$$

It is possible to give $S_q^{(n)}$ a simple yet powerful graphical representation in terms of *trajectories of functions* (see [106, 168, 166, 167, 174] for a discussion of what a trajectory of functions is). To this end, consider a complex-valued functional Φ. A trajectory of functions in the space $D(\Phi)$ is a curve in $D(\Phi)$, which is mapped to a curve in $\mathbb{C}$ (see Figure 3). Furthermore, if the functional is continuous and differentiable, a smooth curve in $D(F)$ is mapped onto a smooth curve in $\mathbb{C}$. The set of trajectories in the complex plane associated with $S_1^{(m)}$ is shown in Figure 4. Each curve is parametrized by only one parameter a_j and it cannot branch into two distinct curves . On the contrary, if we consider $S_2^{(m)}$ we are adding one

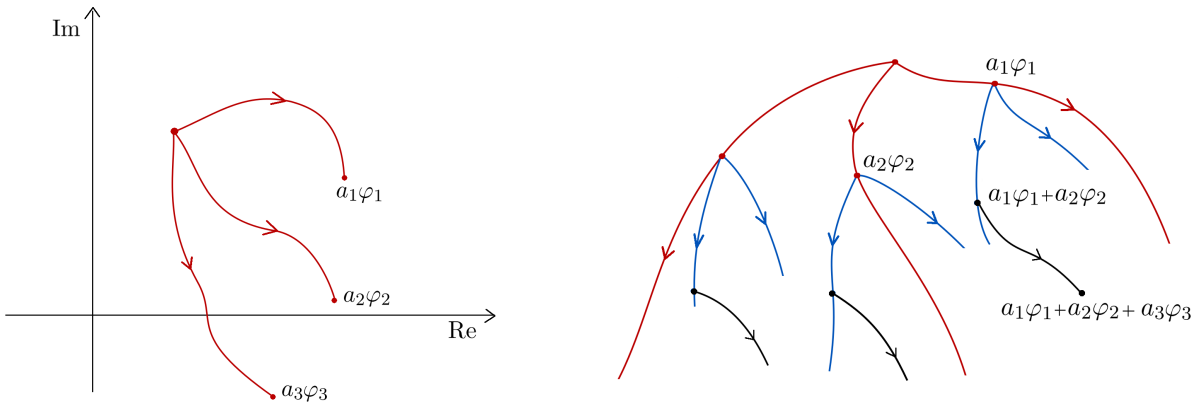

Figure 4: Trajectories in the range of a complex valued functional Φ corresponding to functions in the sets $S_1^{(m)}$ (left) and $S_3^{(m)}$ (right). In the case of $S_1^{(m)}$ each curve is parametrized by only one parameter a_j and it cannot branch into two distinct curves. On the contrary, if we consider $S_3^{(m)}$ we are adding two more degrees of freedom and each curve can branch twice.

more degree of freedom and each curve departing from 1 can branch, but only once. Similarly, we can have three branches in $S_3^{(m)}$, etc. A remarkable distribution of nodes in $S_2^{(m)}$ is associated with *networks of test functions*, i.e., *graphs* in the function space $D(F)$. Vertex and edges are elements of $S_2^{(m)}$. A simple example is shown in Figure 3. In mathematics such network is called *complete graph*, i.e., an undirected graph in which every pair of distinct nodes is connected by a unique edge. If we discretize each edge with p collocation points (including the endpoints) and we have m nodes then the number of degrees of freedom is $m(m-1)(p-2)/2+m$.

Another set of nodes which will be used in the sequel is the one obtained by setting all coefficients a_{i_p} in (100) equal to 1, i.e.,

$$\widehat{S}_q^{(m)} = \left\{\theta_i(x) \in D(F) \mid \theta_i(x) = \varphi_{i_1}(x) + \cdots + \varphi_{i_q}(x)\right\}, \qquad i_s = 0, ..., m, \tag{102}$$

If the set $\{\varphi_j\}$ includes the null element $\{0\}$, then by symmetry (102) is equivalent to

$$\widehat{S}_q^{(m)} = \{\{0\}, \{\varphi_1, .., \varphi_m\}, \{2\varphi_1, .., 2\varphi_m\}, \{(\varphi_1+\varphi_2), ..., (\varphi_1+\varphi_m)\}, \{(\varphi_2+\varphi_3), ..., (\varphi_2+\varphi_m)\}, ...\}. \tag{103}$$

In this case, the number of elements (cardinality) of $\widehat{S}_q^{(m)}$ is

$$\#\widehat{S}_q^{(m)} = \sum_{j=0}^{q} \binom{j+m-1}{j}, \qquad \text{where } \binom{i}{j} \text{ is the binomial coefficient.} \tag{104}$$

For example,

$$\#\widehat{S}_1^{(10)} = 11, \qquad \#\widehat{S}_2^{(10)} = 66 \qquad \#\widehat{S}_3^{(10)} = 286, \qquad \#\widehat{S}_5^{(10)} = 3003, \qquad \#\widehat{S}_{10}^{(10)} = 184756. \tag{105}$$

In addition, the cardinality of $\widehat{S}_q^{(m)}$ satisfies the recursion relation

$$\#\widehat{S}_q^{(m)} = \#\widehat{S}_{q-1}^{(m)} + \binom{q+m-1}{q}. \tag{106}$$

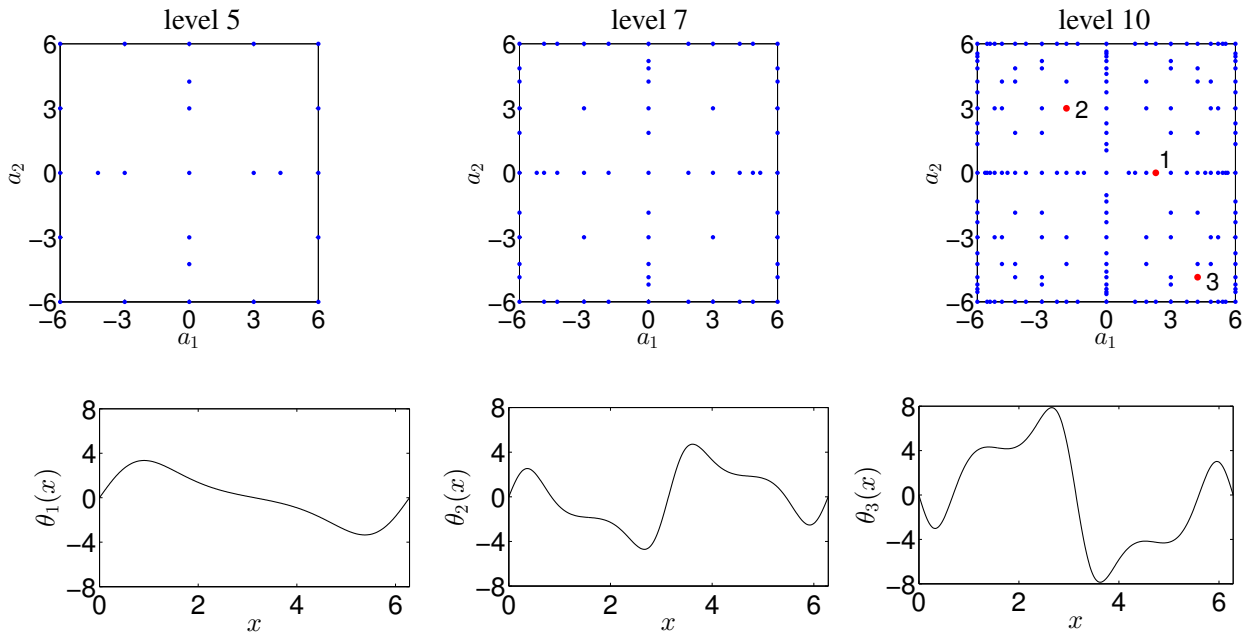

Figure 5: Clenshaw-Curtis point sets and corresponding nodes in $\theta_i(x) = a_{1_i}\varphi_1(x) + a_{2_i}\varphi_2(x)$ $(i = 1, 2, 3)$ in the test function space $\widetilde{S}_2^2$. Specifically, we plot $\theta_i(x)$ corresponding to the nodes 1, 2 and 3 marked in red in the top right Figure. The basis elements $\varphi_k(x)$ here are chosen as $\sin(kx)\exp(\cos(kx))$ $(k = 1, 2)$.

The set of functions $\widehat{S}_q^{(m)}$ is sufficient to uniquely identify a polynomial functional of order q in which each kernel function is represented relative to tensor product basis with m elements in each variable.

However, $\widehat{S}_q^{(m)}$ is, in general, *not* sufficient to accurately interpolate nonlinear functionals. The main problem is that the set of interpolation nodes (102) may not be large enough or may not cover the function space $D(F)$ appropriately. Another open question is related to the selection of optimal interpolation nodes in $D(F)$ yielding highly accurate representations. This question is addressed in Section 4.4.1.

In a finite-dimensional setting, we can sample the coefficients a_{i_p} in (100) at sparse grids locations [9, 21], i.e., at union of appropriate tensorizations of one-dimensional point sets such as Gauss-Hermite, Clenshaw-Curtis, Chebyshev or Leja [120]. This yields the set

$$\widetilde{S}_q^{(m)} = \left\{\theta_i(x) \in D(F) \mid \theta_i(x) = a_{i_1}\varphi_{i_1}(x) + \cdots + a_{i_q}\varphi_{i_q}(x)\right\}, \qquad i_s = 1, ..., m, \tag{107}$$

where the vector $(a_{i_1}, ..., a_{i_q})$ takes discrete values at sparse grid nodes. As an example, in Figure 5 we plot three Clenshaw-Curtis grids and few samples of the corresponding interpolation nodes in $\widetilde{S}_2^{(2)}$. For illustration purposes, the basis elements $\varphi_1(x)$ and $\varphi_2(x)$ here are chosen as

$$\varphi_1(x) = \sin(x)e^{\cos(x)}, \qquad \varphi_2(x) = \sin(2x)e^{\cos(2x)}. \tag{108}$$

We recall that, the construction of sparse grids usually follows the Smolyak algorithm. Other dimension-adaptive schemes and greedy Leja rules were recently proposed in [29, 120, 122].

4.2.2 Polynomial Interpolation of Nonlinear Functionals

Let $D(F)$ and Y be vector spaces and let $F : D(F) \to Y$ be a nonlinear functional on $D(F)$. Consider the set of polynomial functionals of degree n

$$\Pi_n([\theta]) = L_0 + L_1([\theta]) + L_2([\theta], [\theta]) + \cdots + L_n([\theta], ..., [\theta]), \tag{109}$$

where $L_0 \in Y$, $L_k : D(F)^k \to Y$ are k-linear *symmetric* functionals

$$L_k([\theta_1], ..., [\theta_p]) = \int \cdots \int K_k(x_1, .., x_k)\theta_1(x_1) \cdots \theta_k(x_k)dx_1 \cdots dx_k, \qquad k = 1, ..., n. \tag{110}$$

A comparison between equations (109) and (85) yields

$$P_k([\theta]) = L_k([\theta], ..., [\theta]), \tag{111}$$

and therefore we can equivalently write (109) as

$$\Pi_n([\theta]) = \sum_{k=1}^{n} P_k([\theta]). \tag{112}$$

The symmetry assumption on L_k implies that $K_k(x_1, ..., x_k)$ are a symmetric kernels, i.e., any permutation of x_1, ..., x_n leaves K_k unchanged. It is obviously possible to define polynomial functionals with non-symmetric kernels. However, such functionals can be *always* written in a symmetric form by re-writing the kernel functions appropriately. For example, let $H_2(x_1, x_2)$ be non-symmetric. It is easy to verify that

$$\int_a^b \int_a^b H_2(x_1, x_2)\theta(x_1)\theta(x_2)dx_1dx_2 = \int_a^b \int_a^b K_2(x_1, x_2)\theta(x_1)\theta(x_2)dx_1dx_2, \qquad \forall\theta \in D(F), \tag{113}$$

where

$$K_2(x_1, x_2) = \frac{1}{2}\left(H_2(x_1, x_2) + H_2(x_2, x_1)\right). \tag{114}$$

In other words, the value of the integral does not change if we replace $H_2(x_1, x_2)$ with its symmetrized version $K_2(x_1, x_2)$. More generally, we can symmetrize any kernel $H_p(x_1, ..., x_p)$ by summing up all terms corresponding to all possible permutations of $(x_1, ..., x_p)$ and then dividing up by the factorial of p. For example,

$$\begin{aligned} K_3(x_1, x_2, x_3) = \frac{1}{3!}\left(H_3(x_1, x_2, x_3) + H_3(x_1, x_3, x_2) + H_3(x_2, x_1, x_3) + H_3(x_2, x_3, x_1) + \right. \\ \left. H_3(x_3, x_1, x_2) + H_3(x_3, x_2, x_1)\right). \end{aligned} \tag{115}$$

As we shall see below, the symmetry of the operators L_k significantly reduces the number of collocation nodes in the function space $D(F)$ needed to identify kernels K_k, provided these are of finite-rank.

The polynomial functional interpolation problem can be stated as follows: Given a set of m nodes $\{\theta_1(x), ..., \theta_m(x)\}$ in $D(F)$, find a polynomial functional in the form (109) satisfying the interpolation conditions

$$\Pi_n([\theta_i]) = F([\theta_i]), \qquad i = 1, ..., m. \tag{116}$$

The Stone-Weierstrass Theorem The possibility of approximating an arbitrary continuous functional in Hilbert or Banach spaces in terms polynomial functionals is justified by theorems analogous to the classical Weierstrass theorem for continuous functions. We recall that such theorem states that if $f(x)$ is a continuous, real-valued function on the closed interval $[a, b]$, then given any $\epsilon > 0$ there exists a real polynomial $p(x)$ such that $|f(x) - p(x)| < \epsilon$ for all $t \in [a, b]$. A remarkable generalization of this result is the *Stone-Weierstrass theorem*, which states the following: suppose X is a compact metric space and K is an algebra of continuous, real-valued functions on X that separates points[9]. Then for any continuous,

[9]The algebra K separates points if for any two distinct elements u_1 ,$u_2 \in X$ there exists a $\Pi_n \in K$ such that $\Pi_n([u_1]) - \Pi_n([x_2]) \neq 0$ of X and that contains the constant function.

real-valued functional F on X and for any $\epsilon > 0$ there exists a polynomial functional $\Pi \in K$ such that $\|F([u]) - \Pi([u])\| < \epsilon$ for all $u \in X$. The first paper dealing with this subject is due Frechét [52]. He showed that any continuous functional can be represented by a series of polynomial functionals whose convergence is uniform in all compact sets of *continuous functions*. This result was generalized to compact sets of functions in Hilbert and Banach spaces by Prenter [142] and Istratescu [73], respectively. Other relevant work in this area is [56, 140, 15, 25, 133, 138].

4.2.3 Porter Interpolants

An effective way to construct finite-order polynomial functionals with minimal norm interpolating arbitrary continuous functionals in Hilbert spaces was proposed by W. Porter in [139]. The key idea relies on minimizing the norm of (109), subject to interpolation conditions (116), here imposed as standard Lagrange multipliers, i.e.,

$$\min_{K_1,..,K_n} \|\Pi_n\|^2 + \sum_{j=1}^{m} \left(\lambda, \Pi_n([\theta_i]) - F([\theta_i])\right). \tag{117}$$

The minimum is relative to arbitrary variations of the kernel functions $K_j(x_1, ..., x_j)$. Also, denotes $\|\Pi_n\|^2$ the norm of the polynomial functional (109), defined as

$$\|\Pi_n\|^2 = \sum_{p=0}^{n} \int \cdots \int |K_p(x_1, ..., x_p)|^2 \, dx_1 \cdots dx_p, \tag{118}$$

while $(,)$ denotes the inner product in $L_2(X)$, where here X is the domain of $\theta(x)$. The solution to the variational principle (117) allows us to identify the kernel functions $K_j(x_1, ..., x_j)$ and, correspondingly, the polynomial functional with *minimal norm* interpolating $F([\theta])$ at the m nodes $\{\theta_j\}_{j=1,...,m}$. Specifically, the kernel of the homogeneous polynomial functional of order p is obtained as

$$K_p(x_1, ..., x_p, t) = \sum_{j,k=1}^{m} \pi_j^{(p)}(x_1, .., x_p) H_{jk}^{-1} F([\theta_k], t) \qquad i = 0, ..., n \tag{119}$$

where $\pi_j^{(p)}(x_1, .., x_p) = \theta_j(x_1) \cdots \theta_j(x_p)$ ($\pi_j^{(0)} = 1$) and the (symmetric) matrix H_{ij} is defined as[10]

$$H_{ij} = 1 + (\theta_i, \theta_j) + (\theta_i, \theta_j)^2 + \cdots + (\theta_i, \theta_j)^n. \tag{120}$$

The polynomial functional Π_n constructed in this way exists if $F([\theta_k])$ is in the range of the matrix H (see [139] for further details). If one wants to approximate $F([\theta])$ in terms of a superimposition of monomials with orders defined by an index set $\mathcal{I}$ then[11]

$$H_{ij} = \sum_{p \in \mathcal{I}} (\theta_i, \theta_j)^p \tag{121}$$

The *total degree* of the polynomial functional is the largest number in the index set $\mathcal{I}$. It is convenient to write Porter's interpolant in terms of basis functionals $g_i([\theta])$ as

$$\Pi_n([\theta]) = \sum_{k=1}^{m} F([\theta_k]) \, g_k([\theta]) \tag{122}$$

[10] In equation (120), $H_{ij} = 1$ means a full matrix of ones.

[11] Note that if $\{\theta_j\}_{j=1,...,m}$ is an orthonormal basis and $\{0\} \notin \mathcal{I}$ then $H_{ij} = |\mathcal{I}|\delta_{ij}$ and $H_{ij}^{-1} = \delta_{ij}/|\mathcal{I}|$, where $\|\mathcal{I}\|$ is the number of elements in $\mathcal{I}$.

where

$$g_k([\theta]) = \sum_{j=1}^{m} H_{jk}^{-1} \sum_{p \in \mathcal{I}} (\theta_j, \theta)^p \tag{123}$$

At this point some remarks are in order:

1. $\{g_k([\theta])\}$ is a set of cardinal basis functionals, i.e., $g_k([\theta_q]) = \delta_{kq}$. This implies that Porter's interpolant is a *cardinal Lagrangian interpolant*.

2. Porter's interpolant is degenerate for $\mathcal{I} = \{0\}$ as the matrix H is rank one and therefore not invertible. The Moore-Penrose pseudoinverse H^+, however, exists and it provides the correct form of the interpolant. To show this in a simple case, consider the constant functional $F([\theta]) = c \in \mathbb{R}$ and the zero-order polynomial interpolant at $\{\theta_1, ..., \theta_m\}$

$$\Pi_0([\theta]) = K_0 = \sum_{k,j=1}^{m} H_{jk}^{-1} F([\theta_j]) \qquad H_{ij} = 1. \tag{124}$$

   Clearly, H_{jk}^{-1} does not exist since $H_{ij} = 1$ and therefore rank$(H) = 1$. However, the Moore-Penrose pseudoinverse of H is $H_{ij}^{+} = 1/m^2$, and therefore $\Pi_0([\theta]) = c = F([\theta])$.

3. In general, the polynomial functional (122)-(123) is an interpolant if and only if the matrix (121) is invertible, i.e., full rank. This depends on both the choice of interpolation nodes and on the index set $\mathcal{I}$. The Moore-Penrose pseudoinverse H^+, in general, *does not allow* to satisfy the interpolation condition. Indeed, by evaluating (122) at the interpolation nodes θ_k we obtain

$$\Pi_n\left([\theta_i]\right) = \sum_{k=1}^{m} F\left([\theta_k]\right) \sum_{j=1}^{m} H_{jk}^{-1} H_{ji} = F([\theta_i]) \tag{125}$$

   However, if we replace H_{jk}^{-1} with H_{jk}^{+} we get $\Pi_n\left([\theta_i]\right) \neq F\left([\theta_i]\right)$, since $H^+ H \neq I$.

4. In order for the matrix (121) to be invertible, the interpolation nodes $\theta_j(x)$ must be carefully chosen, also in relation to the order of Porter's interpolant defined by the index set $\mathcal{I}$.

5. Consider the approximation of constant functionals $F([\theta]) = c$ by polynomial functionals of order one, i.e., $\Pi_1([\theta]) = L_0 + L_1([\theta])$. Assume that the interpolation nodes $\{\theta_k\}_{k=1,...,m}$ are orthogonal functions with norm that decreases with m as $1/m$ (see Section 6.1). Let $H_{ij} = 1 + h\delta_{ij}$ where $h = \|\theta_j\|^2$ be the matrix (121) corresponding to the index set $\mathcal{I} = \{0, 1\}$. By using the identity

$$\lim_{h \to 0} \frac{1}{h} \left(1 + h\delta_{ij}\right)^{-1} = \delta_{ij} - \frac{1}{m} \tag{126}$$

   we obtain

$$\Pi_1([\theta]) \simeq c \sum_{k,j=1}^{m} \left(h\delta_{jk} - \frac{h}{m} \right) (1 + (\theta, \theta_j)) \qquad \text{as} \qquad h \to 0 \quad \text{and} \quad m \to \infty. \tag{127}$$

   This means that $\lim_{m \to \infty} \Pi_1([\theta]) = c$, i.e., the polynomial interpolant is *consistent* with the functional F in the sense that the linear term becomes smaller and smaller as we increase the number of test functions θ_k. In the limit $m \to \infty$ (infinite number of test functions) we see the linear term is completely absent.

By extending these arguments to higher-order polynomial functionals in Hilbert spaces, one can show that Porter's interpolants of order n *converge pointwise to entire functionals or any polynomial functional of order* n *or less* as the number of interpolation nodes θ_k goes to infinity (see [84] and Theorem 1 in [82]).

Functional Derivatives The functional derivatives of Porter interpolants can be easily determined by computing the functional derivatives of the basis functionals $g_i([\theta])$ defined in (123). To this end, we first notice that

$$\frac{\delta(\theta,\theta_k)^p}{\delta\theta(x)} = p(\theta,\theta_k)^{p-1}\theta_k(x), \qquad p \geq 1. \tag{128}$$

A substitution of this formula into (123) yields

$$\frac{\delta g_k([\theta])}{\delta\theta(x)} = \sum_{j=1}^{m} \theta_j(x) H_{jk}^{-1} \sum_{p\in\mathcal{I}} p\,(\theta_j,\theta)^{p-1} \tag{129}$$

By evaluating $g_k([\theta])$ at the nodes $\theta_j(x)$ we obtain a functional generalization of the classical differentiation matrix [64]

$$D_{ji}^{(1)}(x) = \frac{\delta g_i([\theta_j])}{\delta\theta(x)}. \tag{130}$$

Similarly, the second-order functional derivative of $g_k([\theta])$ is

$$\frac{\delta^2 g_k([\theta])}{\delta\theta(x)\delta\theta(y)} = \sum_{j=1}^{m} \theta_j(x)\theta_j(y) H_{jk}^{-1} \sum_{p\in\mathcal{I}} p(p-1)\,(\theta_j,\theta)^{p-2}\,, \tag{131}$$

and it yields the following second-order functional differentiation matrix

$$D_{ji}^{(2)}(x,y) = \frac{\delta^2 g_i([\theta_j])}{\delta\theta(x)\delta\theta(y)}. \tag{132}$$

At this point it is useful to provide simple examples of functional interpolation in Hilbert spaces:

- *Homogeneous polynomial functionals of first-order:*

$$P_1([\theta]) = \int_a^b K_1(x)\theta(x)dx. \tag{133}$$

  To represent $P_1([\theta])$ in terms of a functional interpolant it is sufficient to consider the set of orthonormal functions $\widehat{S}_1^{(m)} = \{\varphi_1,...,\varphi_m\}$ (see Eq. (102)). In this case, Porter's cardinal basis functionals (123) reduce to

$$g_i([\theta]) = (\varphi_i,\theta)\,, \tag{134}$$

  and the functional interpolant can be written as

$$\Pi_1([\theta]) = \sum_{i=1}^{m} P_1([\varphi_i]) g_i([\theta]). \tag{135}$$

  Clearly, we have that $\Pi_1([\theta]) \to P_1$ as $m \to \infty$.

- *Homogeneous polynomial functionals of second-order:*

$$P_2([\theta]) = \int_a^b \int_a^b K_2(x,y)\theta(x)\theta(y)dxdy. \tag{136}$$

  To represent $P_2([\theta])$ in terms of a functional interpolant it is sufficient to consider the set of orthonormal functions

$$\hat{\widehat{S}}_2^{(m)} = \{\varphi_1,...,\varphi_m,(\varphi_1+\varphi_2),...,(\varphi_1+\varphi_m),(\varphi_2+\varphi_3),...,(\varphi_2+\varphi_m),...\} \tag{137}$$

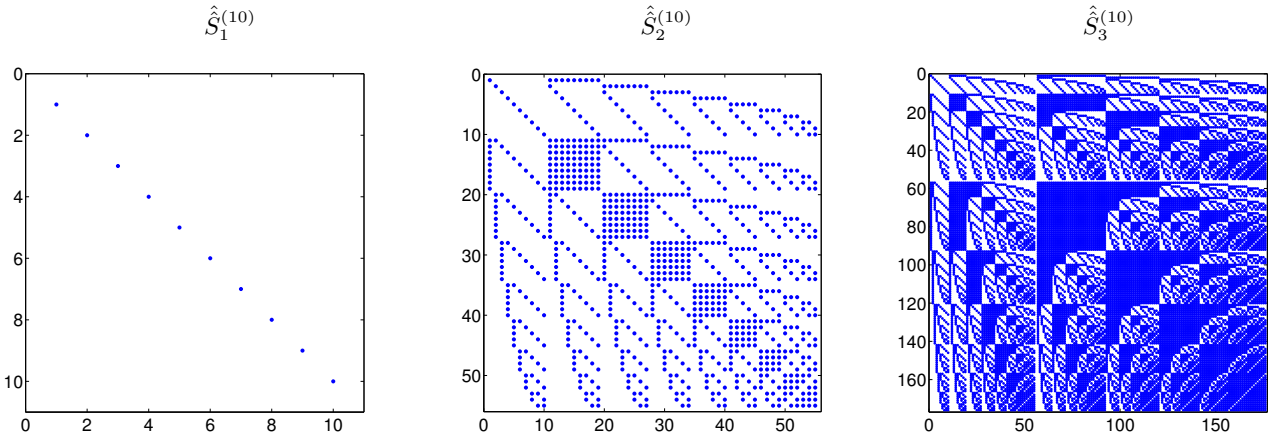

Figure 6: Structure of the H-matrix (121) associated with the function set $\hat{\hat{S}}_1^{(10)}$, $\hat{\hat{S}}_2^{(10)}$ and $\hat{\hat{S}}_3^{(10)}$ defined in Eq. (137). We consider $\mathcal{I}=1$, $\mathcal{I}=2$ and $\mathcal{I}=3$, respectively.

which is similar (but not equal) to (102). The matrix (121) associated with this set has the structure shown in Figure 6. The cardinal basis functionals (123) reduce to

$$g_k([\theta]) = \sum_{j=1}^{\#\hat{\hat{S}}_2^{(m)}} H_{jk}^{-1}\left(\theta_j,\theta\right)^2, \tag{138}$$

where $\#\hat{\hat{S}}_2^{(m)}$ is the number of elements of $\hat{\hat{S}}_2^{(m)}$, $\theta_k=\varphi_k$ $(k=1,...,m)$, $\theta_{m+1}=\varphi_1+\varphi_2$, etc. The functional interpolant can be written as

$$\Pi_2([\theta]) = \sum_{i=1}^{\#\hat{\hat{S}}_2^{(m)}} P_2([\theta_i])g_i([\theta]), \tag{139}$$

and it converges P_2 as $m\to\infty$ (see Section 6).

- *Homogeneous polynomial functionals of third-order:*

$$P_3([\theta]) = \int_a^b\int_a^b\int_a^b K_3(x_1,x_2,x_3)\theta(x_1)\theta(x_2)\theta(x_3)dx_1dx_2dx_3. \tag{140}$$

To represent $P_3([\theta])$ in terms of a functional interpolant it is sufficient to consider the set of functions $\hat{\hat{S}}_3^{(m)}\subset\hat{S}_3^{(m)}$ defined as

$$\hat{\hat{S}}_3^{(m)} = \hat{\hat{S}}_2^{(m)}\cup\{(\varphi_i+\varphi_j+\varphi_k),\quad k>j>i\} \tag{141}$$

where $\hat{\hat{S}}_2^{(m)}$ is as in (137). The matrix (121) associated with this set has the structure shown in Figure 6 The cardinal basis functionals (123) reduce to

$$g_k([\theta]) = \sum_{j=1}^{\#\hat{\hat{S}}_3^{(m)}} H_{jk}^{-1}\left(\theta_j,\theta\right)^3. \tag{142}$$

The functional interpolant can be written as

$$\Pi_3([\theta]) = \sum_{i=1}^{\#\widehat{S}_3^{(m)}} P_3([\theta_i]) g_i([\theta]). \tag{143}$$

More-Penrose Pseudoinverse and Non-Cardinal Basis Functionals The matrix H_{ij} defined in (121) may be not invertible in some cases. This happens, for example, if the interpolation nodes $\theta_k(x)$ are linearly dependent or if there exist a symmetry such the inner product of θ_k and θ_j yields linearly dependent rows/columns in (121). In this cases we can still construct a polynomial functional with *minimal norm* which, however, *does not* interpolate F at θ_k. To this end, we simply use the Moore-Penrose pseudoinverse of H_{ij} to obtain a representation of Porter's polynomial functionals in terms of a *non-cardinal basis* $g_k^+([\theta])$ as

$$\Pi_n([\theta]) = \sum_{k=1}^{m} F([\theta_k])\, g_k^+([\theta]). \tag{144}$$

where

$$g_k^+([\theta]) = \sum_{j=1}^{m} H_{jk}^+ \sum_{p\in\mathcal{I}} (\theta_j, \theta)^p \,. \tag{145}$$

In the last equation H_{ij}^+ denotes the Moore-Penrose pseudoinverse of H_{ij}. We will study the approximation properties of polynomial functionals in the form (144) in Section 6.3.2 and Section 6.4.

Recursive Porter Interpolation The number of interpolation nodes θ_k required to represent exactly a polynomial functional of order n is given in (104). For example, $m = 10$ and $n = 12$ yields 646646 interpolation nodes! Such a large number of nodes may be an issue when computing Porter's interpolants. In fact, computing the inverse of (121) rapidly becomes intractable as we increase either m or q. To overcome this problem we can resort to a triangulation of the function space $D(F)$ and construct a set of *local* polynomial functional approximations of small order, in analogy with classical finite element methods.

Alternatively, we can split the process of inverting the matrix (121) into a recursive algorithm, e.g., by using Schur complements and blockwise inversion. To this end, consider the set of nodes

$$\left\{\{\theta_1, ..., \theta_m\}, \{\theta_{m+1}, ..., \theta_{2m}\}, \{\theta_{2m+1}, ..., \theta_{3m}\}, ..., \{\theta_{(N-1)m+1}, ..., \theta_{Nm}\}\right\}, \tag{146}$$

and define the matrices

$$H_{ij}^{(I,J)} = \sum_{p\in\mathcal{I}} (\theta_i, \theta_j)^p \qquad i = (I-1)m+1, .., Im \quad j = (J-1)m+1, .., Jm, \tag{147}$$

where $\mathcal{I}$ denotes the index set of Porter's monomials while I and J run from 1 to N. The H-matrix (121) corresponding to the set (146) can be represented in block-wise form

$$H_N = \begin{bmatrix} H^{(1,1)} & \dots & H^{(1,N)} \\ \vdots & & \vdots \\ H^{(N,1)} & \dots & H^{(N,N)} \end{bmatrix}. \tag{148}$$

The computational cost of inverting such matrix is prohibitive if Nm is large. However, we can use the following recursive procedure. We first build and invert $H_1 = H^{(1,1)}$, corresponding to the first set of m.

This allows us to determine Porter's interpolant on the first set of m nodes in (146). Next we add the second set, i.e., the nodes $\{\theta_{m+1}, ..., \theta_{2m}\}$. The matrix (121) corresponding to the nodal set $\{\theta_1, ..., \theta_{2m}\}$ is

$$H_2 = \begin{bmatrix} H_1 & C_1 \\ C_1^T & H^{(2,2)} \end{bmatrix} \qquad C_1 = H^{(1,2)} \tag{149}$$

and it can be inverted by using the block-wise formula. To this end, let us assume that H is invertible in the classical sense. This allows us to use the well-known formula

$$H_2^{-1} = \begin{bmatrix} H_1^{-1} + B_1 A_1 B_1^T & -B_1 A_1 \\ -A_1 B_1 & A_1 \end{bmatrix} \tag{150}$$

where

$$B_1 = H_1^{-1} C_1, \tag{151}$$

$$A_1 = \left(H^{(2,2)} - C_1^T B_1 \right)^{-1} \qquad \text{(inverse of the Schur complement).} \tag{152}$$

If H is not invertible then we can compute a block-wise Moore-Penrose pseudo-inverse (see [113]). Now we bring in the third set of nodes $\{\theta_{2m+1}, ..., \theta_{3m}\}$. The matrix (121) corresponding to the nodal set $\{\theta_1, ..., \theta_{3m}\}$ is

$$H_3 = \begin{bmatrix} H_2 & C_2 \\ C_2^T & H^{(3,3)} \end{bmatrix} \qquad C_2 = \begin{bmatrix} H^{(1,3)} \\ H^{(2,3)} \end{bmatrix}, \tag{153}$$

and its inverse is, as before,

$$H_3^{-1} = \begin{bmatrix} H_2^{-1} + B_2 A_2 B_2^T & -B_2 A_2 \\ -A_2 B_2 & A_2 \end{bmatrix} \tag{154}$$

where

$$B_2 = H_2^{-1} C_2, \qquad A_2 = \left(H^{(3,3)} - C_2^T B_2 \right)^{-1}. \tag{155}$$

At this point it is clear that the procedure can be iterated as many times as needed. This generates a sequence of basis functionals (123), and an interpolating polynomial functional with minimal norm that passes through an increasing number of nodes. In this way, we have reduced the problem of computing Porter's interpolant through a very large number of nodes into a sequence of matrix inversions of dimension at most $m \times m$. The storage requirements of the algorithm just described, however, cannot be overcome because Porter's basis functionals are ultimately defined by H_N^{-1}. Thus, we need such matrix to proceed with the calculations. It would be nice to identify interpolation nodes in function space leading to minimal complexity/storage requirements for H_N^{-1}.

An alternative interpolation method makes use of residuals. The main idea is sketched in Figure 7. The functional $F([\theta])$ is interpolated by a polynomial of order n, denoted as $\Pi_n^{(1)}([\theta])$, at just three nodes $\{\theta_1, \theta_2, \theta_3\}$. Subtracting $\Pi_n^{(1)}([\theta])$ from $F([\theta])$ yields the functional residual

$$R_n^{(1)}([\theta]) = F([\theta]) - \Pi_n^{(1)}([\theta]) \tag{156}$$

which is zero at θ_1, θ_2 and θ_3 because of the interpolation condition. Now we add three more nodes $\{\theta_4, \theta_5, \theta_6\}$ and construct a Porter's interpolant of $R_n^{(1)}([\theta])$ at $\{\theta_1, ..., \theta_6\}$. We denote such interpolant by $\Pi_n^{(2)}([\theta])$. The computation of $\Pi_n^{(2)}([\theta])$ can be carried out as above by using Schur complements and block-wise inversion of (121). The polynomial functional $\Pi_n^{(1)}([\theta]) + \Pi_n^{(2)}([\theta])$ interpolates $F([\theta])$ at $\{\theta_1, ..., \theta_6\}$. The recursive construction proceeds with the definition of the new residual

$$R_n^{(2)}([\theta]) = F([\theta]) - \Pi_n^{(1)}([\theta]) - \Pi_n^{(2)}([\theta]), \tag{157}$$

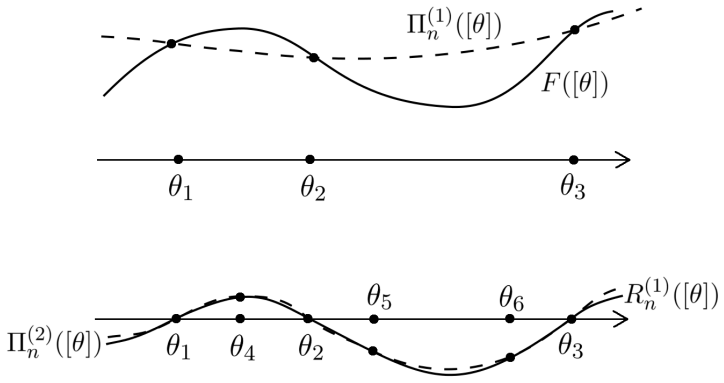

Figure 7: Recursive polynomial interpolation: Minimal residual approach.

three more nodes $\{\theta_7, \theta_8, \theta_9\}$, and a Porter's polynomial $\Pi_n^{(3)}([\theta])$, interpolating $R_n^{(2)}([\theta])$ at $\{\theta_1, ..., \theta_9\}$. Proceeding recursively with higher-order residuals up to order r, we obtain the polynomial functional

$$Q_n([\theta]) = \sum_{k=1}^{r} \Pi_n^{(k)}([\theta]). \tag{158}$$

Clearly $Q_n([\theta])$ interpolates $F([\theta])$ at all nodes θ_k and therefore it is completely equivalent to $\Pi_n([\theta])$, i.e., $Q_n([\theta]) = \Pi_n([\theta])$.

Hierarchical Matrices The algorithm described in the previous Section aims at reducing the computational cost of computing polynomial functional interpolants by inverting the matrix H defined in (121) in a blockwise fashion or recursively. The structure of such matrix obviously depends on how we select the interpolation nodes in the function space $D(F)$. Can we determine sets of nodes for which the interpolation problem can be solved at a minimal cost? Stated in matrix terms, can we identity sets of nodes yielding structured matrices that can be easily inverted, e.g., *hierarchical matrices*? Apparently, the matrices shown in Figure 6 have a self similar structure which can be used to speed up their inversion. We leave this question open for future research. For uniquely solvable interpolation problems we could equivalently construct Khlobystov polynomial functionals (see subsequent Sections) and determine the coefficients of the expansion by using the method of moments (see equation (167)).

4.2.4 Prenter Interpolants

Another method to determine polynomial interpolants in Hilbert and Banach spaces was introduced by Prenter in [143]. She proved that if $F([\theta])$ is a functional in a Hilbert space then we have

$$\Pi_n([\theta]) = \sum_{i=1}^{n} F([\theta_i]) g_i([\theta]), \tag{159}$$

where

$$g_i([\theta]) = \prod_{\substack{j=1 \\ j \neq i}}^{n} \frac{(\theta - \theta_j, \theta_i - \theta_j)}{(\theta_i - \theta_j, \theta_i - \theta_j)} \qquad \text{(cardinal basis)}. \tag{160}$$

As before, here $(,)$ denotes the inner product in $L_2(X)$, where X is the domain of $\theta_k(x)$. Note that each basis element $g_i([\theta])$ is a polynomial functional of order n. On the other hand, Porter's method yields polynomial basis functionals of total degree $\max(\mathcal{I})$, where the index set $\mathcal{I}$ does not depend on the number of collocation points. Porter [138] applied Prenter's theorems to causal systems, while Bertuzzi, Gandolfi and Germani [14, 15] extended Prenter's results to causal approximation of input-output maps in Hilbert spaces. Generalizations to Banach spaces can be found in Chapter 3 of [169] (see also [107] and the references therein). The functional derivatives of Prenter's polynomial functionals can be obtained by computing the functional derivatives of (160). This yields[12]

$$\frac{\delta g_i[\theta]}{\delta \theta(x)} = \sum_{\substack{k=1 \\ k \neq i}}^{n} \frac{\theta_i(x) - \theta_k(x)}{\|\theta_i - \theta_k\|^2} g_{ik}[\theta], \tag{162}$$

$$\frac{\delta^2 g_i[\theta]}{\delta \theta(x) \delta \theta(y)} = \sum_{\substack{k=1 \\ k \neq i}}^{n} \frac{\theta_i(x) - \theta_k(x)}{\|\theta_i(x) - \theta_k(x)\|^2} \sum_{\substack{s=1 \\ s \neq k}}^{n} \frac{\theta_i(y) - \theta_s(y)}{\|\theta_i(y) - \theta_s(y)\|^2} g_{iks}[\theta], \tag{163}$$

where,

$$g_{ik}[\theta] = \prod_{\substack{j=1 \\ j \neq i,k}}^{n} \frac{(\theta - \theta_j, \theta_i - \theta_j)}{\|\theta_i - \theta_j\|^2}, \qquad g_{iks}[\theta] = \prod_{\substack{j=1 \\ j \neq i,k,s}}^{n} \frac{(\theta - \theta_j, \theta_i - \theta_j)}{\|\theta_i - \theta_j\|^2}. \tag{164}$$

Note that the expressions (162)-(163) are more complicated than those we obtained for Porter's basis (129). As noted by Allasia and Bracco in [3], Prenter's interpolants are badly conditioned as the number of interpolation nodes in function space increases. This unfortunate feature is common to many Lagrange interpolants.

4.2.5 Khlobystov Interpolants

Continuous functionals in Hilbert or Banach spaces can be approximated (uniformly) in terms of polynomial functionals [141, 15, 73, 107, 71, 169]. Such polynomial functionals may be built based on an interpolation process (see Section 4.2.3 and Section 4.2.4). What are the convergence properties of such interpolants? To address this question, let us consider a polynomial functional $\Pi_n([\theta])$ in the form (112), where $D(\Pi_n)$ is a Hilbert space of test functions. Let us introduce an orthonormal basis $\{\varphi_1, ..., \varphi_m\}$ in $D(\Pi_n)$, and consider the following expansion

$$\Pi_n^I([\theta]) = \sum_{k=1}^{n} \sum_{i_1=1}^{m} \cdots \sum_{i_k=1}^{m} (\theta, \varphi_{i_1}) \cdots (\theta, \varphi_{i_k}) a_k(\varphi_{i_1}, ..., \varphi_{i_k}), \tag{165}$$

where $(,)$ is an inner product in $D(\Pi_n)$ and $a_k(\varphi_{i_1}, ..., \varphi_{i_k})$ are real- or complex-valued coefficients. Clearly Π_n^I is an interpolant of $\Pi_n([\theta])$ at φ_k, i.e.,

$$\Pi_n^I([\varphi_k]) = \Pi_n([\varphi_k]). \tag{166}$$

[12] These expressions can be easily proved by noting that

$$\frac{d}{d\epsilon} g_i[\theta + \epsilon\eta]\Big|_{\epsilon=0} = \sum_{\substack{k=1 \\ k \neq i}}^{n} \frac{(\eta, \theta_i - \theta_k)}{\|\theta_i - \theta_k\|^2} \prod_{\substack{j=1 \\ j \neq k,i}}^{n} \frac{(\theta - \theta_j, \theta_i - \theta_j)}{\|\theta_i - \theta_j\|^2}. \tag{161}$$

The next step is to write the coefficients $a_k(\varphi_{i_1},...,\varphi_{i_k})$ in terms of $\Pi_n([\varphi_j])$. To this end, we can use the method for finding orthonormal moments of regular polynomial functionals (Theorem 1 in [81]). This yields

$$\begin{aligned} n!a_n(\varphi_{i_1},...,\varphi_{i_n}) =&\Pi_n([\varphi_{i_1}+\cdots+\varphi_{i_n}]) - \left\{\Pi_n([\varphi_{i_1}+\cdots+\varphi_{i_{n-1}}])+\right. \\ &\Pi_n([\varphi_{i_1}+\cdots+\varphi_{i_{n-2}}+\varphi_{i_n}])+\cdots+\Pi_n([\varphi_{i_2}+\cdots+\varphi_{i_n}])\Big\}+ \\ &\Big\{\Pi_n([\varphi_{i_1}+\cdots+\varphi_{i_{n-2}}])+\Pi_n([\varphi_{i_1}+\cdots+\varphi_{i_{n-3}}+\varphi_{i_{n-1}}])+\cdots+ \\ &\Pi_n([\varphi_{i_3}+\cdots+\varphi_{i_n}])\Big\}\cdots+(-1)^{n-1}\left\{\Pi_n([\varphi_{i_1}])+\cdots+\Pi_n([\varphi_{i_n}])\right\}+ \\ &(-1)^n\Pi_n([0]). \end{aligned} \tag{167}$$

Once $a_n(\varphi_{i_1},...,\varphi_{i_n})$ are available, we can construct the polynomial

$$\Pi_n - a_n(\varphi_{i_1},...,\varphi_{i_n})\prod_{z=1}^{n}(\theta,\varphi_{i_z})$$

and apply (167) again to determine $a_{n-1}(\varphi_{i_1},...,\varphi_{i_{n-1}})$. After n iterations, we have available all coefficients to construct the polynomial functional (165).

Error Analysis The following error estimate holds true (Theorem 2 in [81])

$$\left\|\Pi_n^I([\theta])-\Pi_n([\theta])\right\| \leq \sum_{k=1}^{n}\|P_k\|\left[\left(\|\theta\|+\epsilon_m([\theta])\right)^k-\|\theta\|^k\right], \tag{168}$$

where

$$\|P_k\| = \int\cdots\int |K_k(x_1,...,x_k)|\,dx_1\cdots dx_k, \tag{169}$$

$$\epsilon_m([\theta]) = \left\|\theta-\sum_{k=1}^{m}(\theta,\varphi_k)\varphi_k\right\|. \tag{170}$$

This means that the interpolant (165) converges *pointwise* to the polynomial functional $\Pi_n([\theta])$ in (109) as the number of nodes $\{\varphi_k\}$ in the function space $D(\Pi_n)$ goes to infinity[13]. As noted by Khlobystov [82], Porter's interpolant (122) can be written exactly in the form (165) if we consider test functions in the form $\theta_i=\varphi_{i_1}+...+\varphi_{i_n}$ (see the Lemma in [82]). In this sense, *Porter's interpolants represent the Lagrangian form of Khlobystov's interpolants*. An interesting and very important question is the approximation of polynomial functionals of order n in terms interpolants over nodal sets $\widehat{S}_q^{(m)}$, with $q<n$ (see Eq. (102)). A specific example would be the approximation of $P_3([\theta])$ in (140) by using an interpolant built on the set of nodes $\widehat{S}_1^{(m)}$. In some very special cases we may get uniform convergence as $m\to\infty$, for example when K_3 is diagonal

$$K_3(x_1,x_2,x_3)=\sum_{j=1}^{m}a_j\varphi_j(x_1)\varphi_j(x_2)\varphi_j(x_3). \tag{171}$$

However, this won't happen in general, and therefore we will have to accept a systematic truncation error in representing continuous nonlinear functionals. Such error is similar the error committed when we approximate infinite-variate functions, e.g., by second-order HDMR [185].

[13]Note that $\epsilon_m([\theta])\to 0$ as $m\to\infty$. Thus, the right hand side of the error estimate (168) goes to zero as $m\to\infty$, i.e., $\Pi_n^I([\theta])\to\Pi_n([\theta])$ pointwise as $m\to\infty$.

Khlobystov interpolants with Hilbert-Schmidt Kernels In this Section we present a procedure to construct interpolants of polynomial operators in Hilbert spaces with separable kernels. To this end, let us consider an orthonormal basis $\{\varphi_1, \varphi_2, ..., \varphi_m\}$ and represent K_p in (110) as

$$K_1(x_1) = \sum_{i=1}^{m} a_i \varphi_i(x), \tag{172}$$

$$K_2(x_1, x_2) = \sum_{i,j=1}^{m} a_{ij} \varphi_i(x_1) \varphi_j(x_2), \tag{173}$$

$$K_3(x_1, x_2, x_3) = \sum_{i,j,k=1}^{m} a_{ijk} \varphi_i(x_1) \varphi_j(x_2) \varphi_k(x_3), \tag{174}$$

$$\cdots .$$

Without loss of generality we can assume that K_2, K_3, ... are symmetric, i.e., that the coefficients $a_{ijk\cdots}$ are invariant under any permutation of the indices i, j, k, etc. A substitution of (172), (173), etc., into (109) yields the polynomial functional

$$\Pi_n([\theta]) = K_0 + \sum_{i=1}^{m} a_i(\varphi_i, \theta) + \sum_{i,j=1}^{m} a_{ij}(\varphi_i, \theta)(\varphi_j, \theta) + \sum_{i,j,k=1}^{m} a_{ijk}(\varphi_i, \theta)(\varphi_j, \theta)(\varphi_k, \theta) + \cdots . \tag{175}$$

At this point we pose the following question: How many test functions do we need to identify the coefficients a_i, a_{ij}, a_{ijk}, etc., uniquely? To clarify the question, consider the following second-order polynomial functional

$$\Pi_2([\theta]) = K_0 + \sum_{i=1}^{m} a_i(\varphi_i, \theta) + \sum_{i,j=1}^{m} a_{ij}(\varphi_i, \theta)(\varphi_j, \theta). \tag{176}$$

The total number of degrees of freedom (number of independent coefficients K_0, a_i and a_{ij}) is

$$1 + m + m + \binom{m}{2} = 1 + \frac{3m + m^2}{2}. \tag{177}$$

To determine such coefficients, we need to test $\Pi_2([\theta])$ at $(2 + 3m + m^2)/2$ distinct nodes [14], e.g.,

$$\left\{0, \{\varphi_i\}_{i=1}^{m}, \{\varphi_i + \varphi_j\}_{i,j=1\,(j\geq i)}^{m}\right\}. \tag{178}$$

In this case, we obtain the linear system

$$\begin{aligned} \Pi_2([0]) &= K_0 \\ \Pi_2([\varphi_p]) &= K_0 + a_p + a_{pp} \\ \Pi_2([\varphi_p + \varphi_q]) &= K_0 + a_p + a_q + a_{pp} + a_{qq} + 2a_{pq} \end{aligned}$$

which can be immediately solved for a_{pq}, a_p and K_0, yielding

$$a_{pq} = \frac{1}{2}\left(\Pi_2([\varphi_p + \varphi_q]) - \Pi_2([\varphi_p]) - \Pi_2([\varphi_q]) + \Pi_2([0])\right), \tag{179}$$

$$a_p = -\frac{1}{2}\Pi_2([2\varphi_p]) + 2\Pi_2([\varphi_p]) - \frac{3}{2}\Pi_2([0]), \tag{180}$$

$$K_0 = \Pi_2([0]). \tag{181}$$

[14] Note, that testing a second-order polynomial functional in $\varphi_i(x)$ or $2\varphi_i(x)$ yields different results.

This allows us to identity finite-rank kernels in the form (172)-(174) and therefore polynomial functionals in the form (176). Note that if the basis elements in (178) are not normalized (but still orthogonal) then we simply need to replace a_{pq} and a_p in (179)-(181) with $\|\varphi_p\|^2 \|\varphi_q\|^2 a_{pq}$ and $\|\varphi_p\|^2 a_p$, respectively. Higher-order polynomial functionals can be constructed in the same way. However, the number of degrees of freedom may increase significantly with the order of the polynomial (see equation (104)). For example, a twelve-order polynomial functional in which each kernel is represented relative to $m = 10$ basis functions (tensor product) yields 646646 degrees of freedom!

Remark: The fact that we can get analytical expressions for the coefficients of the polynomial interpolant means that Porter's matrix (130) is *invertible analytically* for uniquely solvable interpolation problems and orthonormal bases.

The procedure we just described to identify the coefficients of the symmetric kernel functions K_n relies on tensor product representations, i.e., series expansions in the form

$$K_n(x_1, x_2, ..., x_n) = \sum_{i_1,...,i_n=1}^{m} a_{i_1 \cdots i_n} \varphi_{i_1}(x_1) \cdots \varphi_{i_n}(x_n). \tag{182}$$

The number of independent coefficients $a_{i_1 \cdots i_n}$ is

$$\binom{n+m-1}{n} = \frac{(n+m-1)!}{n!(m-1)!}. \tag{183}$$

Such number can pose serious computational challenges even for moderate values of m and n. To alleviate this problem one could use HDMR expansions [145, 99, 98], i.e., represent $K_n(x_1, x_2, \cdots, x_n)$ in terms of a superimposition of functions involving a lower number of variables (interaction terms). This yields, for example

$$K_n(x_1, x_2, ..., x_n) = f_0 + \sum_{i=1}^{n} f_i(x_i) + \sum_{i<j}^{n} f_{ij}(x_i, x_j) + \sum_{i<j<k}^{n} f_{ijk}(x_i, x_j, x_k) + \cdots. \tag{184}$$

The function f_0 is a constant. The functions $f_i(x_i)$ (first-order interactions) give us the overall effects of the variables x_i in f as if they were acting independently of the other input variables. The functions $f_{ij}(x_i, x_j)$ (second-order interactions) describe the cooperative effect of the variables x_i and x_j. Similarly, higher-order terms reflect the cooperative effects of an increasing number of variables. Representing f_i, f_{ij}, f_{ijk} relative to the orthonormal basis $\{\varphi_j(x)\}$ yields the series

$$\begin{aligned} K_n(x_1, x_2, ..., x_n) =& f_0 + \sum_{i=1}^{n} \sum_{s=1}^{m} a_s^i \varphi_s(x_i) + \sum_{i<j}^{n} \sum_{s,q=1}^{m} a_{sq}^{ij} \varphi_s(x_i) \varphi_q(x_j) + \\ & \sum_{i<j<k}^{n} \sum_{s,q,r=1}^{m} a_{sqr}^{ijk} \varphi_s(x_i) \varphi_q(x_j) \varphi_r(x_j) + \cdots. \end{aligned} \tag{185}$$

Given the symmetry of each function f_i, f_{ij}, f_{ijk}, the total number of degrees of freedom of an HDMR expansion of order Z is

$$\sum_{k=0}^{Z} \binom{n}{k} \binom{m+k-1}{k} = 1 + \binom{n}{1}\binom{m}{1} + \binom{n}{2}\binom{m+1}{2} + \binom{n}{3}\binom{m+2}{3} + \cdots. \tag{186}$$

For example, the second- and third-order truncations of a $n = 10$ dimensional kernel relative to $m = 10$ yield 2576 and 28976 degrees of freedom, respectively. On the other hand, the tensor product representation yields 92378 degrees of freedom. Similarly, one can use a separated series expansion (SSE) [16, 30] of each kernel to reduce the number of degrees of freedom. The coefficients of the expansion can be determined by interpolation, least-squares or projection [126, 125].

4.3 Functional Approximation on Cylindrical Sets

Polynomial functionals suffer from severe limitations when approximating nonlinear functionals $F([\theta])$. One of the main issues is related to the fact that the computation of a high-order polynomial expansion requires representing kernel functions in many independent variables. To get an idea of how serious this problem could be, simply consider that representing a polynomial functional of order 6 is as computationally expensive as representing the solution to the steady-state Boltzmann equation [35], a well-known challenging problem in computational physics. Expanding each kernel in terms of HDMR [145] or separated series expansions (SSE) [16] can mitigate the dimension problem, but it may not be the most efficient way to represent a nonlinear functional.

In this Section we discuss a new approach based on a s *cylindrical representation* of $F([\theta])$. To introduce the new method, consider a set of linearly independent elements in a Hilbert space $\{\varphi_1, ..., \varphi_m\}$ (e.g., an orthonormal basis) and look for an approximant of $F([\theta])$, say $\widehat{F}$, in the form

$$F([\theta]) = \widehat{F}((\theta, \varphi_1), ..., (\theta, \varphi_m)) + R([\theta]), \tag{187}$$

where R is a (functional) reminder term and $(,)$ denotes an inner product in $D(F)$, e.g.,

$$(\theta, \varphi_k) = \int_a^b \theta(x)\varphi_k(x)dx, \qquad k = 1, ..., m. \tag{188}$$

The variables (θ, φ_k) can be either real or complex numbers. In the theory of stochastic processes the set

$$\{\theta \in D(F) \,|\, ((\theta, \varphi_1), ..., (\theta, \varphi_m)) \subseteq \mathbb{R}^m\} \tag{189}$$

is known as *cylindrical set* (see, e.g., [173] p. 56 or [162] p.45). Therefore, according to Eq. (187), we are looking for an approximant of $F([\theta])$ in the space of *cylindrical functionals*, i.e., functionals defined on cylindrical sets. The representation (187) is very general. For example, it includes the case where $\widehat{F}$ is a polynomial functional, e.g., (165) or (122), or the case where the functional is defined on a finite-dimensional function space (see, e.g., (58)).

Example: Consider a finite dimensional space of test functions defined by the span of an orthonormal basis $\{\varphi_k\}$. An element of such space can be written as

$$\theta(x) = \sum_{k=1}^{m} (\theta, \varphi_k)\varphi_k(x). \tag{190}$$

In this setting, (187) becomes a multivariate function of m variables (θ, φ_k), i.e., the residual $R([\theta])$ is zero. For example,

$$\begin{aligned} F([\theta]) &= \int_a^b e^{\theta(x)} dx \\ &= \sum_{k=0}^{\infty} \frac{1}{k!} \int_a^b \left(\sum_{j=1}^{m} (\theta, \varphi_j)\varphi_j(x) \right)^k dx \end{aligned} \tag{191}$$

This yields $F([\theta]) = \widehat{F}((\theta,\varphi_1),...,(\theta,\varphi_m))$, where

$$\widehat{F}((\theta,\varphi_1),...,(\theta,\varphi_m)) = \sum_{k=0}^{\infty} \frac{1}{k!} \int_a^b \left(\sum_{j=1}^{m} (\theta,\varphi_j)\varphi_j(x) \right)^k dx. \tag{192}$$

Remark: Cylindrical functionals in the form (187) can approximate any continuous functional[15] in a Hilbert or a Banach space. This is a consequence of the Stone-Weierstrass theorem. The computational cost of such representation obviously depends on the criterion we use to construct $\widehat{F}$. Hereafter, we propose different ones.

4.3.1 Functional HDMR

The HDMR expansion of the nonlinear functional $\widehat{F}((\theta,\varphi_1),...,(\theta,\varphi_m))$ appearing in Eq. (187) can be defined as

$$\widehat{F}((\theta,\varphi_1),...,(\theta,\varphi_m)) = \widehat{F}_0 + \sum_{k=1}^{m} \widehat{F}_k((\theta,\varphi_k)) + \sum_{\substack{k,j=1 \\ k<j}}^{m} \widehat{F}_{kj}((\theta,\varphi_k),(\theta,\varphi_j)) + \cdots . \tag{198}$$

Each nonlinear function $\widehat{F}_k$, $\widehat{F}_{kj}$, ..., can be determined by expanding it relative to a known basis and then applying either interpolation, least-squares or projection operator techniques (see, e.g., [145, 99, 98] the multivariate function setting). For example, consider the first-order truncation of (198)

$$\widehat{F}((\theta,\varphi_1),...,(\theta,\varphi_m)) \simeq \widehat{F}_0 + \sum_{k=1}^{m} \widehat{F}_k((\theta,\varphi_k)). \tag{199}$$

Here

$$\widehat{F}_k((\theta,\varphi_k)) = \sum_{i=1}^{P} \alpha_{ik} L_i((\theta,\varphi_k)), \tag{200}$$

where L_i could be, e.g., orthogonal polynomials.

[15] Let us recall that a functional F is continuous at a point $\theta_0(x)$ if for any sequence $\{\theta_n(x)\}$ which converges to θ_0, i.e.

$$\lim_{n\to\infty} \|\theta_n - \theta_0\| \to 0, \tag{193}$$

the sequence $\{F([\theta_n])\}$ converges to $\{F([\theta_0])\}$, i.e.,

$$\lim_{n\to\infty} \|F([\theta_n]) - F([\theta_0])\| \to 0. \tag{194}$$

An example of a continuous functional may be

$$F([\theta]) = \theta(x_1)^2 + \int_a^b \sin(\theta(x))dx, \qquad x_1 \in [a,b]. \tag{195}$$

Indeed, let us pick $\{\theta_n\}$ in (complete) compact metric space. Also choose an integrable function $g(x)$ such that $|\theta_n(x)| \leq g(x)$. In this condition, the Lebesgue dominated convergence theorem applies and we have

$$\lim_{n\to\infty} \int_a^b \sin(\theta_n(x))dx = \int_a^b \sin(\theta(x))dx, \tag{196}$$

that is

$$\theta_n \to \theta \;\Rightarrow\; F([\theta_n]) \to F([\theta]). \tag{197}$$

4.3.2 Functional SSE

The separated series expansion (SSE) of $\widehat{F}$ in Eq. (187) takes the form

$$\widehat{F}((\theta,\varphi_1),...,(\theta,\varphi_m)) = \sum_{l=1}^{r}\prod_{i=1}^{m} G_i^l((\theta,\varphi_i)), \tag{201}$$

where G_i^l are suitable functions. We shall call call r *separation rank*. In the statistics literature, representations of the form (201) are known as *parallel factorizations* or *canonical decompositions* (see [91, 96]). They are also related to multipartite generalizations of the classical Schmidt decomposition often used in quantum field theory [24]. Although there are at present no useful theorems on the size of the separation rank r needed to represent with accuracy general classes of functionals $\widehat{F}$, there are cases where the expansion (201) is *exponentially more efficient* than one would expect a priori. Perhaps the simplest example in which this happens is the functional (68), here rewritten for convenience

$$F([\theta]) = \sin\left(\int_a^b K(x)\theta(x)dx\right). \tag{202}$$

Assuming that the kernel $K(x)$ admits the finite-dimensional expansion

$$K(x) = \sum_{j=1}^{m} k_j\varphi_j(x) \tag{203}$$

and substituting it into (202) we obtain

$$\widehat{F}([\theta]) = \sin\left(\sum_{j=1}^{m} k_j(\theta,\varphi_j)\right) = \sum_{j=1}^{m}\sin(k_j(\theta,\varphi_j))\prod_{\substack{i=1\\ i\neq j}}^{m}\frac{\sin(k_i(\theta,\varphi_i)+\chi_i-\chi_j)}{\sin(\chi_i-\chi_j)}, \tag{204}$$

for all χ_i such that $\chi_i \neq \chi_j$. The last equality, derived in [114], shows that the separation rank of (202)-(203) is $r = m$, i.e., that we can represent $\widehat{F}([\theta])$ exactly in terms of a separated series with m terms. Furthermore, if we allow the functionals $G_i^l((\theta,\varphi_i))$ to be complex[16]. then

$$\sin\left(\sum_{j=1}^{m} k_j(\theta,\varphi_j)\right) = \prod_{j=1}^{m}\frac{e^{ik_j(\theta,\varphi_j)}}{2i} - \prod_{j=1}^{m}\frac{e^{-ik_j(\theta,\varphi_j)}}{2i}, \tag{205}$$

i.e., we can reduce the separation rank to $r = 2$. More generally, the separation rank depends on the complexity of the functional. As in the HDMR method, the separated series expansion (201) can be determined by using different methods, e.g., interpolation, projection operators, or least squares. If the dependence on the free parameters of the expansion is linear, e.g., if $G_i^l((\theta,\varphi_i))$ is of the form

$$G_i^l((\theta,\varphi_i)) = \sum_{k=1}^{P}\beta_{ik}^l\phi_k((\theta,\varphi_i)) \tag{206}$$

(ϕ_k are known basis functions), then these methods reduce to *solving linear systems* (see [16, 36, 38]). Furthermore, the computation of functional approximant $\widehat{F}$ is usually collapsed into small subproblems that are solved iteratively by using alternating direction (ADI) algorithms.

[16]Constraints on the functions G_i^l such as positivity can be also imposed, e.g., if one is interested in probability functionals.

4.3.3 The Distance Between two Functionals

The computation of SSE and HDMR representations relies on an appropriate definition of a distance between two functionals. In a collocation setting, such distance (norm) can be defined as

$$\left\| F([\theta]) - \widehat{F}([\theta]) \right\|_D^2 = \sum_{j=1}^{N} \left(F([\theta_j^*(x)]) - \widehat{F}([\theta_j^*(x)]) \right)^2 w_j, \tag{207}$$

where $\{\theta_1^*, ..., \theta_N^*\}$ are collocation nodes in $D(F)$ and the weights w_j are positive numbers. To compute the norm $\| \cdot \|_D$ we could sample $\theta(x)$ at random and then evaluate (207) with $w_j = 1/N$. In this case, we are basically performing a Monte Carlo estimate of the distance between the two functionals F and $\hat{F}$ relative to a specific ensemble of nodes (paths) in the function space $D(F)$. The definition (207) represents a discretized version of the continuum norm (functional integral)

$$\left\| F([\theta]) - \widehat{F}([\theta]) \right\|_W^2 = \int \left(F([\theta]) - \widehat{F}([\theta]) \right)^2 W([\theta]) \mathcal{D}[\theta], \tag{208}$$

where $W([\theta]) > 0$ is a functional weight. In fact, by replacing $(F([\theta]) - \widehat{F}([\theta]))^2$ in (208) with the Lagrangian interpolant (see Section 4.2.2)

$$\Pi_N \left([\theta_k^*] \right) = \sum_{k=1}^{N} \left(F([\theta_k^*]) - \widehat{F}([\theta_k^*]) \right) g_k([\theta]) \tag{209}$$

we obtain (207), where the weights w_k are

$$w_k = \int g_k([\theta]) W([\theta]) \mathcal{D}[\theta]. \tag{210}$$

The norms (207) and (208) can be induced by functional inner products

$$(F, G)_D^* = \sum_{i=1}^{N} F([\theta_i^*]) G([\theta_i^*]) w_i, \tag{211}$$

$$(F, G)_W^* = \int F([\theta]) G([\theta]) W([\theta]) \mathcal{D}[\theta]. \tag{212}$$

We recall that depending on the way we discretize the set of functions $\theta(x)$ we can have different representations of the functional integral measure $\mathcal{D}[\theta]$ (see Appendix C). For instance, if we use a collocation representation of $\theta(x)$, then of course the independent variables are $\theta(x_j)$, i.e., the function values at the nodes x_j, and we formally have

$$\mathcal{D}[\theta] = \lim_{n \to \infty} \prod_{j=1}^{n} d\theta(x_j). \tag{213}$$

On the other hand, if we expand θ in a series

$$\theta(x) = \sum_{k=1}^{\infty} a_k \phi_j(x), \tag{214}$$

then the independent variables are the Fourier coefficients of the expansion and we have

$$\mathcal{D}[\theta] = \lim_{n \to \infty} \prod_{j=1}^{n} da_j. \tag{215}$$

4.3.4 Functional SSE: Alternating Least Squares Formulation

Let us consider the functional residual

$$R([\theta]) = F([\theta]) - \sum_{l=1}^{r} \prod_{k=1}^{m} G_k^l((\theta, \varphi_k)), \tag{216}$$

In the least squares formulation, we aim at computing the SSE expansion of F by minimizing the norm of $R([\theta])$ relative to variations of G_k^l. In particular, if we assume that G_k^l is in the form (206), then variations of G_k^l are represented by variations of β_{hj}^n. In other words, the separated series expansion is determined by the variational principle[17]

$$\min_{\beta_{hj}^n} \|R([\theta])\|_W^2 \tag{217}$$

The Euler-Lagrange equations of (217) yield a symmetric and positive definite system for β_{hj}^n. The dimension of such system is $m \times P \times r$, which may be very large. However, we can split (217) into a *sequence* of lower-dimensional optimization problems (alternating least-squares). For example, (217) can be iteratively minimized relative to

$$\{\beta_{1j}^1, ..., \beta_{Pj}^1, ..., \beta_{1j}^r, ..., \beta_{Pj}^r\} \qquad \text{(for fixed } j\text{)}. \tag{218}$$

This yields a sequence of m linear systems, each one of size $P \times r$, in the form

$$\sum_{l=1}^{r} \sum_{q=1}^{P} A_{jhp}^{ln} \beta_{jp}^l = f_{jh}^n \qquad \text{(fixed } j \text{ and } h\text{)}, \tag{219}$$

where

$$A_{jhp}^{ln} = \int \mathcal{D}[\theta] W([\theta]) \phi_h((\theta, \varphi_j)) \phi_p((\theta, \varphi_j)) \prod_{\substack{k=1 \\ k \neq j}}^{m} G_k^l((\theta, \varphi_k)) G_k^n((\theta, \varphi_k)), \tag{220}$$

$$f_{jh}^n = \int \mathcal{D}[\theta] W([\theta]) F([\theta]) \phi_h((\theta, \varphi_j)) \prod_{\substack{k=1 \\ k \neq j}}^{m} G_k^n((\theta, \varphi_k)). \tag{221}$$

As we will see in the subsequent Section, these functional integrals can be simplified and eventually computed by using techniques for high-dimensional integration, such as quasi-Monte Carlo [34].

Remark: Functional SSE with alternating least squares can be used to compute the solution to functional differential equations. In this case, the residual (216) and the stationary points of (217) depend on the specific equation (see Section 5).

Remark: In the context of approximation of functionals, minimizing the residual is equivalent to imposing orthogonality relative to a space spanned by suitable basis functions. To show this, let us consider a simple example in just two dimensions. Let $f(a_1, a_2)$ be a regular function defined on the unit square $[0, 1]^2$. We look for a separated representation of $f(a_1, a_2)$ in the form

$$\widehat{f}(a_1, a_2) = \sum_{j=1}^{r} G_1^j(a_1) G_2^j(a_2), \quad \text{where} \quad G_k^j(a_k) = \sum_{p=1}^{P} \beta_{kp}^j \phi_p(a_k). \tag{222}$$

[17] In (217) we can use either continuum or discrete norms (see (208) and (207)).

To determine β_{kp}^j we first define the residual,

$$R(a_1, a_2) = f(a_1, a_2) - \sum_{j=1}^{r} G_1^j(a_1) G_2^j(a_2) \tag{223}$$

and then minimize its weighed norm

$$(R, R)_W = \int_0^1 \int_0^1 R(a_1, a_2)^2 W(a_1, a_2) da_1 da_2 \tag{224}$$

relative to independent variations of β_{1p}^j and β_{2p}^j. This yields

$$\begin{cases} \Big(R, \phi_p(a_1) G_2^j(a_2)\Big)_W = 0 & \text{equations for } \beta_{1p}^j, \\ \Big(R, G_1^j(a_1) \phi_p(a_2)\Big)_W = 0 & \text{equations for } \beta_{2p}^j. \end{cases} \tag{225}$$

In this form it is clear that minimizing the residual with respect to independent variations of β_{1p}^j and β_{2p}^j is equivalent impose orthogonality relative to a space spanned by the basis functions $\phi_p(a_1) G_2^j(a_2)$ and $G_1^j(a_1)\phi_p(a_2)$, respectively.

4.3.5 Functional SSE - Alternating Galerkin Formulation

So far we discussed separated series expansions computed by alternating least-squares. In practice, we required that the residual (216) is minimal relative to variations of β_{jh}^n in (206). We also noticed that minimizing the residual is equivalent to imposing orthogonality relative to a space spanned by a suitable set of functions. In the context of SSE representations of functionals this yields the following alternating Galerkin formulation (m equations)

$$\begin{cases} \Big(R, \phi_p((\theta, \varphi_1)) G_2^j((\theta, \varphi_2)) \cdots G_m^j((\theta, \varphi_m))\Big)_W^* &= 0, \\ \Big(R, G_1^j((\theta, \varphi_1)) \phi_p((\theta, \varphi_2)) \cdots G_m^j((\theta, \varphi_m))\Big)_W^* &= 0, \\ \vdots & \\ \Big(R, G_1^j((\theta, \varphi_1)) G_2^j((\theta, \varphi_2)) \cdots \phi_p((\theta, \varphi_m))\Big)_W^* &= 0. \end{cases} \tag{226}$$

Remark: As before, $R([\theta])$ could be either the residual (216) or, more generally, the residual arising from a discretization of a functional differential equation (see Section 5).

The Method of Hierarchical Bases Among different methods to compute the functional integrals in (226), let us consider the one that discretizes the space of functions $D(F)$ in terms of the span of the finite-dimensional orthonormal basis $\{\varphi_1, ..., \varphi_N\}$ (see Appendix C.1). In other words, let us expand the test function $\theta(x)$ relative to the very same orthonormal basis we use to define the cylindrical set (187), i.e.

$$\theta(x) = \sum_{k=1}^{N} a_k \varphi_k(x) \quad \text{where} \quad |a_k| \leq b \quad (b \text{ finite})^{18}. \tag{227}$$

[18] In this setting, $\theta(x)$ is bounded, i.e., there exists c such that $\sup_x |\theta(x)| \leq c$.

The basis functions appearing in (187) and (227) then are *hierarchical*, in the sense that for $N \geq m$ we obviously have

$$\{\varphi_1, ...\varphi_m\} \subseteq \{\varphi_1, ...\varphi_N\}. \tag{228}$$

This allows us to simply the functional integrals (220) and (221) significantly. In particular, assuming that $W([\theta]) = 1$, we obtain

$$A^{ln}_{jph} = (2b)^{N-m} \int_{-b}^{b} \phi_h(a_j)\phi_p(a_j)da_j \prod_{\substack{k=1 \\ k\neq j}}^{m} \int_{-b}^{b} G^l_k(a_k)G^n_k(a_k)da_k, \tag{229}$$

$$f^n_{jh} = \int_{[-b,b]^m} \overline{F(a_1, ..., a_m)}\phi_h(a_j) \prod_{\substack{k=1 \\ k\neq j}}^{m} G^n_k(a_k)da_1 \cdots da_m, \tag{230}$$

where

$$\overline{F(a_1, ..., a_m)} = \int_{[-b,b]^{N-m}} F(a_1, ..., a_N)da_{m+1} \cdots da_N. \tag{231}$$

Furthermore, if we select the basis functions $\phi_p(a_j)$ to be orthogonal[19] in $[-b, b]$, i.e.,

$$\int_{-b}^{b} \phi_h(a)\phi_k da = \delta_{hk}\eta_h \qquad \eta_h = \|\phi_h\|^2 \tag{232}$$

then (219) simplifies to a block-diagonal linear system in the form

$$\sum_{l=1}^{r} L^{ln}_j \beta^l_{jh} = \frac{1}{\eta_h} f^n_{jh} \qquad \text{(fixed } j\text{)}, \tag{233}$$

where f^n_{jh} is given in (230) and

$$L^{ln}_j = \prod_{\substack{k=1 \\ k\neq j}}^{m} \sum_{q=1}^{P} \beta^l_{kq}\beta^n_{kq}\eta_q. \tag{234}$$

The integral (230) has to be evaluated numerically, e.g., by sparse collocation [128, 120] or quasi-Monte Carlo methods [34].

Remark According to equation (230), the SSE representation of a functional $F([\theta])$ on a cylindrical set of dimension m (see (187)) becomes a *mean field theory* in which we basically decompose the phase-space average of $F([\theta])$.

Remark The accuracy of the separated series expansion is bounded from below by the accuracy by which we can compute the functional integrals (230).

Choice of The Basis Functions The basis functions ϕ_k appearing in (206) represent the variability of functional F along different directions in the test function space $D(F)$. As such, they have to satisfy the boundary conditions of F. For example, if F is defined on a hypercube $[-b, b]^N$ that is large enough to set zero (periodic) boundary conditions then we can use, e.g., rescaled trigonometric polynomials

$$\phi_k(a) = l_k\left(\pi\left(\frac{a}{b} + 1\right)\right) \qquad a \in [-b, b] \quad \text{(Fourier)}, \tag{235}$$

[19]Examples of such functions are the trigonometric polynomials and Legendre orthogonal polynomials in $[-b, b]$.

where

$$l_{k+1}(x) = \frac{1}{P}\frac{\sin\left(\frac{P}{2}(x-x_k)\right)}{\sin\left(\frac{x-x_k}{2}\right)}, \qquad x_k = \frac{2\pi}{P}k \qquad k = 0, ..., (P-1). \tag{236}$$

For more general boundary conditions we can use a polynomial basis, e.g., rescaled Legendre orthogonal polynomials

$$\phi_k(a) = L_k\left(\frac{a}{b}\right) \qquad a \in [-b, b] \quad \text{(Legendre)}, \tag{237}$$

where

$$\begin{aligned} L_0(x) &= 1, \\ L_1(x) &= x, \\ &\vdots \\ L_{n+1}(x) &= \frac{2n+1}{n+1}xL_n(x) - \frac{n}{n+1}L_{n-1}(x), \quad (n = 1, ..., P-1). \end{aligned}$$

The norm of (235) and (237) is easily obtained as

$$\eta_h = \frac{b}{\pi}\frac{2\pi}{P} \quad \text{(Fourier)} \qquad \eta_h = \frac{2b}{2h+1} \quad \text{(Legendre)} \tag{238}$$

These quantities appear in equations (233) and (234).

Choice of the Number of Active Dimensions The choice of the basis functions φ_k and the number of active dimensions, i.e., the parameter m in (201), is *critical* for the accuracy of the SSE representation. Smaller values of m yield faster computations but at the same time can lead to *ill-posed approximation problems*. For example, consider the residual

$$\|R([\theta])\|^2 = \int \mathcal{D}[\theta]\left(F([\theta]) - \sum_{l=1}^{r}\prod_{k=1}^{m} G_k^l((\theta, \varphi_k))\right)^2. \tag{239}$$

Does the SSE expansion converge to $F([\theta])$ as we increase r for fixed m? Clearly, the answer depends on the functional $F([\theta])$, but in general we can say that if m is not large enough then we may have accuracy problems, no matter how much we push the separation rank r or the expansion order P. In fact, there exist a non-zero lower bound for $\|R([\theta])\|^2$ that depends only on m. The reason for such lower bound can be easily understood with the following simple example. Suppose we are interested in approximating a 3D function $f(a_1, a_2, a_3)$ in $[-1, 1]^3$ by a 2D separated series expansion. The residual we aim at minimizing is

$$\int_0^1\int_0^1\int_0^1\left(f(a_1, a_2, a_3) - \sum_{l=1}^{r} G_1^l(a_1)G_2^l(a_2)\right)^2 da_1 da_2 da_3. \tag{240}$$

Clearly this can be done to some extent if and only if the dependence of f on x_3 is not significant. The same is true in the functional approximation setting. Consider, as an example, a fourth-order homogeneous polynomial functional

$$F([\theta]) = \sum_{i,j,k,p=1}^{\infty} a_{ijkp}(\theta, \varphi_i)(\theta, \varphi_j)(\theta, \varphi_k)(\theta, \varphi_p) \tag{241}$$

where a_{ijkp} are the Fourier coefficients arising from the fourth-order kernel expansion. A functional SSE approximation with $m = 2$ in this case would work only under very particular circumstances, e.g., when $a_{ijkp} \simeq c_{ij}d_{kp}$ and both c_{ij} and d_{ij} decay sufficiently fast with both i and j. In such case, there is some hope to make the norm of the residual (239) smaller by increasing r or P.

Remark: A procedure to identify the set of active subspaces within the domain of a nonlinear functional is still lacking, although methods for finite-dimensional systems could be eventually applied [31].

4.3.6 Functional Derivatives of SSE

Consider the following approximation of a functional $F([\theta])$ on the cylindrical set $\{(\theta, \varphi_1), ..., (\theta, \varphi_m)\}$

$$F([\theta]) \simeq \widehat{F}((\theta, \varphi_1), ..., (\theta, \varphi_m)). \tag{242}$$

By evaluating the Gâteaux differential of $\widehat{F}$ at $\theta(x)$ in the direction of an arbitrary function $\eta(x)$ we obtain

$$\int_a^b \frac{\delta \widehat{F}}{\delta \theta(x)} \eta(x) dx = \frac{d}{d\epsilon} \left[\widehat{F}((\theta + \epsilon\eta, \varphi_1), ..., (\theta + \epsilon\eta, \varphi_m)) \right]_{\epsilon=0} \tag{243}$$

$$= \sum_{k=1}^{m} \frac{\partial \widehat{F}}{\partial a_k} (\eta, \varphi_k), \tag{244}$$

where $a_k = (\theta, \varphi_k)$. Setting $\eta(x) = \delta(x - y)$ yields the following expression for the functional derivative

$$\frac{\delta \widehat{F}}{\delta \theta(y)} = \sum_{k=1}^{m} \frac{\partial \widehat{F}}{\partial a_k} \varphi_k(y). \tag{245}$$

On the other hand, by projecting (245) onto φ_j we obtain

$$\int_a^b \frac{\delta F}{\delta \theta(x)} \varphi_j(x) dx = \frac{\partial \widehat{F}}{\partial a_j}, \tag{246}$$

i.e. the partial derivative of $\widehat{F}$ relative to $a_k = (\theta, \varphi_k)$ is the projection of the functional derivative of F along φ_k. Equations (245) and (246) are consistent with previous results on functional derivatives in finite-dimensional spaces (see Eqs. (71) and (72)). By following the same procedure, we can construct functional derivatives of $\widehat{F}$ of higher-order, e.g.,

$$\frac{\delta^2 \widehat{F}}{\delta \theta(x) \delta \theta(y)} = \sum_{k,j=1}^{m} \frac{\partial^2 \widehat{F}}{\partial a_k \partial a_j} \varphi_k(x) \varphi_j(y), \tag{247}$$

$$\frac{\delta^3 \widehat{F}}{\delta \theta(x) \delta \theta(y) \delta \theta(z)} = \sum_{k,j,i=1}^{m} \frac{\partial^3 \widehat{F}}{\partial a_k \partial a_j \partial a_i} \varphi_k(x) \varphi_j(y) \varphi_i(z). \tag{248}$$

To compute (245), (247) and (248) we first need to partially differentiate $\widehat{F}$ relative to different arguments $a_k = (\theta, \varphi_k)$, and subsequently evaluate the partial derivatives at (θ, φ_k). By using (201) we have

$$\frac{\partial \widehat{F}}{\partial a_i} = \sum_{l=1}^{r} \frac{\partial G_i^l}{\partial a_i} \prod_{k=1//k\neq i}^{m} G_k^l(a_k), \tag{249}$$

$$\frac{\partial \widehat{F}}{\partial a_i \partial a_j} = \begin{cases} \displaystyle\sum_{l=1}^{r} \frac{\partial^2 G_i^l}{\partial a_i^2} \prod_{\substack{k=1 \\ k\neq i}}^{m} G_k^l(a_k) & i = j, \\ \displaystyle\sum_{l=1}^{r} \frac{\partial G_i^l}{\partial a_i} \frac{\partial G_j^l}{\partial a_j} \prod_{\substack{k=1 \\ k\neq i,j}}^{m} G_k^l(a_k) & i \neq j. \end{cases} \tag{250}$$

Note that for each selected test function $\theta(x)$ we have that $\partial \widehat{F}/\partial a_j$, $\partial^2 \widehat{F}/\partial a_j \partial a_j$, etc., are numbers, i.e., the Fourier coefficients of the series expansion of the functional derivatives (245), (247) and (248).

Regularity of Functional Derivatives It easy to show that functional derivatives of nonlinear functionals can easily be *singular*, e.g., defined in terms of Dirac delta functions. For example, let $h \in C^\infty(\mathbb{R})$. Then any functional in the form $F([\theta]) = h((\theta,\theta))$ has a singular second-order functional derivative. In fact,

$$\frac{\delta F([\theta])}{\delta \theta(x)} = 2 \left.\frac{\partial h}{\partial a}\right|_{a=(\theta,\theta)} \theta(x) \tag{251}$$

$$\frac{\delta^2 F([\theta])}{\delta \theta(x) \delta \theta(y)} = 2\delta(x-y) \left.\frac{\partial h}{\partial a}\right|_{a=(\theta,\theta)} + 4 \left.\frac{\partial^2 h}{\partial a^2}\right|_{a=(\theta,\theta)} \theta(x)\theta(y). \tag{252}$$

The Gaussian functional

$$F([\theta]) = e^{-(\theta,\theta)} \tag{253}$$

belongs to this class, i.e., it has a singular second-order functional derivative. On the other hand, the functional

$$G([\theta]) = h\left(\int K(x)\theta(x)dx\right) \tag{254}$$

where $K_1(x) \in C^\infty$ is a given kernel, has smooth functional derivatives

$$\frac{\delta G[\theta]}{\delta \theta(x)} = \left.\frac{\partial h}{\partial x}\right|_{x=(K,\theta)} K(x), \tag{255}$$

$$\frac{\delta^2 G[\theta]}{\delta \theta(x) \delta \theta(y)} = \left.\frac{\partial^2 h}{\partial x^2}\right|_{x=(K,\theta)} K(x)K(y). \tag{256}$$

The fact that the functional derivatives of F can be singular poses serious challenges when approximating them numerically. In particular, it is very hard to obtain an approximation of the second-order functional derivative of $h((\theta,\theta))$ by using, e.g., a finite-dimensional set of trigonometric polynomials φ_k.

4.4 Generalized Lagrangian Interpolation

We have seen that the classical Lagrange interpolation problem for multivariate functions can be generalized to functionals in Hilbert or Banach spaces, i.e., objects depending on an infinite number of variables. Given a real-valued continuous functional

$$F : D(F) \to \mathbb{R}, \tag{257}$$

and a set of elements $\{\theta_1(x), ..., \theta_n(x)\}$ in $D(F)$, the Lagrangian interpolant of F is a continuous functional

$$\Pi : D(F) \to \mathbb{R}, \tag{258}$$

such that

$$\Pi([\theta_i]) = F([\theta_i]). \tag{259}$$

A simple representation of $\Pi([\theta])$ can be given in terms of *cardinal basis functionals* $g_i : D(F) \to \mathbb{R}$ as

$$\Pi([\theta]) = \sum_{i=1}^{n} F([\theta_i]) g_i([\theta]), \quad \text{where} \quad g_i([\theta_j]) = \delta_{ij}. \tag{260}$$

Similarly to classical Lagrange interpolation for functions from $\mathbb{R}^n$ to $\mathbb{R}^m$, we have a great freedom in selecting $g_i([\theta])$. We have already seen, for example, Porter's and Prenter's cardinal bases defined in equation (123) and equation (160), respectively. Now, let

$$\kappa : D(F) \times D(F) \to \mathbb{R} \tag{261}$$

be any continuous (not necessarily symmetric) functional subject to the sole requirement that

$$\kappa([\theta], [\eta]) = 0 \quad \Leftrightarrow \quad \theta(x) = \eta(x). \tag{262}$$

Examples of such functional are

$$\kappa_1([\theta], [\eta]) = \|\theta(x) - \eta(x)\|^p, \qquad p > 0 \tag{263}$$

$$\kappa_2([\theta], [\eta]) = \|\theta(x) - \eta(x)\| + \|\theta(x)\| - \|\eta(x)\| \tag{264}$$

$$\kappa_3([\theta], [\eta]) = 1 - \exp\left(-\|\theta(x) - \eta(x)\|^2\right). \tag{265}$$

By using $\kappa([\theta], [\eta])$ we can define the following cardinal basis associated with the elements $\{\theta_1(x), ..., \theta_n(x)\}$ in $D(F)$ (see [27], Ch. 10)

$$g_i([\theta]) = \prod_{\substack{j=1 \\ j \neq i}}^{n} \frac{\kappa([\theta], [\theta_j])}{\kappa([\theta_i], [\theta_j])} \qquad i = 1, ..., n. \tag{266}$$

Equation (260) and (266) define a *generalized Lagrangian interpolant* that depends on the choice of $\kappa([\theta], [\eta])$. An advantage of such interpolant over Porter's method is that the basis functionals (266) are given analytically and do not require any precomputation such as the inversion (and storage) of the H-matrix (121). On the other hand, we have no guarantee that (266) have good approximation properties, while in the case of Porter's polynomials we know that they are of minimal norm. The Lagrange interpolation formula (260)-(266) can be written in a *barycentric form*. To this end, we first rewrite the numerator of (266) as

$$\Omega([\theta]) = \prod_{i=k}^{n} \kappa([\theta], [\theta_k]) \tag{267}$$

divided by $\kappa([\theta], [\theta_i])$. Then define the *barycentric weights*

$$w_i = \prod_{\substack{j=1 \\ j \neq i}}^{n} \frac{1}{\kappa([\theta_i], [\theta_j])}. \tag{268}$$

Clearly,

$$g_i([\theta]) = \Omega([\theta]) \frac{w_i}{\kappa([\theta], [\theta_i])}. \tag{269}$$

Substituting this expression into (260) and applying it to the constant functional $F([\theta]) = 1$ yields

$$\Omega([\theta]) = \frac{1}{\sum_{i=1}^{n} \frac{w_i}{\kappa([\theta], [\theta_i])}}. \tag{270}$$

Therefore,

$$\Pi([\theta]) = \left(\sum_{i=1}^{n} \frac{w_i}{\kappa([\theta],[\theta_i])} \right)^{-1} \sum_{i=1}^{n} \frac{w_i F([\theta_i])}{\kappa([\theta],[\theta_i])} \qquad \text{(barycentric formula).} \tag{271}$$

This expression can be evaluated in $\mathcal{O}(n)$ operations, provided we have available w_i, which needs $\mathcal{O}(n^2)$ operations. What about updating? Adding a new interpolation node θ_{n+1} entails two calculations: 1) divide each w_j by $\kappa([\theta_j],[\theta_{n+1}])$ and 2) compute w_{n+1} using the formula (268).

Remark: The interpolation processes defined by (260) and (266) has a variation known as Shepard's method [48, 94]. Such method was studied by Allasia and Bracco [3] for functional interpolation in Banach spaces and it relies on the cardinal basis

$$g_i([\theta]) = \frac{1}{1 + \sum\limits_{\substack{k=1 \\ k \neq i}}^{n} \dfrac{\kappa([\theta],[\theta_i])}{\kappa([\theta],[\theta_k])}}, \qquad i = 1, ..., n. \tag{272}$$

The kernel $\kappa([\theta],[\eta])$ here satisfies (262) and the additional positivity requirement

$$\kappa([\theta],[\eta]) > 0 \qquad \text{if} \qquad \theta(x) \neq \eta(x), \tag{273}$$

(see e.g., the kernel (263)). This implies that the basis functionals (272) have the following properties

$$0 \leq g_i([\theta]) \leq 1 \quad \forall \theta \qquad g_i([\theta_j]) = \delta_{ij}. \tag{274}$$

One unfortunate consequence of these conditions is that the functional derivative of $g_i([\theta])$ (if it exists) is identically zero at all nodes θ_j. In fact, $g_i([\theta])$ is always positive, it has a maximum (equal to 1) at θ_i and many minima (equal to 0) at all other nodes. This is bad news when computing functional differentiation matrices (see equation (130)), as such matrices will be be identically zero in this case. Functional Lagrangian interpolation can also be defined in terms of *radial basis functionals* $\kappa(\|\theta - \theta_j\|)$, for suitable choices of κ. In this cases, the cardinal basis $g_i([\theta])$ can be obtained by standard techniques such as the ratio of two Vandermonde determinants. Interpolation using radial basis functionals can converge towards polynomial functional interpolants if we take increasingly flat radial bases (see, e.g., [158, 40, 163]).

The Lagrangian interpolation process defined by (260), (262) and (266) can be generalized further by considering a family of continuous functionals

$$\kappa_i : D(F) \times D(F) \to \mathbb{R}, \tag{275}$$

as many as the number of interpolation nodes, satisfying $\kappa_i([\theta],[\theta_j]) \neq 0$ for $i \neq j$, $\kappa_i([\theta],[\theta_i]) = 0$ and $\kappa_i([\theta],[\theta]) = 0$. The cardinal basis corresponding to $\{\kappa_1, ..., \kappa_n\}$ is

$$g_i([\theta]) = \prod_{\substack{j=1 \\ j \neq i}}^{n} \frac{\kappa_i([\theta],[\theta_j])}{\kappa_i([\theta_i],[\theta_j])}. \tag{276}$$

In particular, the choice

$$\kappa_i([\theta],[\eta]) = (\theta - \eta, \theta_i - \eta) \tag{277}$$

yields Prenter's cardinal basis (160). It fact,

$$\kappa_i([\theta],[\theta_j]) = (\theta - \theta_j, \theta_i - \theta_j), \tag{278}$$

$$\kappa_i([\theta_i],[\theta_j]) = \|\theta_i - \theta_j\|^2, \tag{279}$$

$$\kappa_i([\theta],[\theta_i]) = 0. \tag{280}$$

Another generalization of the Lagrange interpolation process can be obtained along the lines of Porter's functional interpolants. To this end, let $\kappa([\theta],[\eta])$ be any symmetric functional such that the matrix

$$H_{ij} = \kappa([\theta_i],[\theta_j]) \tag{281}$$

is invertible for every set of distinct nodes $\{\theta_j(x)\}$. Then the functional

$$\Phi_n([\theta]) = \sum_{k=1}^{m} F(\theta_k) \underbrace{\sum_{j=1}^{m} \kappa([\theta_k],[\theta_j])^{-1} \kappa([\theta],[\theta_j])}_{g_k([\theta])}, \tag{282}$$

where $\kappa([\theta_k],[\theta_j])^{-1}$ denotes the inverse matrix of (281), interpolates $F([\theta])$ at $\theta_k(x)$ $(k = 1, ..., m)$. The question of how to select the symmetric functional κ depends on the requirements we impose on the behavior of the function away from the interpolation nodes. In particular, the choice

$$\kappa([\theta],[\eta]) = \sum_{p=0}^{n} (\theta, \eta)^p \tag{283}$$

yields Porter's interpolants, i.e., polynomial functionals of order n with minimal norm.

4.4.1 Optimal Interpolation Nodes

In this Section we briefly address the question of how to select the interpolation nodes in the function space $D(F)$ in such a way that the corresponding functional interpolant, e.g., the Porter one (122)-(123), exhibits good approximation properties.

Adaptive Leja Sequences An effective approach to select sub-optimal interpolation nodes relies on adaptive Leja sequences [120, 19]. In this setting, given the set of nodes $\{\theta_1(x), ..., \theta_n(x)\}$ in $D(F)$, the problem of finding the new node $\theta^*(x)$ is reduced to the problem of computing

$$\arg\max_{\{\theta^*(x)\}} |\det(V)| \tag{284}$$

where V is a Vandermonde-like operator (infinite-dimensional matrix) (see [19, 120, 122, 108] for details). This results in the so-called *Leja construction* of the test function $\theta^*(x)$, a greedy version of the well-known Fekete construction involving nonlinear optimization. There are also non-determinant versions of multivariate Leja interpolation nodes, which are related to *potential theory* [102, 72]. In this setting, given a symmetric functional $\kappa([\theta(x)],[\eta(x)])$ we can construct a *greedy κ-energy sequence* in which $\theta^*(x)$ is chosen to satisfy

$$\sum_{i=1}^{n} \kappa([\theta^*(x)],[\theta_i(x)]) = \arg\min_{\theta^* \in D(\Phi)} \sum_{i=1}^{n} \kappa([\theta^*(x)],[\theta_i(x)]), \tag{285}$$

assuming $\{\theta_1(x), ..., \theta_n(x)\}$ are available The element $\theta^*(x)$ obtained in this way is not unique. Also, depending on the choice of the kernel function $\kappa([\theta(x)], [\eta(x)])$, we can have different sets of nodes. A relevant kernel for the κ-energy sequence is the so-called *Riesz p-kernel*

$$\kappa_p([\theta(x)], [\eta(x)]) = \begin{cases} \dfrac{1}{\|\theta(x) - \eta(x)\|^p} & \text{if } p > 0 \\ -\ln(\|\theta(x) - \eta(x)\|) & \text{if } p = 0 \end{cases} \tag{286}$$

Such kernel avoids placing points too close to each other (the potential κ_p is rather large in such regions), while decreasing monotonically at larger distances. The asymptotic behavior of greedy κ-energy sequences has been studied theoretically by López-García and Saff [102], in a finite-dimensional setting.

Minimization of Lebesgue Functionals Another approach to determine sub-optimal nodes in the function space $D(F)$ relies on greedy algorithms minimizing *Lebesgue-like functionals*. This problem has been recently studied in a finite-dimensional setting by Narayan and Xiu [122, 121], Maday *et al.* [104, 105] and Van Barel *et. al* [8]. The basic idea is simple and can be generalized to the infinite-dimensional case. Suppose we have available $\{\theta_1(x), ..., \theta_n(x)\}$. We look for a new node $\theta^*(x)$ maximizing a suitable objective functional, e.g., related to the well-known Lebesgue function in finite-dimensional interpolation problems. In particular, following the weighed approach of Narayan and Xiu [122], we can look for a new node $\theta^*(x)$ satisfying the following (greedy) optimization problem

$$\underset{\theta^* \in D(F)}{\arg\max}\, \chi([\theta^*]), \qquad \chi([\theta]) = \omega([\theta])^2 \sum_{k=1}^{n} \frac{g_k([\theta])^2}{\omega([\theta_k])^2}, \tag{287}$$

where $\omega([\theta])$ is a positive functional and $g_i([\theta])$ is a cardinal basis. Other choices of $\chi([\theta])$ yield different sets of nodes. For example,

$$\chi([\theta]) = \omega([\theta]) \sum_{k=1}^{n} \frac{g_i([\theta])^2}{\omega([\theta_k])} \tag{288}$$

yields an infinite-dimensional extension of the Fejér points. The sequence of nodes $\theta_i(x)$ we obtain in this way *strongly depends on the initial set of nodes*, on the weight $\omega([\theta])$ and on the cardinal basis $\{g_i([\theta])\}$. Finding the maximum of (287) involves computing the solution to an optimization problem in infinite dimensions [12]. An equivalent formulation relies on Euler-Lagrange equations. Indeed, the stationary points of (287) are solutions to the Euler-Lagrange equation (functional differential equation)

$$\frac{\delta \chi([\theta])}{\delta \theta(x)} = 0. \tag{289}$$

Remark: The condition (289) can be written explicitly for Porter's interpolants. To this end, substitute (123) in (288) and set $\omega = 1$ to obtain

$$\chi([\theta]) = \sum_{k=1}^{n} \sum_{j,z=1}^{m} H_{jk}^{-1} H_{zk}^{-1} \sum_{p,q=0}^{h} (\theta_j, \theta)^p \, (\theta_z, \theta)^q \, . \tag{290}$$

This allows us to write explicitly the Euler-Lagrange equations identifying the stationary points of of $\chi([\theta])$, e.g., in the function space

$$D_N = \left\{ \theta(x) \in D(F) \;\middle|\; \theta(x) = \sum_{k=1}^{N} b_k \varphi_k(x) \right\}. \tag{291}$$

We emphasize that optimal sampling strategies in function spaces yielding functional interpolants with high accuracy have not been addressed.

Remark: In a one-dimensional setting, Gauss points yields quasi-optimal approximation properties [64] but they are not obtained through optimization, e.g., they do not maximize the Lebesgue constant. Similarly, sparse grid points [21] are not obtained through optimization. Maximizing the Lebesgue function (or any variant of it) is challenging even in low dimensions and when using greedy algorithms [120]. Attempting this maximization in an infinite number of dimensions (function spaces) is even more challenging (infinite-dimensional optimization). To overcome this problem, it would be incredibly useful to derive an equation that allows us to identify the interpolation nodes $\theta_k(x)$ directly, i.e., without getting involved in complex non-convex optimization problems in infinite dimensions. Such equation may be the Euler-Lagrange equation (289).

4.5 The Cluster Expansion

We have seen that restriction of the Hopf functional to the finite-dimensional space (56) (see Figure 2) yields the joint characteristic function

$$\phi(a_1, ..., a_N) = \left\langle e^{i(a_1 U_1(\omega) + \cdots + a_N U_N(\omega))} \right\rangle, \qquad U_k(\omega) = \int_a^b u(x;\omega)\varphi_k(x)dx. \tag{292}$$

To represent the high-dimensional function $\phi(a_1, ..., a_N)$ one could use techniques such as HDMR [99, 23], separated representations [38], or sparse grids [37, 127]. One of the problems with such techniques is that they do not preserve important properties of the characteristic function, e.g., $\phi(0, ..., 0) = 1$, and marginalization rules. However, in the case of (292), we do know the structure of multivariate function we are approximating. Therefore, we can use such structure to determine an expansion that preserves marginalization rules and other properties. To this end, let us first define the following reduced-order characteristic functions

$$\phi_n(a_n) = \left\langle e^{ia_n U_n(\omega)} \right\rangle, \tag{293}$$

$$\phi_{nm}(a_n, a_m) = \left\langle e^{ia_n U_n(\omega) + ia_m U_m(\omega)} \right\rangle \tag{294}$$

$$\phi_{nmk}(a_n, a_m, a_k) = \left\langle e^{ia_n U_n(\omega) + ia_m U_m(\omega) + ia_k U_k(\omega)} \right\rangle \tag{295}$$

$$\cdots$$

We clearly have

$$\phi_{nmk}(a_n, 0, 0) = \phi_{nm}(a_n, 0) = \phi_n(a_n), \qquad \text{(marginalization rule).} \tag{296}$$

By using well-known cumulant series representations [92], we expand the joint characteristic function (292) as

$$\left\langle \exp\left[i \sum_{j=1}^{N} a_j U_j(\omega) \right] \right\rangle = \exp\left[\sum_{\nu_1, ..., \nu_N = 0}^{\infty} \left\langle U_1^{\nu_1} \cdots U_N^{\nu_N} \right\rangle_c \prod_{k=1}^{N} \frac{(ia_k)^{\nu_k}}{\nu_k!} \right], \tag{297}$$

where the last summation is over ν_1, ..., ν_N excluding the case in which all indices are zero, i.e., excluding $\nu_1 = \cdots = \nu_N = 0$. The cumulants averages in (297) can be written in terms of moments of U_j. For example, we have

$$\begin{aligned}
\langle U_j \rangle_c &= \langle U_j \rangle \\
\langle U_j U_k \rangle_c &= \langle U_j U_k \rangle - \langle U_j \rangle \langle U_k \rangle \\
\langle U_j U_k U_m \rangle_c &= \langle U_j U_k U_m \rangle - \langle U_j \rangle \langle U_k U_m \rangle - \langle U_k \rangle \langle U_j U_m \rangle - \langle U_m \rangle \langle U_k U_j \rangle + 2 \langle U_j \rangle \langle U_k \rangle \langle U_m \rangle .
\end{aligned}$$

At this point, it is useful to write the (297) explicitly for simple cases, e.g., for (294) and (295). We have,

$$\phi_{nm}(a_n, a_m) = \phi_n(a_n)\phi_m(a_m) \exp\left[\sum_{j,k=1}^{\infty} \left\langle U_m^k U_n^j \right\rangle_c \frac{(ia_m)^k (ia_n)^j}{k!j!}\right] \quad \text{and} \tag{298}$$

$$\begin{aligned}\phi_{nmk}(a_n, a_m, a_k) =& \phi_n(a_n)\phi_m(a_m)\phi_k(a_k)\phi_{nm}(a_n, a_m)\phi_{mk}(a_m, a_k)\phi_{nk}(a_n, a_k)\times \\ & \exp\left[\sum_{j,z,q=1}^{\infty} \left\langle U_m^j U_n^z U_k^q \right\rangle_c \frac{(ia_m)^j (ia_n)^z (ia_k)^q}{j!z!q!}\right].\end{aligned} \tag{299}$$

By generalizing these results to N variables, we find the following *cluster expansion*

$$\begin{aligned}\phi(a_1, ..., a_N) = & \prod_{n=1}^{N} \phi_n(a_n) \prod_{n<m}^{N} \frac{\phi_{nm}(a_n, a_m)}{\phi_n(a_n)\phi_m(a_m)} \times \\ & \prod_{n<m<k}^{N} \frac{\phi_{nmk}(a_n, a_m, a_k)}{\phi_n(a_n)\phi_m(a_m)\phi_k(a_k)\phi_{nm}(a_n, a_m)\phi_{mk}(a_m, a_k)\phi_{nk}(a_n, a_k)} \times \cdots\end{aligned} \tag{300}$$

Any truncation of (300) to a certain order in the multi-point characteristic functions $\phi_{lmn\cdots}$ yields approximations[20]. In particular, the second-order truncation (Gaussian approximation)

$$\phi(a_1, ..., a_N) \simeq \prod_{n=1}^{N} \phi_n(a_n) \prod_{n<m}^{N} \frac{\phi_{nm}(a_n, a_m)}{\phi_n(a_n)\phi_m(a_m)} \tag{301}$$

involves $N(N-1)/2$ functions ϕ_{ln} (ϕ_l can be determined from ϕ_{lm}), and it has been extensively used. The main reason is that if U_1,..., U_N are jointly Gaussian, then (301) is exact (the nth-order cumulants of a multivariate Gaussian are zero if $n \geq 3$). We can establish an interesting connection between the networks of test functions we discussed in Section 4.2.1 and the truncation order in (300). In particular, based (100) the

Representation in $S_1^{(N)}$: The representation of the Hopf functional in $S_1^{(N)}$ (see Eq. (100)) is defined in terms of one-dimensional functions

$$\Phi([a_j \varphi_j(x)]), \qquad j = 1, ..., N. \tag{302}$$

The corresponding approximation takes the form

$$\Phi([a_1\varphi_1(x) + \cdots + a_N\varphi_N(x)]) \simeq \prod_{j=1}^{N} \Phi([a_j\varphi_j(x)]). \tag{303}$$

In statistical physics this is known as *mean-field approximation*, and it relies on a statistical independence hypothesis between the random variables $U_k(\omega)$ in (292).

[20]The rationale behind this approximation relies on the fact that the joint cumulants of U_k often decay with the order, and therefore the exponential function (see (299)) tends to 1 quickly.

Representation in $S_2^{(N)}$: The representation of the Hopf functional in $S_2^{(N)}$ involves two-dimensional functions in the form

$$\Phi([a_j\varphi_j(x) + a_k\varphi_k(x)]), \qquad k, j = 1, ..., N. \tag{304}$$

With this set we consider the second-order truncation of (300), i.e.,

$$\begin{aligned}\Phi([a_1\varphi_1(x) + \cdots + a_N\varphi_N(x)]) &\simeq \prod_{j=1}^{N} \Phi([a_j\varphi_j(x)]) \prod_{j<k}^{N} \frac{\Phi([a_j\varphi_j(x) + a_k\varphi_k(x)])}{\Phi([a_j\varphi_j(x)])\Phi([a_k\varphi_k(x)])} \\ &= \prod_{j<k}^{N} \Phi([a_j\varphi_j(x) + a_k\varphi_k(x)]) \prod_{j=1}^{N} \Phi([a_j\varphi_j(x)])^{2-N}. \end{aligned} \tag{305}$$

Clearly, the one-dimensional functions $\Phi([a_j\varphi_j(x)])$ can be obtained from (304) by setting $a_k = 0$.

4.6 Functional Approximation Based on Random Processes

So far we discussed representations of functionals in terms of polynomial interpolants, separated series expansions, and cluster expansions. The construction of such representations can be seen as an identification problem of a nonlinear operator, given a collection of input/output functions. In this Section we briefly discuss another way of constructing polynomial functional expansions of nonlinear functionals. The method, pioneered by N. Wiener [187], relies on stochastic processes. Suppose we are given an *infinite collection* of input-output signals in the form of a pair of stochastic processes $\{w(x;\omega), F([w(x;\omega)])\}$, where $w(x;\omega)$ has known statistical properties. Based on the statistical analysis of $\{w(x;\omega), F([w(x;\omega)])\}$, it is possible to determine a polynomial expansion of the functional $F([\theta])$.

The key point is that the stochastic signal $w(x;\omega)$ is somehow equivalent to an infinite collection of nodes $\theta_k(x)$ (either discretely or continuously indexed) whose span is hopefully sufficient to identify $F([\theta])$. The representation of such functional takes the general form (see [187, 159, 130, 44])

$$F([\theta]) = \sum_{k=0}^{\infty} G_k([\theta]), \tag{306}$$

where $G_k([\theta])$ $k = 0, 1, ...$ is a complete set of orthogonal polynomial functionals. Orthogonality here is relative to the probability measure $P[w]$ of the random process $w(x;\omega)$, i.e., relative to the inner product

$$(G_k([w]), G_j([w]))_{dP[w]} = \int_{\Omega} G_k([w])G_j([w])dP[w]. \tag{307}$$

For example, if $w(x;\omega)$ is Brownian motion, then G_k are Hermite polynomial functionals[21]. In this case, (306) is the well-known Wiener-Hermite expansion [187, 22].

[21] For example, the second-order Hermite functional is

$$G_2([w]) = \int_a^b \int_a^b K_2(x_1, x_2)dw(x_1;\omega)dw(x_2;\omega) - \int_a^b K_2(x_1, x_1)dx_1, \tag{308}$$

subject to the normalization condition (see [187], p. 32)

$$\int K_2(x_1, x_2)^2 dx_1 dx_2 = \frac{1}{2}. \tag{309}$$

Note that if $w(x;\omega)$ is Brownian motion then the integral (308) does not exist in the ordinary Stieltjes sense because $w(x;\omega)$ is nowhere differentiable. However, we can interpret the derivative of $w(x;\omega)$ in a distributional sense to get a generalized process, the white noise. Wiener has shown that in such generalized setting, the integral (308) is perfectly well defined for kernel functions $K_2(x_1, x_2)$ in L_2. By using integration by parts we can also transform (308) into an integral involving kernel functions that could be *distributions*, e.g., Dirac deltas. A detailed mathematical analysis such transformation and other convergence results can be found in [133, 187].

The process of determining the kernels of $G_1([\theta])$, $G_2([\theta])$, etc., is known as *identification process* in the theory of nonlinear systems, and it has been extensively studied for obvious reasons (see [124, 155, 161]). By leveraging on the orthogonality of G_k relative to the inner product (307) one can show that (see, e.g., Eq. (4.4) in [187])

$$K_p(x_1,...,x_p) = \frac{1}{p!\epsilon^p}\left(F([w]), G_p(H_p,[w])\right)_{dP(w)}, \qquad H_p(z_1,...,z_p) = \begin{cases} 1 & x_i \le z_i \le x_i + \epsilon \\ 0 & \text{otherwise} \end{cases}. \quad (310)$$

This result relies on the fact that orthogonality of G_k and G_j in the sense of (307) is not dependent on the actual kernel functions appearing in G_k and G_j. In fact, if we consider the inner product of (306) with $G_p(H_p,[w])$ - arbitrary kernel $H_p(x_1,...,x_n)$ - then the only term that survives at the right hand side is $(G_p(K_p,[w])G_p(H_p,[w]))_{dP(w)}$. Such inner product can be written as

$$\left(G_p(K_p,[w])G_p(H_p,[w])\right)_{dP(w)} = p!\int_a^b \cdots \int_a^b K_p(x_1,...,x_p)H_p(x_1,...,x_p)dx_1\cdots dx_p, \quad (311)$$

i.e., all contributions of lower-order terms are identically zero. Thus, if we select H_p, properly (e.g., $H_p(x_1,...,x_p) = 1$ in a small hypercube centered at $(x_1,...,x_p)$ with side length ϵ and zero otherwise) then we can extract $K_p(x_1,...,x_p)$ as in equation (310).

This means that if we know the response $F([w])$ corresponding to the stochastic process $w(x;\omega)$, then we can identify the kernels (310) and therefore construct the corresponding polynomial functional expansion (306). The path integrals in (310) can be evaluated numerically, e.g., by using Monte-Carlo or quasi-Monte Carlo methods. To this end, suppose we have available a collection of N_s of response-excitation signals $\{w^{(i)}(x;\omega), F([w^{(i)}(x;\omega)])\}$ $(i = 1,...,N_s)$, where $w^{(i)}(x;\omega)$ is sampled according to the probability distribution $P[w]$. Then the Monte-Carlo estimate of the kernels (310) is simply

$$K_p(x_1,...,x_p) \simeq \frac{1}{p!\epsilon^p N}\sum_{i=1}^{N} F([\xi^{(i)}])G_k(H_p,[\xi^{(i)}]) \qquad p = 0,1,... \quad (312)$$

Here $\xi^{(i)}(x;\omega)$ is a realization of the distributional derivative of $w^{(i)}(x;\omega)$. In particular, if $w(x;\omega)$ is Brownian motion then $\xi(x;\omega)$ is *spatial white noise*[22]. In this case, we have that the first two functionals $G_1(H_1,[\xi])$ and $G_2(H_2,\xi)$ in (312) are given by

$$G_1(H_1,[\xi]) = \epsilon\xi(x_1;\omega),$$
$$G_2(H_2,[\xi]) = \epsilon^2\left(\xi(x_1;\omega)\xi(x_2;\omega) - 1\right),$$

[22] A simple numerical approximation of white noise $\xi(x;\omega) = dw(x;\omega)/dx$ can be obtained as

$$\xi_{\Delta x}(x;\omega) = \frac{w(x+\Delta x;\omega) - w(x;\omega)}{\Delta x}, \qquad (w \text{ Brownian motion}). \quad (313)$$

This is a Gaussian process with zero mean, variance $1/\Delta x$ and covariance

$$\langle \xi_{\Delta x}(x;\omega)\xi_{\Delta x}(y;\omega)\rangle = \begin{cases} \frac{1}{\Delta x}\left(1 - \frac{|x-y|}{\Delta x}\right) & \text{if } |x-y| \le \Delta x \\ 0 & \text{otherwise} \end{cases} \quad (314)$$

The Fourier transform of $\langle \xi_{\Delta x}(x;\omega)\xi_{\Delta x}(y;\omega)\rangle$ yields a power spectrum which is not flat as it is supposed to be for white noise, but decays at sufficiently large frequencies.

and therefore

$$K_1(x_1) \simeq \frac{1}{N}\sum_{i=1}^{N} F([\xi^{(i)}])h_1(\xi^{(i)}(x_1;\omega)), \tag{315}$$

$$K_2(x_1,x_2) \simeq \frac{1}{N}\sum_{i=1}^{N} F([\xi^{(i)}])h_2(\xi^{(i)}(x_1;\omega),\xi^{(i)}(x_2;\omega)). \tag{316}$$

Here $h_1(x_1) = x_1$ and $h_2(x_1,x_2) = (x_1x_2 - 1)/2$ are the classical first- and second-order Hermite polynomials. A very insightful discussion on how to obtain K_j by using white noise is given by Rugh in [155], §7.4. The expansion (306) obtained in this way can, in principle, be used to compute the value of the functional $F([\theta])$ corresponding to any deterministic function $\theta(x)$. However, since the kernels (310) are built upon stochastic processes and their averages, it is not clear in what sense (306) will converge for deterministic input functions $\theta(x)$. This question was addressed by Palm and Poggio in [133] (Theorems 4 and 5), where necessary and sufficient conditions for pointwise convergence of Wiener-Hermite expansions are provided. The functional expansion in terms of orthogonal polynomial functionals can be generalized to random processes other than Brownian motion and white noise[23]. However, one has to be very careful when performing such generalizations. There are indeed random excitation processes that do not allow for a complete representation of the functional $F([\theta])$ (see [44, 159, 130] for further details).

5 Approximation of Functional Differential Equations

A functional differential equation is an equation involving a nonlinear operator, i.e., a nonlinear functional defined on a suitable function space. Thus, the main goal of approximation theory for functional differential equations is to determine an approximation of such nonlinear operator, e.g., its time evolution given an initial state. This cannot be done analytically, except in very simple cases. In this manuscript we will be mostly concerned with linear equations[24] in the form

$$\frac{\partial F([\theta],t)}{\partial t} = L([\theta])F([\theta],t) + H([\theta],t) \qquad F([\theta],0) = F_0([\theta]), \tag{318}$$

where $F_0([\theta])$ is an initial condition, $H([\theta],t)$ is a known time-dependent forcing functional and $L([\theta])$ is a linear operator in the space of functionals $F([\theta],t)$. Depending on F_0, the solution to (318) can be either a linear or a nonlinear functional of $\theta(x)$, as shown in the following example.

Example: Consider the following instance of equation (318)

$$\frac{\partial F([\theta],t)}{\partial t} + \int_0^{2\pi} \theta(x)\frac{\partial}{\partial x}\frac{\delta F([\theta],t)}{\delta\theta(x)}dx = 0, \qquad F([\theta],0) = F_0([\theta]), \tag{319}$$

[23]The construction of such generalized expansion proceeds as follows. Starting from the constant functional F_0 we look for

$$F_1([w]) = C_1\int K_1(x)dw(x;\omega) + F_0, \tag{317}$$

where $w(x;\omega)$ is a generalized random process, and we make it orthogonal to F_0 in the sense of $dP[w(x;\omega)]$. This yields C_1. Then we construct $F_2([w])$ and we make it orthogonal to both $F_1([w])$ and F_0. All these conditions are ultimately expressed analytically in terms of multi-point averages of the random process $w(x;\omega)$.

[24]We have seen in Section 2 that in most applications of interest functional differential equations are linear, and they involves partial derivatives with respect to independent variables (e.g., space and time) as well as functional derivatives with respect to functions.

where $F_0([\theta])$ is the homogeneous functional

$$F_0([\theta]) = \int_0^{2\pi} K_0(x)\theta(x)dx, \qquad (K_0(x) \text{ is given}). \tag{320}$$

In this case, the solution to (319) is linear and homogeneous for all $t \geq 0$[25], i.e., it is in the form

$$F([\theta], t) = \int_0^{2\pi} R(x,t)\theta(x)dx, \qquad R(x,0) = K_0(x). \tag{322}$$

A substitution of (322) into (319) yields

$$\int_0^{2\pi} \theta(x) \left(\frac{\partial R(x,t)}{\partial t} + \frac{\partial R(x,t)}{\partial x} \right) dx = 0, \qquad \text{i.e.} \qquad \frac{\partial R(x,t)}{\partial t} + \frac{\partial R(x,t)}{\partial x} = 0. \tag{323}$$

Thus, (322) is a solution to (319)-(320) if $R(x,t)$ solves a simple linear advection equation on the real line, with initial condition $K_0(x)$. Now, if we let the initial condition $F_0([\theta])$ to be a nonlinear functional of θ, then things become a little bit more complicated. In particular, the evolution of $F([\theta], t)$ is nonlinear in $\theta(x)$. As an example, consider

$$F([\theta], t) = \left\langle \exp\left[i \int_0^{2\pi} S(x,t;\omega)\theta(x)dx \right] \right\rangle, \tag{324}$$

It can be shown that this is a solution to (319) if $S(x,t;\omega)$ satisfies the stochastic advection equation

$$\frac{\partial S(x,t;\omega)}{\partial t} + \frac{\partial S(x,t;\omega)}{\partial t} = 0, \qquad S(x,0;\omega) \quad \text{random}. \tag{325}$$

Thus, both (322) and (324) are solutions to (319) corresponding to different initial conditions. The first one is linear in $\theta(x)$, the second one is not.

On the Existence and Uniqueness of the Solution A fundamental question is whether such solutions are unique or not given the initial state $F_0([\theta])$. This is a mathematical analysis problem which we hope will be addressed systematically in the near future. At today, there are few general theorems on the existence and the uniqueness of solutions to linear functional differential equations (see, e.g., [50, 62, 188]).

Hereafter we describe different numerical methods to compute the solution to equations in the form (318) These methods, in some sense, provide new means for solving *infinite-dimensional systems of PDEs*, or *PDEs in an infinite number of variables*. We have seen, in fact, that a functional differential equation is equivalent to an infinite hierarchy of PDEs or a PDE in infinite dimensions. Classical approaches to solve these problems are based on mere truncations of PDE systems, power series expansions or cumulant series (see [69, 1, 116, 117, 54]). The approaches we propose hereafter are substantially different, and based mostly on the functional approximation methods we discussed in Section 4.

[25] To see this, it is sufficient to write the first-order Euler scheme

$$F([\theta], \Delta t) = F([\theta], 0) - \Delta t \int_0^{2\pi} \theta(x) \frac{\partial K(x,0)}{\partial x} dx. \tag{321}$$

and note that the term within the integral at the right hand side is a linear functional of θ. This implies that $F([\theta], \Delta t)$ is a linear functional of θ. By applying this argument over and over we see that $F([\theta], t)$ is a linear functional of θ for all $t \geq 0$.

5.1 The Method of Weighted Residuals

The method of weighted residuals illustrates how the choice of different weight (or test) functionals can be used to construct different classes of methods extending Galerkin, least-squares and collocation methods for PDEs to functional differential equations The general framework resembles the classical one for PDEs, in which one minimizes a residual (least-squares method) or imposes its orthogonality relative to a suitable space of test functions (Galerkin or collocation methods). To describe the weighted residuals technique, let us consider the linear functional differential equation (318). In approximating its solution numerically we are typically replacing an infinite expansion with a finite representation

$$\widehat{F}([\theta],t) = \sum_{k=1}^{m} f_k(t) g_k([\theta]), \tag{326}$$

where g_k are known basis functionals satisfying the boundary conditions of the problem. Substitution of the approximation (326) into equation (318) yields the (functional) residual

$$R([\theta],t) = \frac{\partial \widehat{F}([\theta],t)}{\partial t} - L([\theta])\widehat{F}([\theta],t) - H([\theta],t). \tag{327}$$

At this point, we introduce the following inner product in the space of functionals[26]

$$(F,G)^* = \int F([\theta])G([\theta])\mathcal{D}[\theta] \qquad \text{(functional integral)} \tag{328}$$

and consider the set of equations

$$(R([\theta],t), h_k([\theta]))^* = 0 \qquad k = 1, ..., m \tag{329}$$

where $h_k([\theta])$ are test functionals. The system (329) allows us to determine the unknowns $f_k(t)$ in the expansion (326) by imposing that the residual R is orthogonal to the span of the functionals $\{h_1, ..., h_n\}$. The nature of the numerical scheme is determined by the choice of the expansion functionals $g_k([\theta])$ in (326) and the test functionals $h_j([\theta])$ in (329).

5.1.1 Functional Collocation Methods

In this class of methods $g_k([\theta])$ is usually chosen to be a cardinal basis associated with a set of interpolation nodes $\{\theta_1(x), ..., \theta_m(x)\}$ in an appropriate function space $D(F)$. An example of such basis may be (123). On the other hand, the test functionals $h_j([\theta])$ are chosen to be Dirac delta functionals centered at $\theta_j(x)$, i.e., $h_j([\theta]) = \delta[\theta_j(x) - \theta(x)]$. In this setting, the orthogonality condition (329) can be explicitly written as

$$\int R([\theta],t)\delta[\theta_j(x) - \theta(x)]\mathcal{D}[\theta] = R([\theta_j],t) = 0 \tag{330}$$

In other words, in functional collocation methods we impose that the residual $R([\theta],t)$ vanishes at m collocation nodes in $D(F)$, i.e., $\{\theta_1(x), ..., \theta_m(x)\}$. This yields a system of m equations for the unknowns $\{f_1, ..., f_m\}$. If we represent $\theta(x)$ in terms of trigonometric polynomials (93)

$$\theta(x) = \sum_{k=1}^{P} a_k \varphi_k(x), \tag{331}$$

then $\theta_i(x)$ corresponds to a specific sample in the m-dimensional space $(a_1, ..., a_m)$, and $\widehat{F}$ is an interpolant of F at $\theta_i(x)$.

[26] A more general version of the inner product (328) involving a weight functional is defined in equation (212).

5.1.2 Functional Galerkin Methods

In this class of methods we impose that the residual $R([\theta],t)$ is orthogonal to the space spanned by the test functionals $h_j([\theta]) = g_j([\theta])$. There is no particular restriction on g_j. For example, they can be cardinal basis functionals, orthogonal polynomial functionals or other types of basis functionals. In any case, the set of equations (329) can be written explicitly as a system of functional integrals

$$\int R([\theta],t) g_k([\theta]) \mathcal{D}[\theta] = 0, \qquad k = 1, ..., m. \tag{332}$$

The evaluation of such functional integrals is notoriously difficult, but there are techniques available that allow us to compute them (see, e.g., Chapter 4 in [43]). Also, several algorithms have been recently proposed for high-dimensional (possibly infinite-dimensional) integration [7, 136, 185, 34, 33]. In the class of functional Galerkin methods we also find stochastic Galerkin methods. Essentially, these are based on stochastic representations of the solution functional (Section 4.6), and inner products involving probability measures. Stochastic Galerkin methods have been used in the theory of turbulence [111, 112, 95, 17].

5.1.3 Functional Least Squares

In this class of methods we look for an approximate solution functional that minimizes the norm of residual $R([\theta],t)$. Such norm may be defined in terms of the functional inner product (328), i.e., $\|R\|^2 = (R,R)^*$. In this case, we obtain the following variational principle involving a functional integral

$$\min_{\widehat{F} \in D_m(F)} \|R_n([\theta],t)\|^2 = \min_{\widehat{F} \in D_m(F)} \int R_n([\theta],t)^2 \mathcal{D}[\theta]. \tag{333}$$

The stationary points of (333) corresponding to variations of the degrees of freedom f_k in (326) satisfy the the Euler-Lagrange equations

$$\left(R([\theta],t), \frac{\partial R([\theta],t)}{\partial f_k} \right)^* = 0, \qquad k = 1, ..., m. \tag{334}$$

A comparison between (329) and (334) suggests that the test functionals $h_j([\theta])$ in this case are equation-dependent, i.e., they depend on the residual $R([\theta],t)$ through the formula

$$h_k([\theta],t) = \frac{\partial R([\theta],t)}{\partial f_k}. \tag{335}$$

Remark: Error analysis, stability and consistency of functional Galerkin, functional collocation and functional least squares methods is an open question.

5.1.4 An Example: The Hopf-Burgers Equation

Let us illustrate the weighted residual formulation with reference to a prototype functional equation, i.e., the Hopf characteristic functional equation corresponding to the Burgers equation

$$\frac{\partial u}{\partial t} + u \frac{\partial u}{\partial x} = \nu \frac{\partial^2 u}{\partial x^2} \tag{336}$$

with periodic boundary conditions in $[0, 2\pi]$, and random initial state $u_0(x;\omega)$. As is well-known, the probability distribution of $u_0(x;\omega)$ significantly influences the statistical properties of the solution to (336) at later times. For example, initial conditions defined by Gaussian processes [61, 86], white noise processes

[5, 51] and fractional Brownian motion [160] yield completely different statistics of $u(x,t;\omega)$. We have seen in Section 2.4 that the the full probabilistic structure of $u(x,t;\omega)$ can be described by the Hopf functional

$$\Phi([\theta(x)],t) = \left\langle \exp\left[i \int_0^{2\pi} u(x,t;\omega)\theta(x)dx \right] \right\rangle, \tag{337}$$

evolving according to the functional differential equation[27]

$$\frac{\partial \Phi}{\partial t} = \int_0^{2\pi} \theta(x) \left(\nu \frac{\partial^2}{\partial x^2} \frac{\delta \Phi}{\delta \theta(x)} + \frac{i}{2} \frac{\partial}{\partial x} \frac{\delta^2 \Phi}{\delta \theta(x)^2} \right) dx, \qquad \Phi([\theta(x)],0) = \Phi_0([\theta(x)]). \tag{338}$$

Very few attempts have been made to solve this equation numerically. Perhaps, one of the first study is the one of Hosokawa and Yamamoto [70], where the analytical solution to the Burgers equation was used to compute the Hopf characteristic functional for the case of Gaussian random initial conditions. In practice, the exact solution of the Burgers equation was simply substituted into the definition of the Hopf functional for the purpose of computing useful statistical quantities. No attempt has been made so far to solve (338) directly, e.g., based on functional collocation. Hereafter we derive such numerical scheme. The first step to approximate Φ by the series expansion

$$\widehat{\Phi}([\theta],t) = \sum_{k=1}^{m} f_k(t) g_k([\theta]). \tag{339}$$

Here $g_k([\theta])$ could be, for example, a *weighed* Porter's cardinal basis[28]. Substituting (339) into equation (338) yields the residual

$$R([\theta],t) = \sum_{k=1}^{m} \frac{df_k}{dt} g_k([\theta]) - \nu f_k \int_0^{2\pi} \theta(x) \frac{\partial^2}{\partial x^2} \frac{\delta g_k([\theta])}{\delta \theta(x)} dx - \frac{i}{2} f_k \int_0^{2\pi} \theta(x) \frac{\partial}{\partial x} \frac{\delta^2 g_k([\theta])}{\delta \theta(x)^2} dx. \tag{341}$$

In a functional collocation setting, we set such residual equal to zero at m collocation nodes in the domain of the functional Φ, for example the nodes we used to build the interpolant (339). By using the properties of the cardinal basis g_k, we obtain this system of equations

$$\frac{df_j}{dt} = \sum_{k=1}^{m} \nu f_k \int_0^{2\pi} \theta_j(x) \frac{\partial^2}{\partial x^2} \frac{\delta g_k([\theta_j])}{\delta \theta(x)} dx + \frac{i}{2} f_k \int_0^{2\pi} \theta_j(x) \frac{\partial}{\partial x} \frac{\delta^2 g_k([\theta_j])}{\delta \theta(x)^2} dx, \qquad j = 1, ..., m \tag{342}$$

The quantities $\delta g_k([\theta_j])/\delta\theta(x)$ and $\delta^2 g_k([\theta_j])/\delta\theta(x)^2$ are the functionals derivatives of $g_k([\theta])$ evaluated at $\theta_j(x)$. The system (342) is a linear system of ODEs for $f_k(t)$. Once its solution is available, we can substitute it into (339) to obtain an approximation of the Hopf functional (337).

5.2 Alternating Direction Algorithms

In this Section we address the problem of computing the solution to (318) by using alternating direction algorithms, in particular alternating least-squares and alternating Galerkin methods. These algorithms are based on the separated series representations we discussed in Section 4.3.2, and have significant advantages

[27] The boundary conditions for (338) can be set as $\Phi = 0$ for $\|\theta\| \to \infty$.

[28] A weighed Porter's basis can be defined by multiplying each functional $g_k([\theta])$ in (123) by a positive weight that vanishes at infinity, for instance

$$g_k([\theta]) = \exp\left[-\int_0^{2\pi} (\theta - \theta_k)^2 dx \right] \widetilde{g}_k([\theta]), \tag{340}$$

where $\widetilde{g}_k$ here is defined as in (123).

over other approaches in terms of computational cost. To describe the alternating direction algorithms we first consider the functional approximation (201), hereafter rewritten for convenience

$$\widehat{F}([\theta],t)=\sum_{k=1}^{r}\prod_{j=1}^{m}G_j^l((\theta,\varphi_j),t),\qquad G_j^l((\theta,\varphi_j),t)=\sum_{p=1}^{P}\beta_{jp}^l(t)\phi_p((\theta,\varphi_j)),\tag{343}$$

where $(,)$ here denotes an inner product in function space $D(F)$ and r is the separation rank[29]. The basis functions ϕ_p are chosen to satisfy the boundary conditions. The first-order functional derivative of (343) is

$$\begin{aligned}\frac{\delta\widehat{F}([\theta])}{\delta\theta(x)}&=\sum_{j=1}^{m}\frac{\partial\widehat{F}([\theta])}{\partial(\theta,\varphi_j)}\varphi_j(x)\\&=\sum_{j=1}^{m}\sum_{l=1}^{r}\frac{\partial G_j^l}{\partial(\theta,\varphi_j)}\prod_{\substack{k=1\\k\neq j}}^{m}G_k^l((\theta,\varphi_k))\varphi_j(x).\end{aligned}\tag{345}$$

These expressions allow us to write the residual (327) as a function of G_j^l, i.e., as a function of $\beta_{jp}^l(t)$. Next, we need a criterion to determine the unknowns $\beta_{jp}^l(t)$.

5.2.1 Alternating Least-Squares Method

In the alternating least-squares method, we look for a minimizer of (333) computed in a parsimonious way. The standard technique is to decompose the optimization problem into a sequence of sub-problems of smaller dimension, which are solved sequentially through iterative methods. Among different ways to perform such a decomposition, here we choose to update simultaneously the entire rank of coefficients corresponding to the variable $a_k=(\theta,\varphi_k)$. This guarantees that the error can never increase, although it is certainly possible to hit a local minimum. Taking a variation of (333) with respect to β_{qz}^n (for fixed q) yields the Euler-Lagrange equations

$$\left(R([\theta],t),\frac{\partial R([\theta],t)}{\partial\beta_{qz}^n}\right)^*=0,\qquad n=1,...,r,\quad z=1,...,P,\quad\text{and fixed } q.\tag{346}$$

The explicit form of the liner systems (346) is usually quite involved, depending on the specific form of the residual. A different (although related) method that yields simpler computations is the alternating Galerkin method described in the next Section.

5.2.2 Alternating Galerkin Method

In the alternating Galerkin method we impose that the residual (327) is orthogonal (in the sense of the functional inner product (328)) to the space spanned by the basis

$$\phi_h((\theta,\varphi_q))\prod_{p=1}^{m}G_p^n((\theta,\varphi_p),t),\tag{347}$$

[29] We could also expand the time dependence part of $F([\theta],t)$ in a Legendre-Gauss-Radau basis (see, e.g., [144]) to obtain

$$\widehat{F}([\theta],t)=\sum_{l=1}^{r}\psi^l(t)\prod_{j=1}^{m}G_j^l((\theta,\varphi_j)),\qquad G_j^l((\theta,\varphi),t)=\sum_{p=1}^{P}\beta_{jp}^l(t)\phi_p((\theta,\varphi_j)),\qquad\psi^l(t)=\sum_{q=1}^{Q}\gamma_q^l(t)L_q(t).\tag{344}$$

i.e., we set

$$\left(R([\theta],t), \phi_h((\theta,\varphi_q)) \prod_{p=1}^{m} G_p^n((\theta,\varphi_p),t) \right)^* = 0, \quad \text{for all} \quad t > 0. \tag{348}$$

Written in an expanded form this system takes the form

$$\begin{cases} \left(R([\theta],t), \phi_p((\theta,\varphi_1)) G_2^j((\theta,\varphi_2),t) \cdots G_m^j((\theta,\varphi_m),t) \right)^* &= 0 \\ \left(R([\theta],t), G_1^j((\theta,\varphi_1),t) \phi_p((\theta,\varphi_2)) \cdots G_m^j((\theta,\varphi_m),t) \right)^* &= 0 \\ \vdots & \\ \left(R([\theta],t), G_1^j((\theta,\varphi_1),t) G_2^j((\theta,\varphi_2),t) \cdots \phi_p((\theta,\varphi_m)) \right)^* &= 0 \end{cases} \tag{349}$$

where each equation is for $p = 1, ..., P$ and $j = 1, ..., r$. The solution strategy is as follows. We first initialize all coefficients $\beta_{jp}^n(t)$, e.g., by using the solution at the previous time step (or at the initial time). Then we solve the first equation for $\beta_{1p}^j(t)$ only, while keeping all other coefficients constants. At this point we update $\beta_{1p}^j(t)$ and solve second equation for β_{2p}^j, while keeping all other coefficients constants (with updated $\beta_{1p}^j(t)$). We repeat this procedure interatively until convergence. A thorough description of this algorithm together with numerical results will be given in Section 5.2.2 (see also Figure 25).

5.3 Finite Elements in Function Spaces

The great success of numerical methods for PDEs heavily relies on the fact that it is possible to approximate their solution *locally*, for example through local bases defined on a triangulation of the solution domain (e.g., hp-element methods [80]). Can we do the same for functional differential equations? Can we construct a set of local functional interpolants of reasonable order in $D(F)$ that allow us to compute accurate numerical solutions to functional differential equations? The main motivation is the same as in the finite-dimensional case, i.e., a large number of degrees of freedom can yield extreme sensitivity of globally defined interpolants to perturbations (see [85]). The first step in constructing local functional interpolants is to partition the function space $D(F)$ into subdomains, i.e., finite elements. Each subdomain is, in principle, a subset of a function space, and therefore an object in an infinite number of dimensions. The topological properties of such a decomposition, however, are not clear and certainly not trivial. For example, what is the geometry associated with finite element in function spaces? What's the metric? How do connect two different elements? Even in 4 dimensions (finite elements in general relativity) it is not trivial to set up connectivity rules between elements [60, 10]. Given a distribution of nodes θ_k in a function space one can attempt to construct a *Voronoi tessellation* and a low-order local polynomial functional approximation by sampling $F([\theta])$ close enough to each node θ_k. The evaluation of the approximated functional at θ^* is then preceded by a stage in which we need to identify the closest interpolation node θ_k to θ^* and eventually check if θ^* is close enough to θ_k. In this way, the local interpolants, however, will not be continuous across different elements. A possible strategy to enforce continuity of such functionals and their functional derivatives is to consider a weighted approach, in which local interpolants are multiplied by suitable weights chosen to enforce continuity (see [75] for the finite-dimensional case).

6 Numerical Results: Functionals

In this Section we provide numerical results and examples on functional approximation. In particular, we discuss polynomial functional interpolants, functional series expansions and cylindrical representations (SSE).

6.1 Linear functionals

Consider the linear functional

$$F([\theta]) = \int_0^{2\pi} K_1(x)\theta(x)dx \tag{350}$$

on the Hilbert space of square integrable periodic functions in $[0, 2\pi]$

$$D(F) = \{\theta \in L_2([0, 2\pi]) \,|\, \theta(0) = \theta(2\pi)\}. \tag{351}$$

Our aim is to represent $F([\theta])$ in terms of a functional interpolant in $D(F)$, i.e.,

$$F([\theta]) = \sum_{k=1}^{\infty} F([\theta_i])g_i([\theta]). \tag{352}$$

where $g_i([\theta])$ are cardinal basis functionals and $\theta_i(x)$ are interpolation nodes in $D(F)$. In particular, we choose $\theta_i(x) = \varphi_i(x)$ where $\{\varphi_1(x), \varphi_2(x), ...\}$ is an orthonormal basis in $D(F)$. Assuming that $K_1(x)$ is in $D(F)$, i.e.,

$$K_1(x) = \sum_{k=1}^{\infty} (K_1, \varphi_k)\varphi_k(x), \tag{353}$$

it follows from (350) that

$$\begin{aligned} F([\theta]) &= \sum_{k=1}^{\infty} (K_1, \varphi_k)(\varphi_k, \theta), \\ &= \sum_{k=1}^{\infty} F([\varphi_k])(\varphi_k, \theta). \end{aligned} \tag{354}$$

Therefore, we have obtained the following exact representation of the linear functional (350) in terms of cardinal basis functionals $g_k([\theta]) = (\varphi_k, \theta)$

$$F([\theta]) = \sum_{k=1}^{\infty} F([\varphi_k])g_k([\theta]), \qquad g_k([\theta]) = (\varphi_k, \theta). \tag{355}$$

This representation coincides with Porter's series expansion (122)-(123) on the index set $\mathcal{I} = 1$.

6.1.1 Polynomial Functional Interpolation

Let us study numerically an interpolation problem involving specific instance of (350). To this end, we set

$$K_1(x) = e^{\sin(x)}(1 + \sin(\cos(x) - 2) - \frac{1}{2} \qquad \text{(Fig. 8)}, \tag{356}$$

and define the following interpolation nodes in $D(F)$

$$\varphi_{k+1}(x) = \frac{1}{m+1} \frac{\sin\left(\dfrac{m+1}{2}(x - x_k)\right)}{\sin\left(\dfrac{x - x_k}{2}\right)}, \qquad x_k = \frac{2\pi}{m+1}k \qquad k = 0, 1, ..., m \tag{357}$$

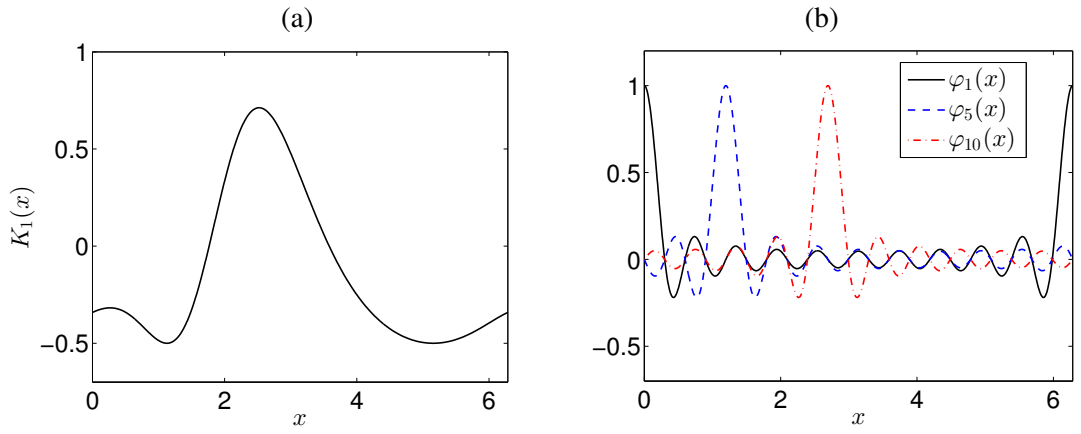

Figure 8: (a) Kernel function defining the linear functional (350). (b) Three elements of the orthogonal basis function set (357) ($m = 20$).

m being an even positive number. These are well-known trigonometric polynomials ([64], p. 28) satisfying the orthogonality conditions

$$(\varphi_j, \varphi_k) = \frac{2\pi}{m+1}\delta_{kj}, \qquad k, j = 1, ..., m+1. \tag{358}$$

Clearly, if $K_1(x)$ is in the span of $\{\varphi_k\}$ then the exact representation of the linear functional $F([\theta])$ involves no more than $m+1$ terms, i.e., a truncation of the series (355) to $m+1$ terms is exact. The kernel (356) is not of this type. Next, we construct a polynomial functional that interpolates $F([\theta])$ at the nodes (357). Specifically we consider Porter's construction (Section 4.2.3), which is very easy to implement and equivalent to Khlobystov polynomials for uniquely solvable interpolation problems. Such interpolants are dense in the space of linear functionals if we consider the set of nodes (102), i.e.,

$$\widehat{S}_1^{(m)} = \{\theta_i(x) \in D(F) \mid \theta_i(x) = \varphi_i(x) \quad i = 0, ..., m\}. \tag{359}$$

This means that testing linear functionals relative to orthogonal bases is sufficient to represent them exactly (see Section 2.1). As we have noticed in Section 4.2.2, this is not the case for higher-order polynomial functionals or general nonlinear functionals. Now, let us consider the general expression of Porter's interpolants

$$F([\theta]) \simeq \sum_{k=1}^{m+1} F([\varphi_k])\, g_k([\theta]), \qquad g_k([\theta]) = \sum_{j=1}^{m+1} H_{jk}^{-1} \sum_{p \in \mathcal{I}} (\varphi_j, \theta)^p, \tag{360}$$

where the matrix H_{ij} is given in (121). Depending on how we choose the index set $\mathcal{I}$ we have different expressions for the basis functionals $g_i([\theta])$. Specifically,

1. Constant polynomial functionals ($\mathcal{I} = \{0\}$). This case is degenerate and it requires Moore-Penrose pseudo-inversion of the matrix (121). This yields the basis functionals

$$g_k([\theta]) = \frac{1}{m+1}. \tag{361}$$

2. Homogeneous polynomial functionals of first order ($\mathcal{I} = \{1\}$):

$$g_k([\theta]) = \left[\frac{2\pi}{m+1}\right]^{-1} (\theta, \varphi_k). \tag{362}$$

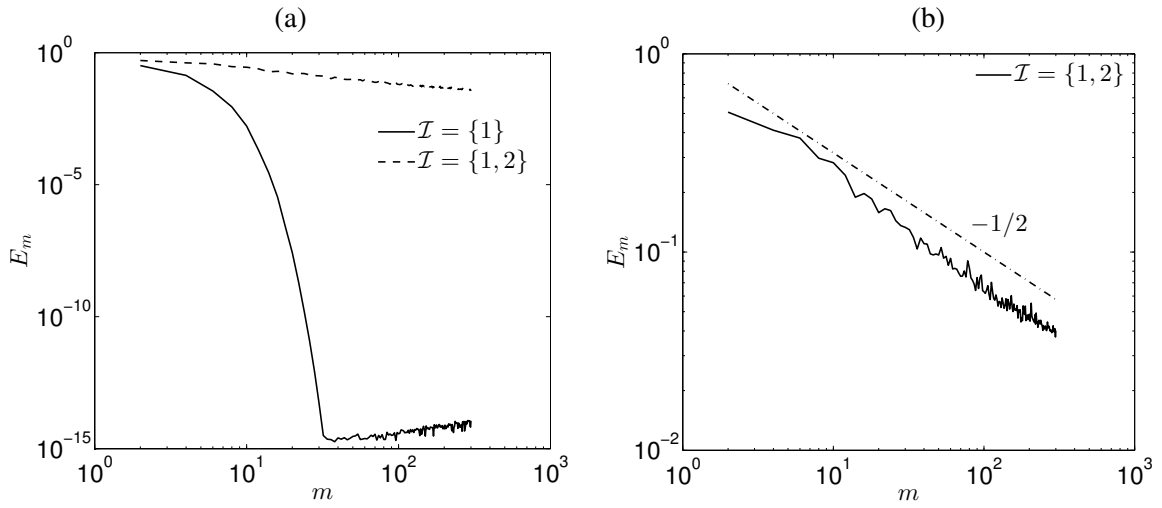

Figure 9: Linear functionals. Functional interpolation errors obtained by using Porter's method. Shown are the pointwise errors (364) versus m for the Gaussian ensemble $\mathcal{G}_{300}(1)$ and Porter's basis functionals (362) ($\mathcal{I} = \{1\}$), and (363) ($\mathcal{I} = \{1,2\}$). The expansion corresponding to $\mathcal{I} = \{1\}$ converges exponentially for obvious reasons, while the expansion corresponding to $\mathcal{I} = \{1,2\}$ has a $O(m^{-1/2})$ convergence rate due to insufficient interpolation nodes (Fig. (b)).

3. Quadratic polynomial functionals ($\mathcal{I} = \{1,2\}$) on the basis set $\{\varphi_1, ..., \varphi_{m+1}\}$. This yields basis functionals

$$g_k([\theta]) = \left[\left(\frac{2\pi}{m+1}\right) + \left(\frac{2\pi}{m+1}\right)^2\right]^{-1} \left((\theta,\varphi_k) + (\theta,\varphi_k)^2\right). \tag{363}$$

In Figure 9 we plot the pointwise error

$$E_m = \sup_{\theta\in\mathcal{G}_q} \left| F([\theta]) - \sum_{k=1}^{m+1} F([\varphi_k]) g_k([\theta]) \right| \tag{364}$$

versus m for test functions θ in the Gaussian ensemble

$$\mathcal{G}_q(\sigma) = \left\{ \theta(x) \in D(F) \;\middle|\; \theta(x) = \sigma \sum_{k=1}^{q+1} b_k \varphi_k(x), \quad \{b_1, ..., b_{m+1}\} \quad \text{i.i.d. Gaussian} \right\}, \tag{365}$$

and interpolants corresponding to the index sets $\mathcal{I} = \{1\}$ and $\mathcal{I} = \{1,2\}$ (bases (362) and (363)). The reason why we obtain exponential convergence with the index set $\mathcal{I} = \{1\}$ is obvious: convergence of the polynomial interpolant is basically defined by the convergence of the trigonometric series to the periodic function $K_1(x)$. On the other hand, Porter's interpolant corresponding to $\mathcal{I} = 1, 2$ shows an algebraic convergence at rate $O(m^{-1/2})$. The reason is that the basis function set $\{\varphi_1, ..., \varphi_{m+1}\}$ does not have enough elements to correctly identify the quadratic part of the interpolant, which is zero in this case. In fact, the off-diagonal terms in (96) or (99) cannot be identified by using an orthogonal basis, unless we consider a set of nodes in the form $\{\varphi_i, (\varphi_i + \varphi_j)\}$ where $i, j = 1, ..., m+1$, and $j \geq i$.

6.1.2 Functional SSE Approach

We look for a representation of (350) in the form (201). The basis functions G_i^l can be equivalently determined in an alternating Galerkin or least squares setting (see Section 4.3.5) by solving the system of

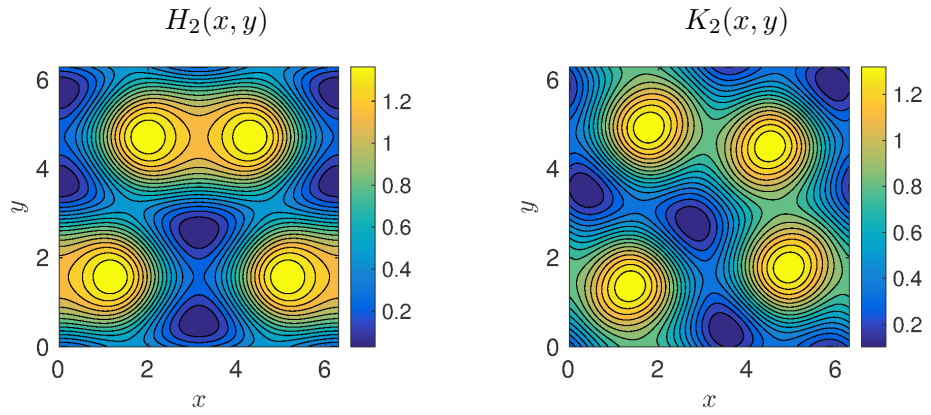

Figure 10: Quadratic functional (370). Kernel function (371) and its symmetrized version (372). Integrating $H_2(x,y)\theta(y)\theta(x)$ or $K_2(x,y)\theta(y)\theta(x)$ over x and y produces exactly the same result, independently on θ.

equations (233) with forcing given by

$$f^n_{jh} = \int_{-b}^{b} \cdots \int_{-b}^{b} \sum_{p=1}^{m+1} Z_p a_p \phi_h(a_j) \prod_{\substack{k=1 \\ k\neq j}}^{m+1} G^n_k(a_k) da_1 \cdots da_{m+1}, \tag{366}$$

$$Z_p = \int_0^{2\pi} K_1(x)\varphi_p(x)dx. \tag{367}$$

All integrals in (366) can be reduced to products of one-dimensional integrals (linear functionals are fully separable). In addition, if we use a polynomial basis for G^l_i (Section 4.3.5), then we can represent (350) exactly as a product of constants and linear polynomials. In fact,

$$\sum_{l=1}^{r} G^l_1(a_1) \cdots G^l_{m+1}(a_{m+1}) = \sum_{l=1}^{m+1} Z_l a_l, \tag{368}$$

which means that the exact separation rank is $r = m+1$ and

$$G^l_l(a_l) = a_l \qquad \text{and} \qquad \prod_{\substack{k=1 \\ k\neq l}}^{m+1} G^l_k(a_k) = Z_l. \tag{369}$$

6.2 Quadratic Functionals

Consider the quadratic functional

$$F([\theta]) = 5 + \int_0^{2\pi} K_1(x)\theta(x)dx + \int_0^{2\pi}\int_0^{2\pi} H_2(x,y)\theta(x)\theta(y)dxdy \tag{370}$$

defined on the space of square integrable periodic functions (351). We set $K_1(x)$ as in (356) and $H_2(x,y)$ as

$$H_2(x,y) = \sin(\cos(x) + \sin(y))\sin(y) + \frac{1}{2}\cos(\cos(x)). \tag{371}$$

Replacing $H_2(x,y)$ with the symmetrized kernel (see Figure 10)

$$K_2(x,y) = \frac{1}{2}\left(H_2(x,y) + H_2(y,x)\right) \tag{372}$$

does not change the functional (370).

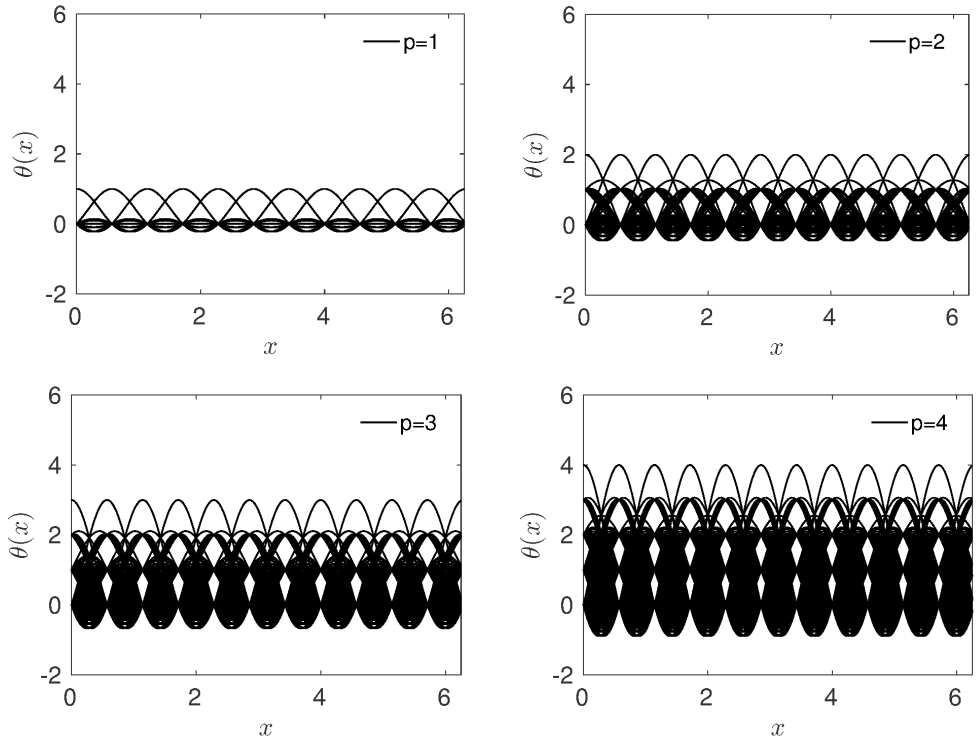

Figure 11: Interpolation nodes in the space of periodic functions (each function is a node). Here we plot the elements in the sets $\widehat{S}_p^{(m+1)}$ (see equation (103)) for $m = 10$ and $p = 1, 2, 3, 4$. The total number of elements within each set is $\#\widehat{S}_1^{(11)} = 12$, $\#\widehat{S}_2^{(11)} = 78$, $\#\widehat{S}_3^{(11)} = 364$ and $\#\widehat{S}_4^{(11)} = 1365$.

6.2.1 Polynomial Functional Interpolation

We first show that Porter's interpolants corresponding to the index set $\mathcal{I} = \{0, 1, 2\}$ and Khlobystov interpolants (176) coincide exactly when the interpolation problem is uniquely solvable, e.g., when we consider the set of nodes (103), here rewritten for convenience

$$\widehat{S}_2^{(m+1)} = \left\{0, \{\varphi_i\}_{i=1}^{m+1}, \{\varphi_i + \varphi_j\}_{j\geq i=1}^{m+1}\right\}. \tag{373}$$

In Figure 11 we plot the elements of such set for $m = 10$. In Figure 12 we plot the pointwise error

$$E_m = \sup_{\theta\in\mathcal{G}_{50}(1)} |F([\theta]) - \Pi_2([\theta])| \tag{374}$$

versus m for functions $\theta(x)$ in the Gaussian ensemble $\mathcal{G}_{50}(1)$ (see equation (365)). In (374), Π_2 represents either Porter's or Khlobystov interpolant at the set of nodes (373). It is seen that both methods achieve exponential convergence rate when interpolating the polynomial functional (370). This is due to the fact that such functional expansions are basically approximating the kernel functions (356) and (371) in terms of a Fourier spectral basis. This also establishes the full equivalence of Porter's and Khlobystov's interpolants for uniquely solvable interpolation problems.

6.2.2 Functional SSE Approach

We have seen in Section 4.3.5 that SSE can be equivalently computed in an alternating least squares or an alternating Galerkin setting. To this end, we need to evaluate the right hand side of the linear systems (233),

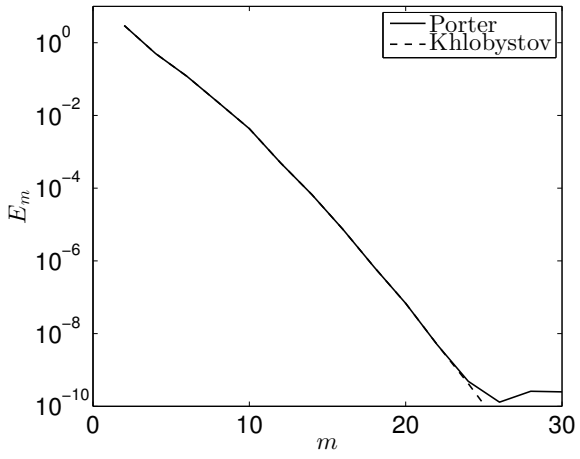

Figure 12: Interpolation of the quadratic functional (370) using Porter and Khlobystov approaches. Shown are the pointwise errors (374) versus m for the Gaussian ensemble $\mathcal{G}_{50}(1)$. The small deviation between Porter's and Khlobystov's error plots observed at $m = 24$ is due to inaccuracies in the computation of the inverse of (121). The number of interpolation nodes required to achieve accuracy of about 10^{-7} ($m = 20$) is $\#\widehat{S}_2^{(21)} = 253$ (see equation 104).

i.e., the forcing term (230). In the case of (370) we obtain

$$f_{jh}^n = \int_{-b}^{b} \cdots \int_{-b}^{b} \left(5 + \sum_{p=1}^{m+1} Z_p a_p + \sum_{q,p=1}^{m+1} Q_{pq} a_p a_q \right) \phi_h(a_j) \prod_{\substack{k=1 \\ k \neq j}}^{m+1} G_k^n(a_k) da_1 \cdots da_m, \tag{375}$$

where

$$Z_p = \int_0^{2\pi} K_1(x) \varphi_p(x) dx, \qquad Q_{pq} = \int_0^{2\pi} \int_0^{2\pi} K_2(x,y) \varphi_p(x) \varphi_q(x) dx dy. \tag{376}$$

Note that, as before, the integrals (375) can be reduced to products of one-dimensional integrals. If we use a Legendre basis ϕ_h (see Section 4.3.5), then we can represent (370) exactly as a product of constants, linear and quadratic polynomials. To show this, let us consider the quadratic part of the functional (370). We have,

$$\sum_{l=1}^{r} G_1^l(a_1) \cdots G_{m+1}^l(a_{m+1}) = \sum_{q,p=1}^{m+1} Q_{qp} a_q a_p. \tag{377}$$

Given the symmetry of Q_{pq}, the separation rank for such quadratic part is $(m+1)(m+2)/2$.

6.3 Hopf Characteristic Functionals

The Hopf characteristic functional can be seen as an infinite-dimensional extension of the joint characteristic function of a set of random variables. It often appears in stochastic analysis and in the theory of stochastic PDEs (Section 2.4) as a primary mathematical tool to determine any statistical property of the solution [89]. In this Section we study the accuracy of polynomial functional interpolation and separated series expansions (SSE) in representing Hopf functionals. To this end, consider the random function

$$u_0(x;\omega) = \frac{1}{\sqrt{q}} \sum_{k=1}^{q} \left[\eta_k \sin(kx) + \xi_k \cos(kx) \right], \tag{378}$$

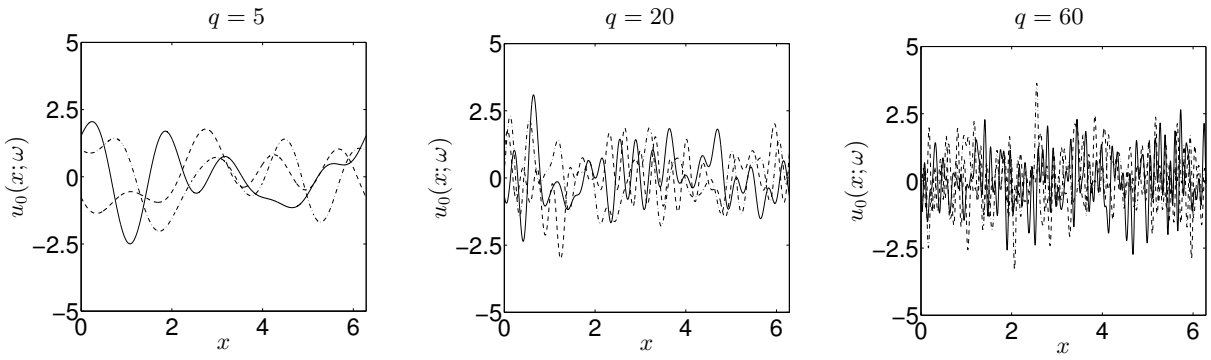

Figure 13: Samples of the random function (378) for different values of q (Gaussian η_k and ξ_k).

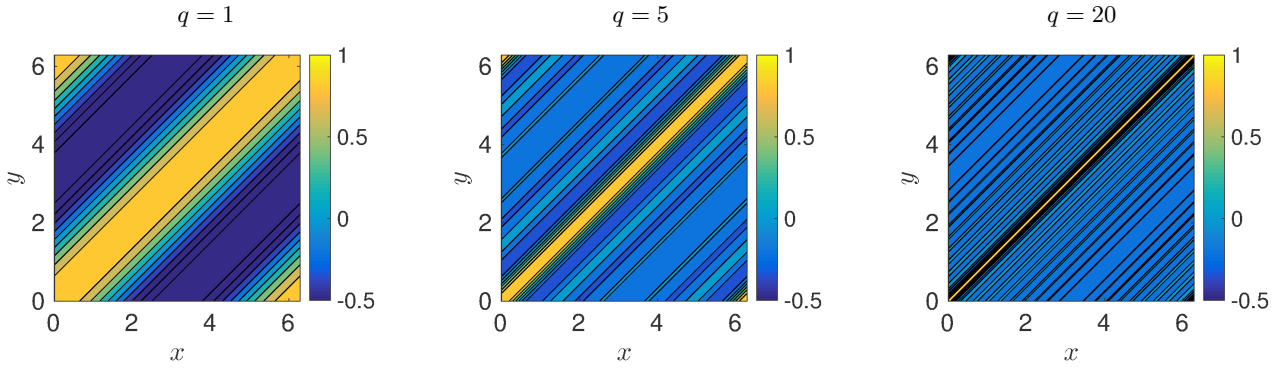

Figure 14: Covariance function (381) for different values of q.

where $\{\eta_k, \xi_k\}_{k=1,\dots,q}$ are i.i.d. random variables satisfying

$$\langle \xi_k \rangle = 0, \quad \langle \eta_k \rangle = 0, \quad \langle \xi_k^2 \rangle = 1, \quad \langle \eta_k^2 \rangle = 1. \tag{379}$$

In Figure 13 we plot few samples of (378), for different values of q in the hypothesis that ξ_i and η_k are Gaussians. From (379) it follows that the first two statistical moments of (378) are independent of q, i.e., we have

$$\langle u_0(x;\omega) \rangle = 0, \qquad \langle u_0(x;\omega)^2 \rangle = 1 \quad \text{for all } q. \tag{380}$$

On the other hand, the covariance function

$$C_0(x,y) = \frac{1}{q} \sum_{k=1}^{q} [\sin(kx)\sin(ky) + \cos(kx)\cos(ky)] \tag{381}$$

does depend on q, as shown in Figure 14. Higher-order moments and cumulants can be computed analytically in a similar way. The Hopf functional of $u_0(x;\omega)$ is defined as

$$\Phi([\theta(x)]) = \left\langle \exp\left[i \int_0^{2\pi} \theta(x) u_0(x;\omega) dx \right] \right\rangle, \tag{382}$$

where the average $\langle \cdot \rangle$ is a multi-dimensional integral with respect to the joint probability density function of ξ_k and η_k. By substituting (378) into (382) we obtain

$$\Phi([\theta(x)]) = \prod_{k=1}^{q} \int e^{ias_k[\theta]} p_{\eta_k}(a) da \prod_{k=1}^{q} \int e^{iac_k[\theta]} p_{\xi_k}(a) da, \tag{383}$$

where

$$s_k[\theta] = \frac{1}{\sqrt{q}} \int_0^{2\pi} \theta(x) \sin(kx) dx, \qquad c_k[\theta] = \frac{1}{\sqrt{q}} \int_0^{2\pi} \theta(x) \sin(kx) dx. \tag{384}$$

Depending on the probability density functions $p_{\eta_k}(a)$ and $p_{\xi_k}(a)$ appearing in (383), we have different expressions of $F([\theta])$.

Gaussian Random Fields Let us assume

$$p_{\eta_k}(a) = \frac{1}{\sqrt{2\pi}} e^{-a^2/2} \qquad p_{\xi_k}(a) = p_{\eta_k}(a). \tag{385}$$

The integrals in (383) are in the form

$$\frac{1}{\sqrt{2\pi}} \int_{-\infty}^{\infty} e^{ias_k[\theta] - a^2/2} da = e^{-s_k^2[\theta]/2}. \tag{386}$$

Therefore, we obtain

$$\Phi([\theta(x)]) = \exp\left[-\frac{1}{2} \sum_{k=1}^{q} \left(s_k^2[\theta] + c_k^2[\theta] \right) \right] \tag{387}$$

$$= \exp\left[-\frac{1}{2} \int_0^{2\pi} \int_0^{2\pi} \theta(x)\theta(y) C_0(x,y) dx dy \right], \tag{388}$$

in agreement with well-known results for Hopf characteristic functionals of Gaussian random fields.

Uniform Random Fields Let us assume

$$p_{\eta_k}(a) = \begin{cases} 1/(2\sqrt{3}) & a \in [-\sqrt{3}, \sqrt{3}] \\ 0 & \text{otherwise} \end{cases} \qquad p_{\xi_k}(a) = p_{\eta_k}(a) \tag{389}$$

In this way the assumptions (379) are satisfied. The integrals in (383) are easily obtained as

$$\frac{1}{2\sqrt{3}} \int_{-\sqrt{3}}^{\sqrt{3}} e^{ias_k[\theta]} da = \frac{\sinh(i\sqrt{3}s_k[\theta])}{i\sqrt{3}s_k[\theta]} = \frac{\sin(\sqrt{3}s_k[\theta])}{\sqrt{3}s_k[\theta]}. \tag{390}$$

A substitution of this formula into (383) yields

$$\Phi([\theta(x)]) = \prod_{k=1}^{q} \frac{\sin(\sqrt{3}s_k[\theta]) \sin(\sqrt{3}c_k[\theta])}{3 s_k[\theta] c_k[\theta]}. \tag{391}$$

Note that in both cases mentioned above, i.e., zero-mean Gaussian and uniform random processes (378), the Hopf functional turns out to be real-valued. Also, in both cases we have $\Phi \to 0$ as $\|\theta\| \to \infty$ (Riemann-Lebesgue lemma), at a rate that depends on the regularity of the underlying probability density functional. In particular, in the Gaussian case Φ goes to zero faster than in the uniform case. Other distributions can be treated similarly, yielding more general complex-valued functionals. In addition, note that both (388) are (391) are *entire functionals* (i.e., analytic on the complex plane). This implies that the polynomial interpolation process converges pointwise [84]).

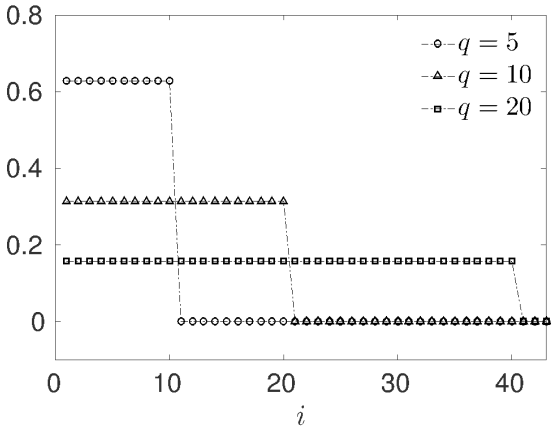

Figure 15: Gaussian Hopf Functional. Spectra of the covariance matrix (395) obtained by projecting the covariance function (381) onto the Fourier modes (392) or the discrete trigonometric polynomials (357). It is seen that the number of active components is exactly $2q$ and all variables are *equally important*. This means that it is impossible to accurately approximate (388) by using polynomial functionals or SSE unless we consider at least $m = 2q$ dimensions.

6.3.1 Effective Dimension

Let us represent $\theta(x)$ in the space of periodic functions in $[0, 2\pi]$. Possible bases are the discrete trigonometric polynomials (357) or the classical set of Fourier modes

$$1, \qquad \sin(kx), \qquad \cos(kx), \qquad k = 1, 2, ... \tag{392}$$

Let us now ask the following question: what is the effective dimension of the Hopf functional (382) in the space of periodic functions? Such dimension is clearly determined by the dimension of the linear functionals s_k and c_k in (384). If we expand the test function θ in a classical Fourier series

$$\theta(x) = a_0 + \sum_{k=1}^{N} a_k \sin(kx) + \sum_{k=1}^{N} b_k \cos(kx) \tag{393}$$

and we substitute it into (384) then we obtain

$$s_k[\theta] = \frac{\pi}{\sqrt{q}} a_k, \qquad \text{and} \qquad c_k[\theta] = \frac{\pi}{\sqrt{q}} b_k. \tag{394}$$

This means that the *effective dimension* of the Hopf functional (382) is *exactly* $2q$. To show this numerically, we consider the Hopf functional (388) (Gaussian case) and plot the spectrum of the covariance matrix

$$Z_{ij} = \int_0^{2\pi} \int_0^{2\pi} C_0(x, y) \varphi_i(x) \varphi_j(y) dx dy, \tag{395}$$

obtained by projecting the covariance function (381) onto the the Fourier modes (392) or, equivalently, onto the discrete trigonometric polynomials (357). As it is clearly seen from Figure 15 the number of active components is exactly $2q$. Note also that the spectrum is flat in all cases, which means that all active variables are equally important. This has important consequences when approximating the functional (388) by polynomial functionals or SSE. In particular, if we use functionals involving less than $2q$ components, e.g., if $m < 2q$ in equation (201), then we cannot approximate (388) accurately, no matter how we push the expansion order.

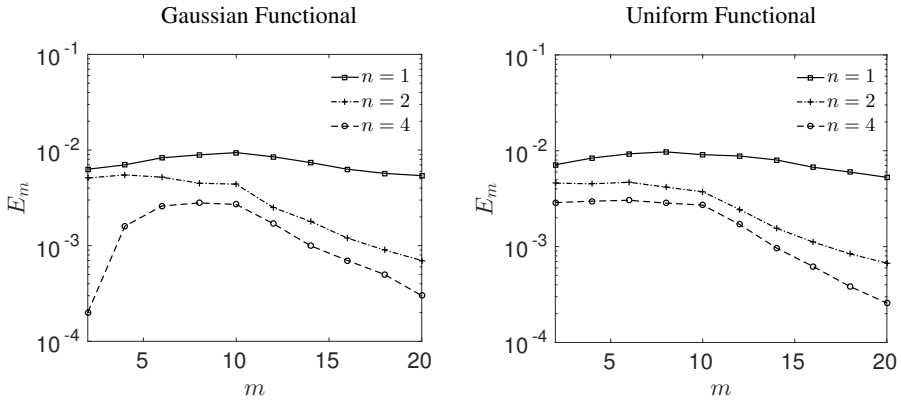

Figure 16: Accuracy of Porter's polynomial functional interpolants in representing the Hopf functionals (387) and (391). Shown are the pointwise errors (397) versus m for different orders of the polynomial interpolant. The errors are computed by sampling 20000 functions from the set $\mathcal{G}_{50}(\sigma)$ with $\sigma = 0.01$ and then computing the supremum (397).

6.3.2 Polynomial Functional Interpolation

Let us expand (388) in a power series

$$\begin{aligned}\Phi([\theta(x)]) =& 1 - \frac{1}{2}\int_0^{2\pi}\int_0^{2\pi} C_0(x_1,x_2)\theta(x_1)\theta(x_2)dx_1dx_2 + \\ & \frac{1}{4}\int_0^{2\pi}\int_0^{2\pi}\int_0^{2\pi}\int_0^{2\pi} C_0(x_1,x_2)C_0(x_3,x_4)\theta(x_1)\theta(x_2)\theta(x_3)\theta(x_4)dx_1dx_2dx_3dx_4 + \cdots .\end{aligned} \tag{396}$$

For small $\theta(x)$ we can truncate the series, and represent Φ in terms of an interpolating polynomial functional of relatively small order, provided we have enough interpolation nodes nearby $\theta(x) = 0$. This is demonstrated in Figure 16, where we study the accuracy Porter's interpolants through the set of nodes $\widehat{S}_n^{(m+1)}$ (see Eq. (103)). Specifically, we plot the error

$$E_m = \sup_{\theta\in\mathcal{G}_{50}(\sigma)} |\Phi([\theta]) - \Pi_n([\theta])| \tag{397}$$

versus m for $q = 5$, $n = 1, 2, 3, 4$ and $\sigma = 0.01$. It is seen that the interpolants converge in both n (polynomial order) and m (number of basis functions). Convergence in m becomes monotonic for $m \geq 10$. This is related to the fact that the effective dimension of the Hopf functionals (387) and (391) is 10 for $q = 5$ (see Section 6.3.1). Therefore for $m \geq 10$ we have enough basis functions to fully resolve them. The accuracy of the polynomial interpolants then depends only on n (polynomial order), the number of interpolation nodes and their location. The number of interpolation nodes in $\widehat{S}_n^{(m+1)}$ is given in (104). For example, the case $m = 20$ and $n = 4$ yields 12650 nodes and an interpolation matrix (121) of size 12650×12650[30]. When evaluating the error (397) it is important to select $\mathcal{G}_{50}(\sigma)$ within the convex hull of the interpolation nodes, e.g., by choosing σ small enough. In this way we avoid inaccuracies due to polynomial extrapolation. To mitigate this phenomenon, we can also consider different sets of interpolation nodes, e.g., the sets $\widetilde{S}_n^{(m+1)}$ defined in equation (107) with a_{i_q} sampled at Gauss-Hermite sparse-grid points. In Figure 17 we plot the elements in $\widetilde{S}_1^{(m+1)}$, $\widetilde{S}_2^{(m+1)}$ and $\widetilde{S}_3^{(m+1)}$ for Gauss-Hermite sparse grids of level 5 (see also Table 3). The symmetry of the nodes a_{i_j} in the Fourier space yields linearly dependent nodes

m	2	4	6	8	10	16	20
$\#\widetilde{S}_2^{(m+1)}$	121	341	673	1117	1673	4013	6133

Table 3: Number of interpolation nodes in $\widetilde{S}_2^{(m+1)}$ with a_{i_j} sampled at Gauss-Hermite sparse grids (level 5).

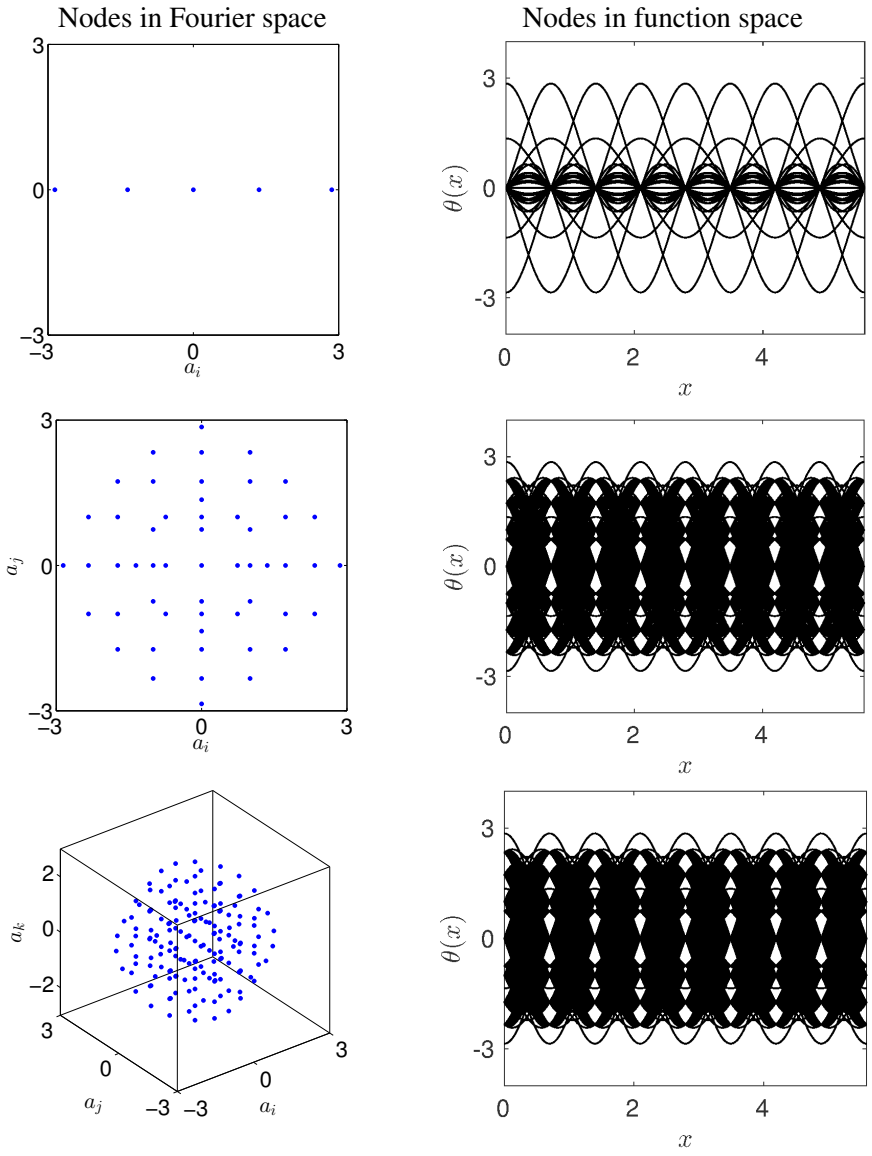

Figure 17: Gauss-Hermite sparse grids (left) and corresponding interpolation nodes in the function space $\widetilde{S}_n^{(m)}$ (right). Specifically, we plot all elements in $\widetilde{S}_1^{(9)}$ (first row, 45 elements), $\widetilde{S}_2^{(9)}$ (second row, 1117 elements) and $\widetilde{S}_3^{(9)}$ (third row, 3949 elements).

in $\widetilde{S}_n^{(m+1)}$. Correspondingly, the interpolation matrix (121) is rank-deficient, i.e., it cannot be inverted in a classical sense. We can overcome this issue by either removing some nodes from the set $\widetilde{S}_n^{(m+1)}$, or by taking the More-Penrose pseudo-inverse of (121). In the latter case we obtain a non-cardinal basis (145)

[30]Recall that the matrix (121) has to be inverted to compute the cardinal basis (123) and the polynomial interpolant (122).

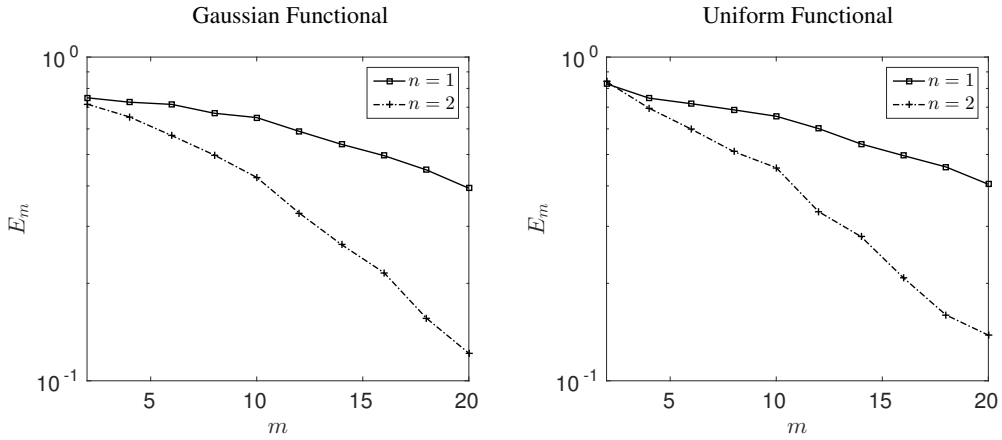

Figure 18: Approximation of the Hopf functionals (387) and (391) by using polynomial functionals of total degree $n = 1$ and $n = 2$. The polynomial are in the form (144) (i.e., non-interpolatory) and they are constructed by using the set of nodes $\widetilde{S}_1^{(m)}$ and $\widetilde{S}_2^{(m)}$ defined in equation (107), with a_{i_j} sampled at Gauss-Hermite sparse grids level 5. Shown are the pointwise errors (397) versus m for $\theta \in \mathcal{G}_{50}(1)$.

and a polynomial functional in the form (144). In Figure 18 we show convergence of such polynomial functional (order 1 and 2) to the Hopf functionals (388) and (391). Specifically, we plot the pointwise errors (397) versus m for a set of 20000 randomly generated evaluation nodes in $\mathcal{G}_{50}(\sigma)$, with $\sigma = 1$.

6.3.3 Functional SSE Approach

Consider the Hopf functionals (388) and (391). We have seen in Section 4.3.5 that we can compute a separated series expansion of such functionals either in an alternating least squares setting or in an alternating Galerkin setting. This can be done efficiently by using the the method of hierarchical bases we discussed in Section 4.3.5 to evaluate the functional integrals (220) and (221). To this end, consider

$$\varphi_0(x) = \frac{1}{2\pi}, \quad \varphi_{k-1}(x) = \frac{\sin(kx/2)}{\sqrt{\pi}}, \quad \varphi_k(x) = \frac{\cos((1+k/2)x)}{\sqrt{\pi}} \qquad (k \text{ even}). \tag{398}$$

This yields the linear systems (233) with simplified forcing term (230) and matrix (234).

Gaussian Functionals In this case, the integrals (230) are in the form[31]

$$f_{jh}^n = \int_{[-b,b]^N} da_1 \cdots da_N \exp\left[-\frac{1}{2}\sum_{p,q=1}^{N} Z_{pq} a_p a_q\right] \phi_h(a_j) \prod_{\substack{k=1 \\ k\neq j}}^{m} G_k^n(a_k), \tag{401}$$

[31]The size of the hypercube that encloses the multi-dimensional Gaussian $g(x) = \exp[-xAx']$, i.e., the set $[-b,b]^N$ such that $g(x) > 10^{-10}$ for all $x \in [-b,b]^N$, can be estimated by computing the smallest (nonzero) eigenvalue λ_{min} of the symmetric positive semi-definite matrix A, and then solving the equation

$$e^{-N\lambda_{min}b^2} = 10^{-10}, \tag{399}$$

where N is the number of dimensions (size of the vector x). This yields the estimate

$$b = \sqrt{\frac{10\ln(10)}{N\lambda_{min}}}. \tag{400}$$

$$Z_{ij} = \int_0^{2\pi} \int_0^{2\pi} C_0(x,y)\varphi_i(x)\varphi_j(y)dxdy \tag{402}$$

where m is the number of active variables (number of basis functions φ_k in the cylindrical representation). It can be verified that

$$Z_{ij} = \begin{cases} \frac{\pi}{q}\delta_{ij} & i,j \leq 2q \\ 0 & \text{otherwise} \end{cases}$$

and therefore

$$f_{jh}^n = (2b)^{N-2q} \int_{[-b,b]^{2q}} da_1 \cdots da_{2q} \exp\left[-\frac{\pi}{2q}\sum_{p=1}^{2q} a_p^2\right] \phi_h(a_j) \prod_{\substack{k=1 \\ k\neq j}}^{m} G_k^n(a_k). \tag{403}$$

This means that the Gaussian functional is fully separated relative to the basis (398), i.e.,

$$F = \exp\left[-\frac{\pi}{2q}\sum_{p=1}^{2q} a_p^2\right]. \tag{404}$$

Therefore a rank one SSE with $m = 2q$ variables is exact in the case. It's important to remark that the Gaussian functional is not fully separated relative to other bases, for example (357).

Uniform Functionals In this case, the integrals (230) are in the form

$$f_{jh}^n = \int_{[-b,b]^N} \prod_{k=1}^{q} \frac{\sin(\sqrt{3}s_k(a_1,..,a_N))\sin(\sqrt{3}c_k(a_1,..,a_N))}{3s_k(a_1,..,a_N)c_k(a_1,..,a_N)} \phi_h(a_j) \prod_{\substack{k=1 \\ k\neq j}}^{m} G_k^n(a_k) \prod_{q=1}^{N} da_q, \tag{405}$$

where $s_k(a_1,..,a_N)$ and $c_k(a_1,..,a_N)$ are obtained from (384) as

$$s_k(a_1,..,a_N) = \frac{1}{\sqrt{q}} \sum_{p=0}^{N} (\sin(kx), \varphi_p(x))a_p, \tag{406}$$

$$c_k(a_1,..,a_N) = \frac{1}{\sqrt{q}} \sum_{p=0}^{N} (\cos(kx), \varphi_p(x))a_p. \tag{407}$$

A substitution of (398) into (406)-(407) yields

$$s_k(a_1,..,a_N) = \sqrt{\frac{\pi}{q}} a_k, \quad k = 1,...,q, \quad \text{(zero otherwise)}, \tag{408}$$

$$c_k(a_1,..,a_N) = \sqrt{\frac{\pi}{q}} a_{k+q}, \quad k = 1,...,q, \quad \text{(zero otherwise)}. \tag{409}$$

This means that, relative to the hierarchical basis (398) the functional (391) is fully separable, i.e.,

$$\Phi = \prod_{k=1}^{2q} \frac{\sin(\sqrt{3\pi}a_k/\sqrt{q})}{3\sqrt{\pi}a_k/\sqrt{q}}. \tag{410}$$

Therefore, a rank one SSE with $m = 2q$ variables is exact[32]. In addition, similarly to the Gaussian case, the uniform functional is not fully separated relative to other bases, for example (357).

[32]Equations (408) and (409) suggest that all the $2q$ variables $a_1, ..., a_{2q}$ are equally important.

	$q=3$	$q=5$	$q=10$	$q=15$
Gaussian	1.5527×10^{-12}	1.1529×10^{-13}	1.8498×10^{-13}	4.3778×10^{-9}
Uniform	1.1834×10^{-25}	2.7762×10^{-22}	4.1825×10^{-26}	1.2993×10^{-24}

Table 4: Hopf Functional. Approximation errors of functional SSE of rank one as a function of q (the effective dimension of the Hopf functional is $2q$). The error is defined in equation (413). These results are obtained by using the alternating direction Galerkin method with Legendre polynomials of order 15 in each variable (θ, φ_j). The size of the hypercube (the domain of the discretized functional) here is set to $b = 2$ and we use one-dimensional Gauss-Legendre-Lobatto quadrature to compute the forcing terms (411) and (412).

Calculation of the Integrals The integrals (401) and (405) can be computed by sparse grids (moderate values of q), HDMR [136, 90] or quasi-Monte Carlo methods (higher values of q), e.g., through a classical low-discrepancy Halton sequence in $2q$ dimensions. If the functional is separable, then the integrals reduce to simple products of one-dimensional integrals. In particular,

$$f^n_{jh} = (2b)^{N-2q} \int_{-b}^{b} e^{-\pi a_j/2q} \phi_h(a_j) da_j \prod_{\substack{k=1 \\ k\neq j}}^{2q} \int_{-b}^{b} e^{-\pi a_k/2q} G^n_k(a_k) da_k \quad \text{(Gaussian case)}, \tag{411}$$

$$f^n_{jh} = (2b)^{N-2q} \int_{-b}^{b} \frac{\sin(\sqrt{3\pi} a_j/\sqrt{q})}{3\sqrt{\pi} a_j/\sqrt{q}} \phi_h(a_j) da_j \prod_{\substack{k=1 \\ k\neq j}}^{2q} \int_{-b}^{b} \frac{\sin(\sqrt{3\pi} a_j/\sqrt{q})}{3\sqrt{\pi} a_j/\sqrt{q}} G^n_k(a_k) da_k \quad \text{(Uniform case)}. \tag{412}$$

In Table 4 we show the approximation error

$$E_2 = \int \mathcal{D}[\theta] \left(\Phi([\theta]) - \sum_{l=1}^{r} \prod_{k=1}^{m} G^l_k((\theta, \varphi_k)) \right)^2 \tag{413}$$

for different values of q. The results are obtained by setting $b = 2$ in (401)-(405) and by using Legendre polynomials of order $P = 15$ in the representation of each G^l_k.

6.3.4 Functional Derivatives

The first- and second-order functional derivatives of the Hopf functional (382)

$$\frac{\delta \Phi([\theta])}{\delta \theta(x)} = i \left\langle u_0(x;\omega) \exp\left[i \int_0^{2\pi} \theta(x) u_0(x;\omega) dx \right] \right\rangle, \tag{414}$$

$$\frac{\delta^2 \Phi([\theta])}{\delta \theta(x) \delta \theta(y)} = - \left\langle u_0(x;\omega) u_0(y;\omega) \exp\left[i \int_0^{2\pi} \theta(x) u_0(x;\omega) dx \right] \right\rangle \tag{415}$$

can be expressed analytically in terms of known functions. To this end, we need a formula to compute the averages in (414) and (415). A lengthy calculation shows that

$$\frac{\delta \Phi([\theta])}{\delta \theta(x)} = \frac{i}{\sqrt{q}} \left(I^{(c)}[\theta] \sum_{k=1}^{q} \sin(kx) I^{(s)}_k[\theta] + I^{(s)}[\theta] \sum_{k=1}^{q} \cos(kx) I^{(c)}_k[\theta] \right), \tag{416}$$

Coefficients Appearing in the Functional Derivatives (416) and (417)

$$G_n(z) = \int_{-\infty}^{\infty} a^n e^{iza} p(a) da$$

Gaussian PDF
$$G_0(z) = e^{-z^2/2}$$
$$G_1(z) = ize^{-z^2/2}$$
$$G_2(z) = (1-z^2)e^{-z^2/2}$$

Uniform PDF
$$G_0(z) = \frac{\sin(\sqrt{3}z)}{\sqrt{3}z}$$
$$G_1(z) = i\frac{\sin(\sqrt{3}z)}{\sqrt{3}z^2} - i\frac{\cos(\sqrt{3}z)}{z}$$
$$G_2(z) = \frac{2\cos(\sqrt{3}z)}{z^2} + \frac{\sqrt{3}\sin(\sqrt{3}z)}{z} - \frac{2\sin(\sqrt{3}z)}{\sqrt{3}z^3}$$

$I^{(s)}[\theta] = \prod_{r=1}^{q} G_0(s_r[\theta])$	$I^{(c)}[\theta] = \prod_{r=1}^{q} G_0(c_r[\theta])$
$I_k^{(s)}[\theta] = G_1(s_k[\theta]) \prod_{\substack{r=1 \\ r\neq k}}^{q} G_0(s_r[\theta])$	$I_k^{(c)}[\theta] = G_1(c_k[\theta]) \prod_{\substack{r=1 \\ r\neq k}}^{q} G_0(c_r[\theta])$
$J_k^{(s)}[\theta] = G_2(s_k[\theta]) \prod_{\substack{r=1 \\ r\neq k}}^{q} G_0(s_r[\theta])$	$J_k^{(c)}[\theta] = G_2(c_k[\theta]) \prod_{\substack{r=1 \\ r\neq k}}^{q} G_0(c_r[\theta])$
$I_{kh}^{(s)}[\theta] = G_1(s_k[\theta])G_1(s_h[\theta]) \prod_{\substack{r=1 \\ r\neq k,h}}^{q} G_0(s_r[\theta])$	$I_{kh}^{(c)}[\theta] = G_1(c_k[\theta])G_1(c_h[\theta]) \prod_{\substack{r=1 \\ r\neq k,h}}^{q} G_0(c_r[\theta])$

Table 5: Coefficients appearing in the functional derivatives (416) and (417).

$$\begin{aligned}\frac{\delta^2\Phi([\theta])}{\delta\theta(x)\delta\theta(y)} = &-\frac{1}{q}\sum_{k,h=1}^{q}\Big(\sin(kx)\cos(hy)I_k^{(s)}[\theta]I_h^{(c)}[\theta] + \cos(kx)\sin(hy)I_k^{(c)}[\theta]I_h^{(s)}[\theta]\Big)\\ &-\frac{1}{q}\sum_{\substack{k,h=1\\k\neq h}}^{q}\Big(I^{(c)}[\theta]\sin(kx)\sin(hy)I_{kh}^{(s)}[\theta] + I^{(s)}[\theta]\cos(kx)\cos(hy)I_{kh}^{(c)}[\theta]\Big)\\ &-\frac{1}{q}\sum_{k=1}^{q}\Big(I^{(c)}[\theta]\sin(kx)\sin(ky)J_k^{(s)}[\theta] + I^{(s)}[\theta]\cos(kx)\cos(ky)J_k^{(c)}[\theta]\Big),\end{aligned} \tag{417}$$

where the functionals $I^{(c)}[\theta]$, $I^{(s)}[\theta]$, $I_k^{(c)}[\theta]$, etc., are given in Table 5. These expressions are general and they hold for any random function in the form (378), with i.i.d. random variables η_k and ξ_j. In summary, the main steps to calculate the functional derivatives of Φ are

1. Select the test function $\theta(x)$;

2. Compute $s_k[\theta]$ and $c_k[\theta]$ in (384) and the coefficients in Table 5;

3. Build the series expansions (416) and (417) by using the results of Table 5[33].

For Gaussian Hopf functionals in the form (388) the expressions (416) and (417) can be significantly simplified. In particular, we obtain[34]

$$\frac{\delta\Phi([\theta])}{\delta\theta(x)} = -\left[\int_0^{2\pi} C_0(x,y)\theta(y)dy\right]\exp\left[-\frac{1}{2}\int_0^{2\pi}\int_0^{2\pi} C_0(x,y)\theta(x)\theta(y)dxdy\right], \tag{419}$$

$$\begin{aligned}\frac{\delta^2\Phi([\theta])}{\delta\theta(x)\delta\theta(y)} = &\left[-C_0(x,y) + \int_0^{2\pi} C_0(x,y)\theta(y)dy\int_0^{2\pi} C_0(x,y)\theta(x)dx\right]\times \\ &\exp\left[-\frac{1}{2}\int_0^{2\pi}\int_0^{2\pi} C_0(x,y)\theta(x)\theta(y)dxdy\right].\end{aligned} \tag{420}$$

In Figure 19 and Figure 20 we plot the first- and second-order functional derivatives of the Hopf functionals (387) and (391), evaluated at different test functions.

Functional Derivatives and SSE The analytical results (416)-(417) can be compared with numerical results of polynomial functional interpolation or functional SSE. Hereafter we consider functional SSE. We have seen is Section 4.3.6 that the functional derivatives of the SSE approximant of Φ can be expressed as

$$\frac{\delta\widehat{\Phi}}{\delta\theta(x)} = \sum_{k=1}^{m}\frac{\partial\widehat{\Phi}}{\partial a_k}\varphi_k(x), \tag{421}$$

$$\frac{\delta^2\widehat{\Phi}}{\delta\theta(x)\delta\theta(y)} = \sum_{k,j=1}^{m}\frac{\partial^2\widehat{\Phi}}{\partial a_k\partial a_j}\varphi_k(x)\varphi_j(y), \tag{422}$$

where $a_k = (\theta, \varphi_k)$. By evaluating (419) and (420) at, e.g.,

$$\theta(x) = \sin(x) + \sin(2x) + \sin(3x) \tag{423}$$

we can easily assess the accuracy of (421) and (422). This is done in Figure 21 where we plot the analytical and the SSE-based first- and second-order functional derivatives evaluated at (423).

6.4 Sine Functional

Consider the nonlinear functional

$$F([\theta]) = \sin\left((K_1,\theta)\right), \qquad (K_1,\theta) = \int_0^{2\pi} K_1(x)\theta(x)dx, \tag{424}$$

[33]Note that in the case of uniform variables the coefficients in Table (5) are such that

$$\lim_{z\to 0} G_0(z) = 1, \qquad \lim_{z\to 0} G_1(z) = 0, \qquad \lim_{z\to 0} G_2(z) = 1. \tag{418}$$

and therefore there are no singularities at $z = 0$. Also, all coefficients decay to 0 when z goes to infinity.

[34]Note that the first-order derivative reduces to 0 (mean field) at $\theta = 0$ while the second-order derivative at $\theta = 0$ reduces to the opposite of the correlation function $C_0(x,y)$.

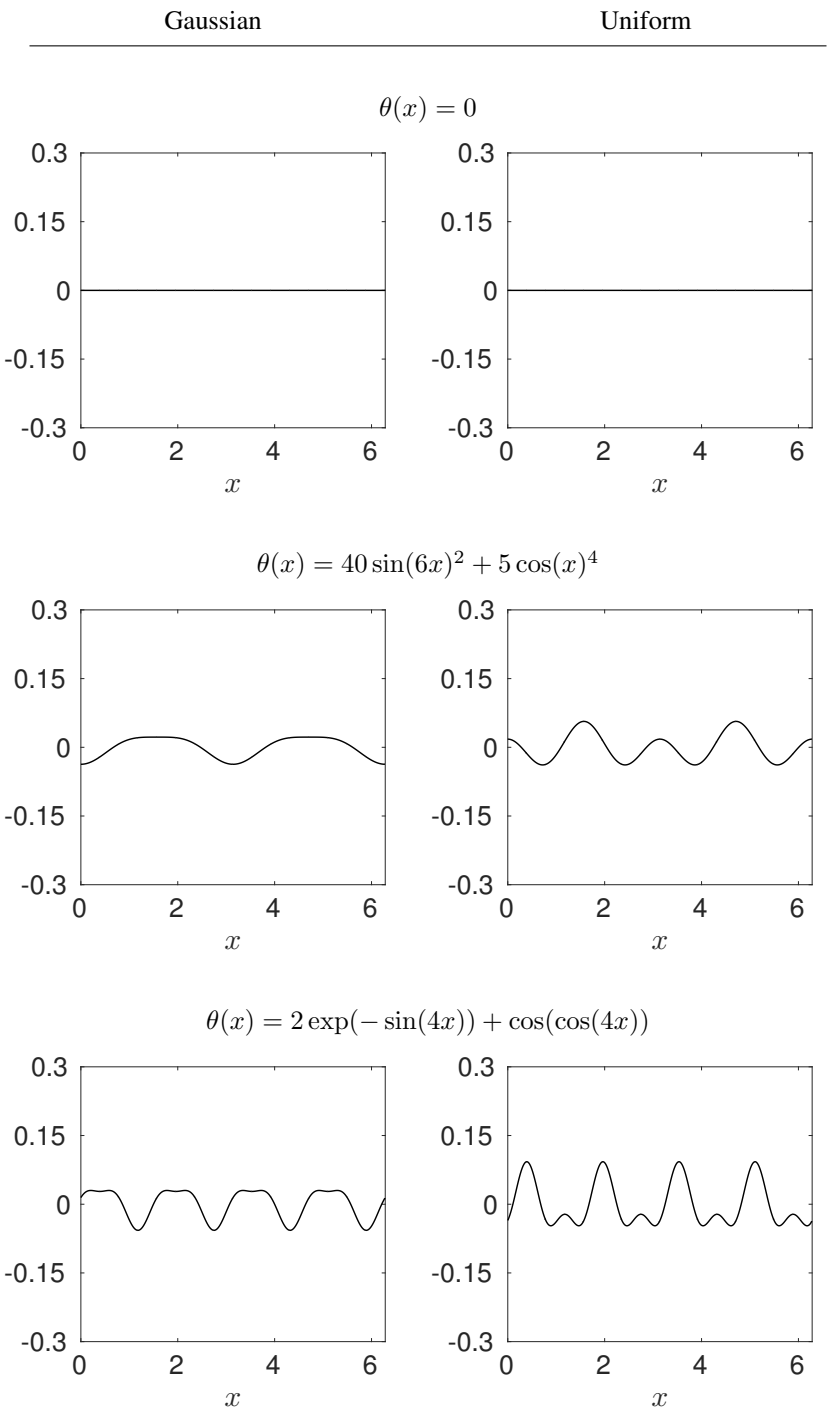

Figure 19: First-order functional derivatives of the Hopf functionals (387) (Gaussian) and (391) (Uniform) for $q = 10$ evaluated at different test functions. The Hopf functionals we are considering here are real-valued and therefore the functional derivatives are real. Note that evaluating the first-order functional derivative at $\theta(x) = 0$ (first row) yields the mean field $\langle u_0(x) \rangle = 0$.

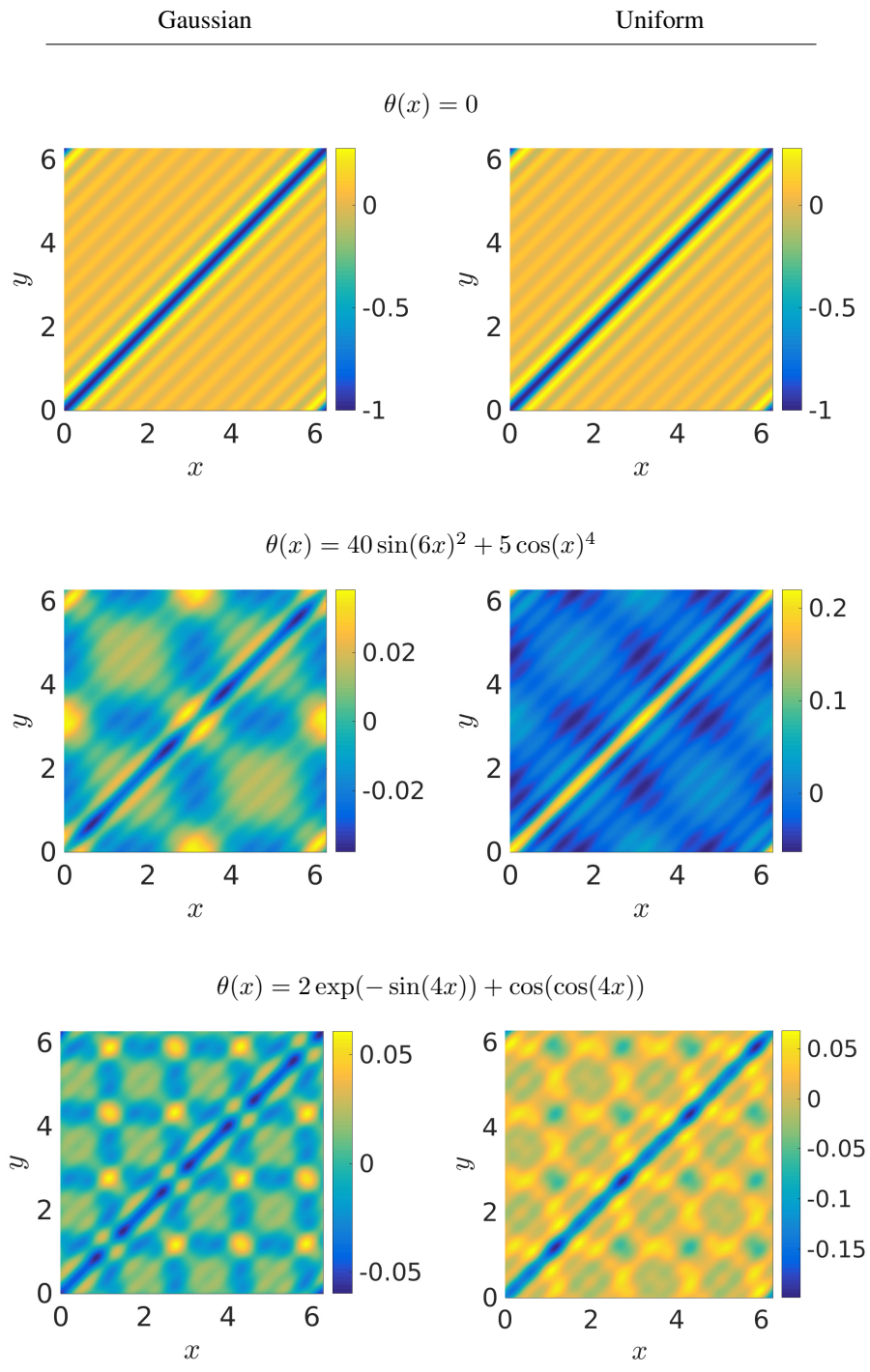

Figure 20: Second-order functional derivatives of the Hopf functionals (387) (Gaussian) and (391) (Uniform) for $q = 10$ evaluated at different test functions. Both functionals are real-valued and therefore the functional derivatives are real. Note that evaluating the second-order functional derivative at $\theta(x) = 0$ (first row) yields the opposite of the correlation function $C_0(x, y)$ in (381).

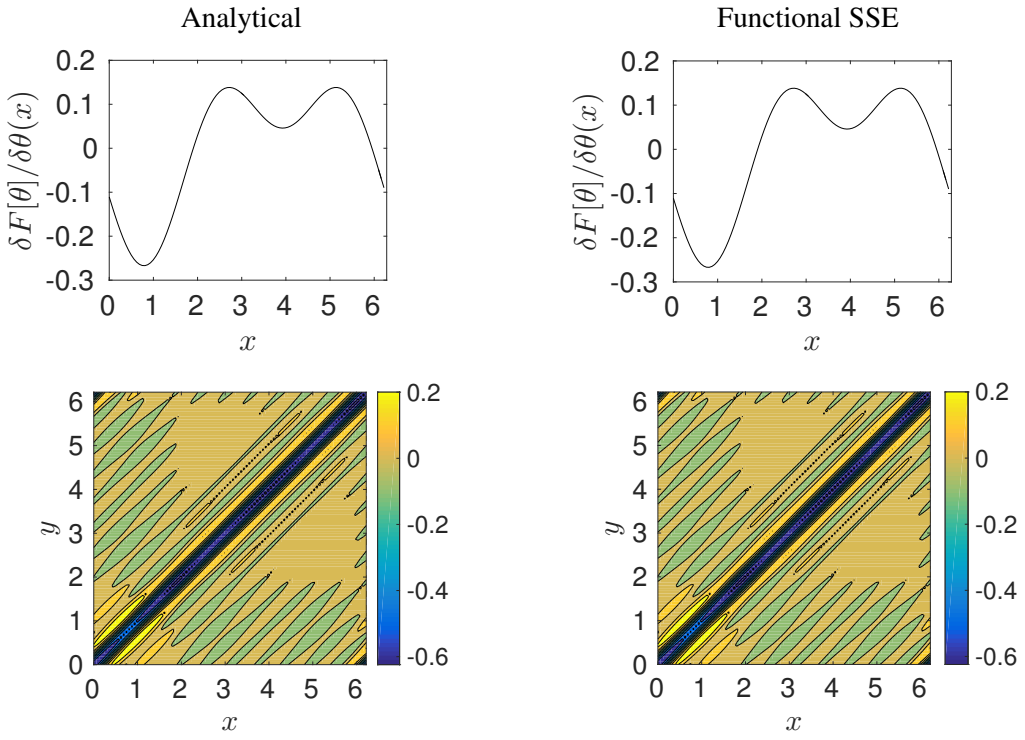

Figure 21: First- and second-order functional derivatives of the Gaussian Hopf functional (388) evaluated at $\theta(x) = \sin(x) + \sin(2x) + \sin(3x)$. Shown are analytical results (419) and (420) versus numerical result obtained by functional SSE (equations (421) and (422)).

where $K_1(x)$ is as in equation (356). By introducing an orthonormal basis $\{\varphi_k\}$ we have

$$K_1(x) \simeq \sum_{k=1}^{N} S_k \varphi_k(x), \qquad S_k = \int_0^{2\pi} K_1(x)\varphi_k(x)dx, \tag{425}$$

and

$$F([\theta]) \simeq \sin\left(\sum_{k=1}^{N} S_k(\varphi_k, \theta)\right). \tag{426}$$

In Figure 22 we compare the accuracy of second-order Porter's polynomial functionals to functional SSE in approximating (426). Specifically, the polynomial functionals are constructed by using the set of nodes $\widetilde{S}_2^{(m+1)}$ defined in equation (103), where a_{i_j} are sampled at Gauss-Hermite sparse grids of level 5. We recall that this set yields a rank-deficient matrix (121), which requires More-Penrose pseudoinversion (see Section 6.3.2). Correspondingly, the polynomial functionals do not interpolate (426). The SSE expansion, on the other hand, is based on Legendre polynomials of order $P = 6$. The functionals $G_k^l((\theta, \varphi_k))$ are shown in Figure 23.

6.4.1 Functional Derivatives

The first- and second-order functional derivatives of (424) are easily obtained as

$$\frac{\delta F([\theta])}{\delta\theta(x)} = K_1(x)\cos((K_1, \theta)), \tag{427}$$

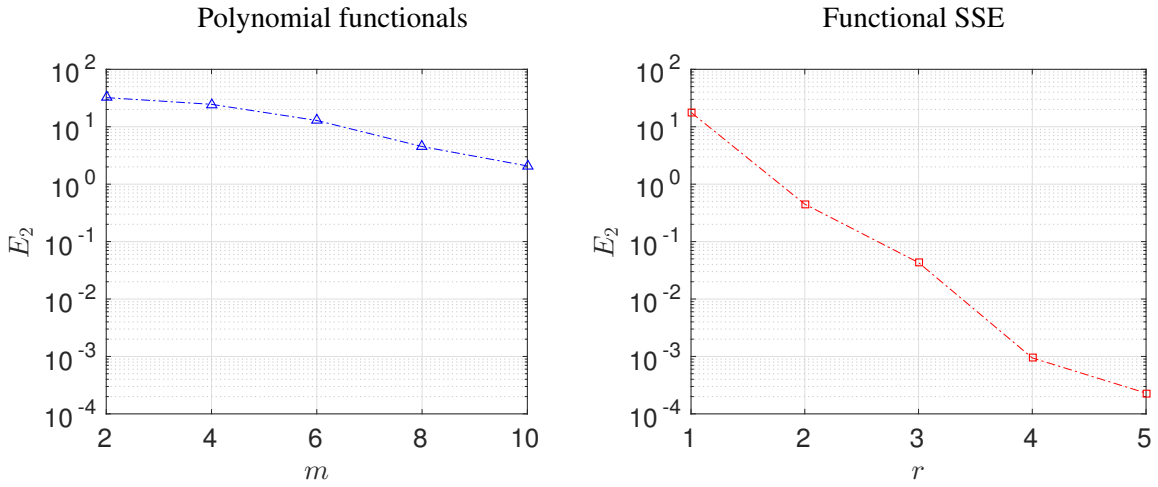

Figure 22: Approximation of the sine functional (426). Shown are the errors (413) obtained by using Porter's polynomial functionals (144) of second-order (left) with non-cardinal basis, and functional SSE (right). Specifically, we study convergence as a function of the number of interpolation nodes in Porter's method: $m = 10$ and sparse grids level 5 yields $\#\widetilde{S}_2^{(m+1)} = 1673$ nodes (see Table 3). In the SSE method we show convergence of (201) as a function of the separation rank (r). The test function space in the SSE method is chosen to be 10-dimensional.

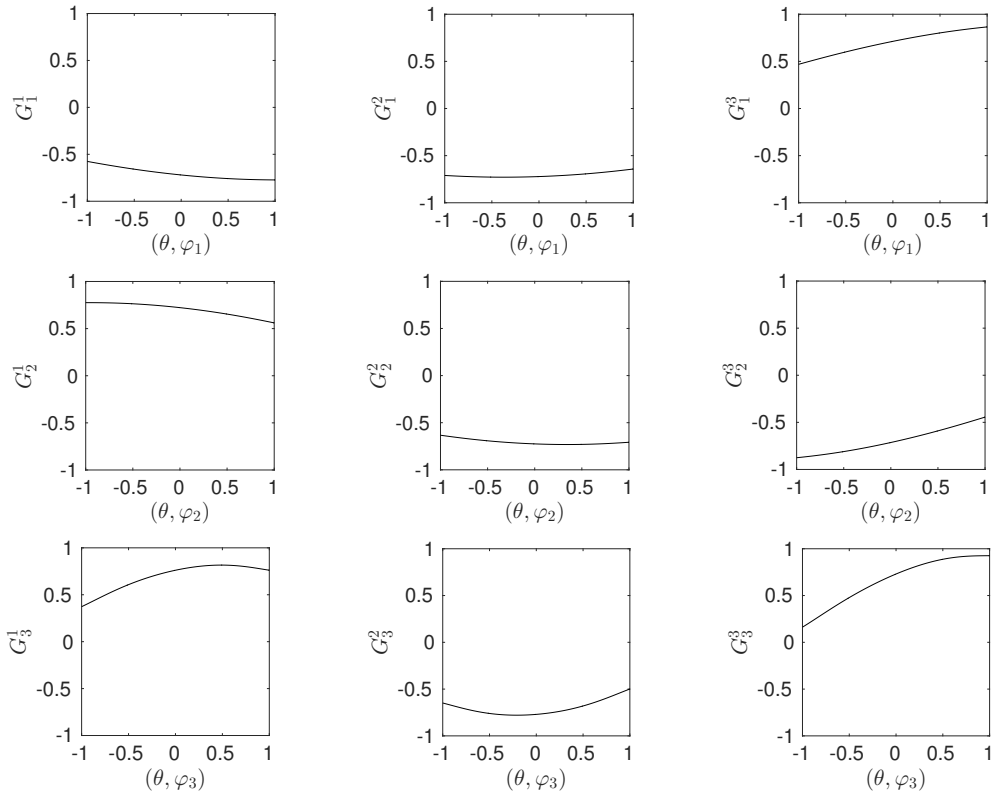

Figure 23: SSE components of the sine functional (426) versus (θ, φ_k).

$$\frac{\delta^2 F([\theta])}{\delta\theta(x)\delta\theta(y)} = -K_1(x)K_1(y)\sin((K_1,\theta)). \tag{428}$$

Note that for each $\theta(x)$, such functional derivatives are basically a rescaled version of the functions $K_1(x)$ and $K_1(x)K_1(y)$. In Figure 24 we compare the exact functional derivatives versus those obtained by functional SSE with separation rank $r = 4$. Recall that the SSE functional derivatives can be expressed as

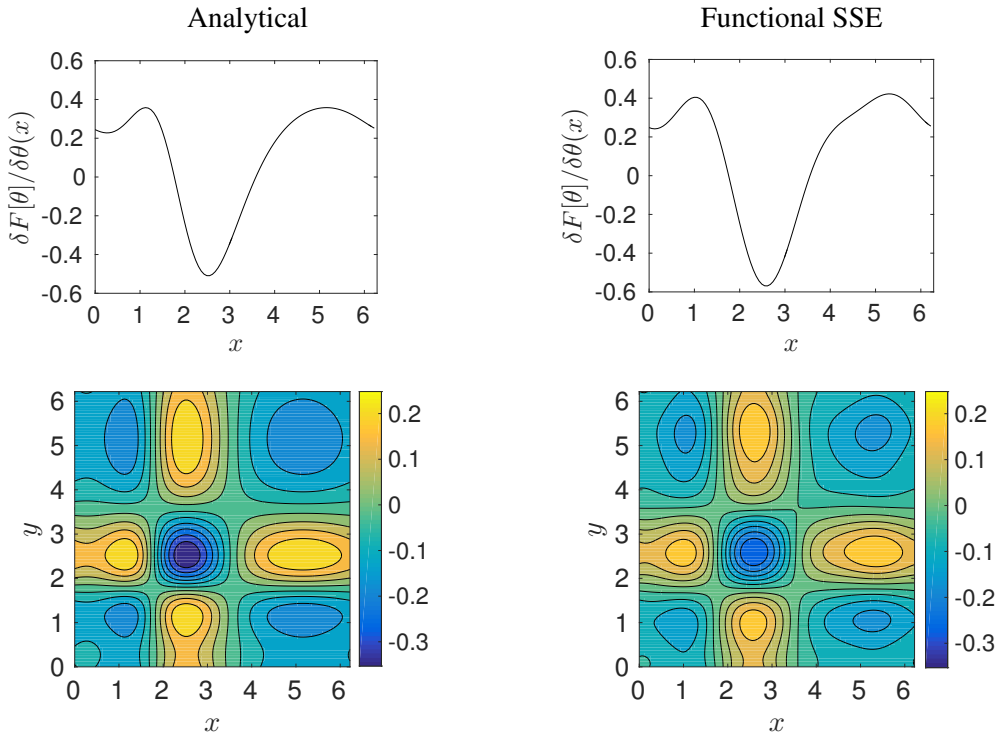

Figure 24: Sine functional (424). First- and second-order functional derivatives evaluated at $\theta(x) = 9(1 + \sin(x) + \sin(2x))/10$. Specifically, we compare the analytical results (427) and (428) (first column) versus results obtained by functional SSE (second column), equations (245) and (247).

$$\frac{\delta\widehat{F}}{\delta\theta(x)} = \sum_{k=1}^{m} \frac{\partial\widehat{F}}{\partial a_k}\varphi_k(x), \tag{429}$$

$$\frac{\delta^2\widehat{F}}{\delta\theta(x)\delta\theta(y)} = \sum_{k,j=1}^{m} \frac{\partial^2\widehat{F}}{\partial a_k \partial a_j}\varphi_k(x)\varphi_j(y), \tag{430}$$

where $\partial\widehat{F}/\partial a_k$ and $\partial^2\widehat{F}/\partial a_j\partial a_k$ are given in (249) and (250), respectively.

7 Numerical Results: Functional Differential Equations

In this Section we study the accuracy of the functional approximation methods we discussed throughout the paper in representing the numerical solution to linear functional differential equations in the form (318). In particular, we consider the following initial value problem (318)

$$\frac{\partial F([\theta],t)}{\partial t} + \int_0^{2\pi} \theta(x)\frac{\partial}{\partial x}\frac{\delta F([\theta],t)}{\delta\theta(x)}dx = H([\theta],t) \qquad F([\theta],0) = F_0([\theta]), \tag{431}$$

where $F_0([\theta])$ is a given initial condition and $H([\theta], t)$ is a known time-dependent functional. We would like to solve (431) in the space of periodic functions

$$D(F) = \{\theta(x) \in L_2([0, 2\pi]),\, \theta(0) = \theta(2\pi)\}. \tag{432}$$

This means that we would like to extract from (431) a *time-dependent nonlinear operator* $F([\theta], t)$ acting on the space of functions $D(F)$. To this end, we first assume that (431) has a *unique* solution[35]. In this hypothesis, it is rather easy to manufacture a nonlinear solution functional. The strategy is to pick an arbitrary $F([\theta], t)$ satisfying $F([\theta], 0) = F_0([\theta])$, plug it in (431) and determine the corresponding forcing functional $H([\theta], t)$. For example,

$$F([\theta], t) = e^{-(\theta,\theta)\cos(t)}, \qquad \text{where} \qquad (\theta, \theta) = \int_0^{2\pi} \theta(x)^2 dx, \tag{433}$$

yields

$$F_0([\theta]) = e^{-(\theta,\theta)} \tag{434}$$

and

$$H([\theta], t) = -\sin(t)F([\theta], t) - 2\cos(t)F([\theta], t) \int_0^{2\pi} \frac{\partial\theta(x)}{\partial x}\theta(x)dx. \tag{435}$$

For computational convenience hereafter we will consider a time-independent separable forcing functional[36]

$$H([\theta]) = e^{-(\theta,\theta)}. \tag{436}$$

In general, this yields a non-separable solution functional $F([\theta], t)$.

7.1 Time Discretization

We discretize (431) in time by using the Crank-Nicolson scheme

$$\frac{F^n([\theta]) - F^{n-1}([\theta])}{\Delta t} + \frac{1}{2}\int_0^{2\pi} \theta(x)\left[\frac{\partial}{\partial x}\frac{\delta F^n([\theta])}{\delta\theta(x)} + \frac{\partial}{\partial x}\frac{\delta F^{n-1}([\theta])}{\delta\theta(x)}\right] dx = H([\theta]), \quad n = 1, 2, ... \tag{437}$$

where $F^i([\theta]) = F([\theta]), t_i)$. This equation can be rewritten as

$$F^n([\theta]) + \frac{\Delta t}{2}\int_0^{2\pi} \theta(x)\frac{\partial}{\partial x}\frac{\delta F^n([\theta])}{\delta\theta(x)}dx = H([\theta]) + F^{n-1}([\theta]) + \frac{\Delta t}{2}\int_0^{2\pi} \theta(x)\frac{\partial}{\partial x}\frac{\delta F^{n-1}([\theta])}{\delta\theta(x)}dx. \tag{438}$$

The integration process proceeds as follows: Given $F^0([\theta]) = F_0([\theta])$ we build the right hand side of (438) and then solve for $F^1([\theta]) = F([\theta], \Delta t)$. This involves inverting linear operator

$$I + \frac{\Delta t}{2}\int_0^{2\pi} \theta(x)\frac{\partial}{\partial x}\frac{\delta}{\delta\theta(x)}dx \tag{439}$$

[35]Existence and uniqueness of solutions to functional differential equations is open problem. There are very few general results on this topic (see [50, 62, 188]). On the other hand, is easy to manufacture examples of linear functional equations for which the solution is not unique. To this end, simply consider the Hopf functional equation corresponding to the characteristic functional of the solution to an ill-posed PDE problem, i.e., a PDE with infinitely many solutions. In this case, the functional equation does not admit a unique solution, as there are many Hopf functionals (one corresponding to each solution of the PDE) solving the same functional equation.

[36]We call the forcing functional (436) separable because any series expansion of θ relative to an orthogonal basis yields a (possibly infinite) product of one dimensional functions.

which can be easily done in a finite-dimensional setting (see Section 7.2.2). Once $F^1([\theta])$ is available, we rebuild the right hand side and compute $F^2([\theta])$, etc. The computation of $F^i([\theta])$ can be done effectively in an alternating least squares or in an alternating Galerkin setting. To describe these schemes, it is convenient to define

$$K^n([\theta]) = H([\theta]) + F^{n-1}([\theta]) + \Delta t \frac{1}{2} \int_0^{2\pi} \theta(x) \frac{\partial}{\partial x} \frac{\delta F^{n-1}([\theta])}{\delta \theta(x)} dx \tag{440}$$

and the residual at time t_n

$$R^n([\theta]) = F^n([\theta]) + \Delta t \frac{1}{2} \int_0^{2\pi} \theta(x) \frac{\partial}{\partial x} \frac{\delta F^n([\theta])}{\delta \theta(x)} dx - K^n([\theta]). \tag{441}$$

In addition, we will drop the superscript n and write (441) simply as

$$R([\theta]) = F([\theta]) + \Delta t \frac{1}{2} \int_0^{2\pi} \theta(x) \frac{\partial}{\partial x} \frac{\delta F([\theta])}{\delta \theta(x)} dx - K([\theta]). \tag{442}$$

In the last equation, K can be computed explicitly by using the solution at time step t_{n-1} (previous time step), while F is the functional we are after, i.e., $F([\theta], t_n)$. In the following Sections we will formulate a numerical method to compute F given K, i.e., a method that allows us to compute $F([\theta], t_n)$ given $F([\theta], t_{n-1})$.

7.2 Functional SSE Approach

We have seen in Section 6.3.2 and Section 6.4 that a separated series expansion (SSE) of a nonlinear functional converges faster than any polynomial functional approximation. Therefore, we look for a separated series representation of the solution to (431), i.e., we replace $F^n([\theta])$ in (438) with

$$\widehat{F}([\theta]) = \sum_{k=1}^{r} \prod_{j=1}^{m} G_j^l((\theta, \varphi_j)), \qquad G_j^l((\theta, \varphi_j)) = \sum_{p=1}^{P} \beta_{jp}^l \phi_p((\theta, \varphi_j)), \tag{443}$$

where $(,)$ denotes the inner product in $L_2([0, 2\pi])$ and r is the separation rank. Note that we dropped the superscript n in agreement with the notation we set at the end of the previous Section. The functional derivative of (443) is (see Eq. (245))

$$\frac{\delta \widehat{F}([\theta])}{\delta \theta(x)} = \sum_{j=1}^{m} \sum_{l=1}^{r} \frac{\partial G_j^l}{\partial (\theta, \varphi_j)} \prod_{\substack{k=1 \\ k \neq j}}^{m} G_k^l((\theta, \varphi_k)) \varphi_j(x). \tag{444}$$

This expression allows us to write the residual (442) as

$$R([\theta]) = \sum_{k=1}^{r} \prod_{j=1}^{m} G_j^l((\theta, \varphi_j)) + \frac{\Delta t}{2} \sum_{j=1}^{m} \sum_{l=1}^{r} \frac{\partial G_j^l}{\partial (\theta, \varphi_j)} \prod_{\substack{k=1 \\ k \neq j}}^{m} G_k^l((\theta, \varphi_k)) \left(\theta, \frac{\partial \varphi_j}{\partial x} \right) - K([\theta]). \tag{445}$$

At this point, we need a criterion to determine the unknowns β_{jp}^l in all G_j^l appearing in (445). As we have mentioned in Section 5.2, we have different possibilities:

- Minimize the (functional) norm of the residual R relative to a variation of the degrees of freedom β_{jp}^l (functional least squares);
- Impose orthogonality of the residual relative to a space spanned by a certain basis (functional Galerkin).

7.2.1 Alternating Least-Squares Method

The norm of the residual (445) can be explicitly written as a functional integral

$$\|R([\theta])\|^2 = \int R([\theta])^2 \mathcal{D}[\theta]. \tag{446}$$

Minimization of (446) relative to variations of β_{qz}^n (for fixed q) yields the Euler-Lagrange equations

$$\left(R, \frac{\partial R}{\partial \beta_{qz}^n}\right)^* = 0, \tag{447}$$

where

$$\begin{aligned}\frac{\partial R}{\partial \beta_{qz}^n} =& \phi_z(a_q) \prod_{\substack{k=1\\k\neq q}}^{m} G_k^{(n)}(a_k) + \frac{\Delta t}{2}\left(\theta, \frac{\partial \varphi_q}{\partial x}\right) \frac{\partial \phi_z(a_q)}{\partial a_q} \prod_{\substack{k=1\\k\neq q}}^{m} G_k^{(n)}(a_k) + \\ & \frac{\Delta t}{2} \sum_{j=1}^{m} \left(\theta, \frac{\partial \varphi_j}{\partial x}\right) \frac{\partial G_j^{(n)}(a_j)}{\partial a_j} \sum_{\substack{q=1\\q\neq j}}^{m} \phi_z(a_q) \prod_{\substack{h=1\\h\neq j,q}}^{m} G_h^{(n)}(a_h),\end{aligned} \tag{448}$$

$$a_j = (\theta, \varphi_j), \qquad (F, G)^* = \int F([\theta]) G([\theta]) \mathcal{D}[\theta]. \tag{449}$$

The explicit form of the liner system (447) is quite involved, and it includes functional integrals in the form (449). Such integrals can be computed by using the methods outlined in Appendix C.

7.2.2 Alternating Galerkin Method

In this setting, we impose that the residual (445) is orthogonal to a suitable set of functionals in the sense of a functional inner product (328) This yields the system of equations

$$\left\{\begin{array}{rcl} \left(R([\theta]), \phi_p((\theta,\varphi_1)) G_2^j((\theta,\varphi_2)) \cdots G_m^j((\theta,\varphi_m))\right)^* &=& 0 \\ \left(R([\theta]), G_1^j((\theta,\varphi_1)) \phi_p((\theta,\varphi_2)) \cdots G_m^j((\theta,\varphi_m))\right)^* &=& 0 \\ \vdots & & \\ \left(R([\theta]), G_1^j((\theta,\varphi_1)) G_2^j((\theta,\varphi_2)) \cdots \phi_p((\theta,\varphi_m))\right)^* &=& 0 \end{array}\right. \tag{450}$$

where $G_j^n((\theta,\varphi_j))$ are known basis functionals which we represent relative to the basis ϕ_h, i.e.,

$$G_j^n((\theta,\varphi_j)) = \sum_{s=1}^{P} \beta_{js}^n \phi_s((\theta,\varphi_j)). \tag{451}$$

We assume that the test function space is bounded, i.e., that all elements in $D(\widehat{F})$ are such that

$$\sup_{x\in[0,2\pi]} |\theta(x)| \leq c \qquad \text{for some } c \in \mathbb{R}^+. \tag{452}$$

In this hypothesis, if we consider a bounded orthonormal basis $\{\varphi_k\}$ we can also bound all Fourier coefficients (θ, φ_k) as

$$|(\theta, \varphi_k)| \leq b \quad \forall k. \tag{453}$$

The functional integrals in (450) then become integrals over an infinite-dimensional bounded domain. A further simplification can be obtained if we represent $\theta(x)$ relative to an orthonormal basis $\{\varphi_k\}$,

$$\theta(x) = \sum_{k=1}^{N} a_k \varphi_k(x), \qquad a_k = (\theta, \varphi_k). \tag{454}$$

Substituting (454) into (450) yields the "method of hierarchical bases" (Section 4.3.5). To simplify the calculation here we consider $N = m$. In this assumption, the system (450) becomes

$$\begin{cases} \int_{-b}^{b} \cdots \int_{-b}^{b} R(a_1, ..., a_m) \phi_p(a_1) G_2^j(a_2) \cdots G_m^j(a_m) da_1 \cdots da_m & = 0 \\ \vdots & \\ \int_{-b}^{b} \cdots \int_{-b}^{b} R(a_1, ..., a_m) G_1^j(a_1) G_2^j(a_2) \cdots \phi_p(a_m) da_1 \cdots da_m & = 0 \end{cases} \tag{455}$$

where the finite-dimensional residual is

$$R(a_1, ..., a_m) = \sum_{l=1}^{r} \prod_{p=1}^{m} G_p^l(a_p) + \frac{\Delta t}{2} \sum_{k,j=1}^{m} a_j C_{jk} \sum_{l=1}^{r} \frac{\partial G_k^l(a_k)}{\partial a_k} \prod_{\substack{p=1 \\ p \neq k}}^{m} G_p^l(a_p) - K(a_1, ..., a_m), \tag{456}$$

and

$$C_{jk} = \int_0^{2\pi} \varphi_j(x) \frac{\partial \varphi_k(x)}{\partial x} dx. \tag{457}$$

In this setting, i.e., when θ is represented relative to the very same orthonormal basis $\{\varphi_1, ..., \varphi_m\}$ appearing in (443) (method of hierarchical bases), we have that the functional differential equation becomes an m-dimensional linear PDE[37].

Calculation of the Projected Residual The projection of the residual (456) onto the test functions

$$\phi_h(a_q) \prod_{\substack{z=1 \\ z \neq q}}^{m} G_z^n(a_z) \tag{459}$$

yields different terms which require separate computations. Let us begin with the first one, i.e.,

$$\sum_{l=1}^{r} \prod_{p=1}^{m} G_p^l(a_p). \tag{460}$$

By using simple algebra we obtain

$$\sum_{l=1}^{r} \int_{-b}^{b} G_q^l(a) \phi_h(a) da \prod_{\substack{z=1 \\ z \neq q}}^{m} \int_{-b}^{b} G_z^l(a) G_z^n(a) da = \sum_{s=1}^{P} \sum_{l=1}^{r} \left(L_q^{ln} \delta_{hs} \eta_s \right) \beta_{qs}^l, \tag{461}$$

[37] If we consider a higher dimensional test function space expressed relative to a different basis $\{\xi_j(x)\}$ then the first equation in (455) is replaced by

$$\int_{-b}^{b} \cdots \int_{-b}^{b} R(a_1, ..., a_N) \phi_p \left(\sum_{i=1}^{N} a_i \alpha_{i1} \right) \prod_{k=2}^{m} G_j^k \left(\sum_{i=1}^{N} a_i \alpha_{ij} \right) da_1 \cdots da_N = 0, \tag{458}$$

where $\alpha_{ij} = (\varphi_i, \xi_j)$. This yields a more complicated system.

where

$$L_q^{ln} = \prod_{\substack{z=1 \\ z\neq q}}^{m} \int_{-b}^{b} G_z^l(a) G_z^n(a) da = \prod_{\substack{z=1 \\ z\neq q}}^{m} \sum_{s=1}^{P} \beta_{zs}^l \gamma_{zs}^n \eta_s. \tag{462}$$

In a matrix-vector form the linear system (461) can be written as

$$\left(\boldsymbol{L}_q^T \otimes \text{diag}(\boldsymbol{\eta})\right) \boldsymbol{\beta}_q, \tag{463}$$

where $\text{diag}(\boldsymbol{\eta})$ is a diagonal matrix with entries $\eta_i = \|\phi_i\|_{L_2}^2$ (L_2 norm of ϕ_i), $\otimes$ is the Kronecker product between two matrices, and the (column) vector $\boldsymbol{\beta}_q$ is defined as

$$\boldsymbol{\beta}_q = \left[[\beta_{q1}^1 \cdots \beta_{qP}^1] \, [\beta_{q1}^2 \cdots \beta_{qP}^2] \cdots [\beta_{q1}^r \cdots \beta_{qP}^r] \right]^T. \tag{464}$$

The second term

$$\sum_{k,j=1}^{m} \int_{-b}^{b} \cdots \int_{-b}^{b} a_j C_{jk} \sum_{l=1}^{r} \frac{\partial G_k^l(a_k)}{\partial a_k} \prod_{\substack{p=1 \\ p\neq k}}^{m} G_p^l(a_p) \phi_h(a_q) \prod_{\substack{z=1 \\ z\neq q}}^{m} G_z^n(a_z) da_1 \cdots da_m \tag{465}$$

is more tricky and it requires further manipulations. In particular, it is convenient to distinguish the following different subcases:

- Terms of type 1 ($j = k = q$). In this case (465) simplifies to

$$C_{qq} \sum_{l=1}^{r} \left(a_q \frac{\partial G_q^l(a_q)}{\partial a_q} \prod_{\substack{p=1 \\ p\neq q}}^{m} G_p^l(a_p), \phi_h(a_q) \prod_{\substack{z=1 \\ z\neq q}}^{m} G_z^n(a_z) \right), \tag{466}$$

  where $(,)$ denotes the inner product associated with the multi-dimensional integrals. Equation (466) can be rewritten as

$$\sum_{l=1}^{r} \sum_{s=1}^{P} C_{qq} L_q^{ln} A_{hs} \beta_{qs}^l, \tag{467}$$

  where L_q^{ln} is as in (462) and

$$A_{hs} = \int_{-b}^{b} a \phi_h(a) \frac{\partial \phi_s(a)}{\partial a} da. \tag{468}$$

  In a matrix-vector form the linear system (467) can be written as

$$C_{qq} \left(\boldsymbol{L}_q^T \otimes \boldsymbol{A}\right) \boldsymbol{\beta}_q. \tag{469}$$

- Terms of type 2 ($j = k, q \neq k, q \neq j$). In this case (465) reduces to

$$\sum_{\substack{k=1 \\ k\neq q}}^{m} C_{kk} \sum_{l=1}^{r} \left(a_k \frac{\partial G_k^l(a_k)}{\partial a_k} \prod_{\substack{p=1 \\ p\neq k}}^{m} G_p^l(a_p), \phi_h(a_q) \prod_{\substack{z=1 \\ z\neq q}}^{m} G_z^n(a_z) \right), \tag{470}$$

i.e.

$$\sum_{\substack{k=1\\k\neq q}}^{m} C_{kk} \sum_{l=1}^{r} \int_{-b}^{b} G_q^l(a)\phi_h(a)da \int_{-b}^{b} a_k \frac{\partial G_k^l(a)}{\partial a} G_k^n(a)da \underbrace{\prod_{\substack{p=1\\p\neq k,q}}^{m} \int_{-b}^{b} G_p^l(a)G_q^n(a)da}_{L_{kq}^{ln}}. \tag{471}$$

The last equation can be rewritten compactly as

$$\sum_{s=1}^{P}\sum_{l=1}^{r} \left(\sum_{\substack{k=1\\k\neq q}}^{m} C_{kk} R_k^{ln} L_{kq}^{ln} \delta_{hs} \eta_s \right) \beta_{qs}^l, \tag{472}$$

where

$$R_k^{ln} = \sum_{i,j=1}^{P} \beta_{ki}^l \gamma_{kj}^n A_{ji} \tag{473}$$

and $\eta_s = \|\phi_s\|_{L2}^2$. Note that L_{jq}^{ln} can be written as

$$L_{jq}^{ln} = \frac{L_q^{ln}}{\int_{-b}^{b} G_j^l(a)G_j^n(a)da} = \frac{L_j^{ln}}{\int_{-b}^{b} G_q^l(a)G_q^n(a)da}. \tag{474}$$

In a matrix-vector notation the linear system (472) can be written as In a matrix-vector form the linear system (467) can be written as

$$\left(\sum_{\substack{k=1\\k\neq q}}^{m} C_{kk} \left(\boldsymbol{L}_{kq} \circ \boldsymbol{R}_k \right)^T \otimes \mathrm{diag}(\boldsymbol{\eta}) \right) \boldsymbol{\beta}_q, \tag{475}$$

where $\circ$ denotes the Hadamard (componentwise) product between two matrices.

- Terms of type 3 ($j \neq k, q = k, q \neq j$). In this case (465) reduces to

$$\sum_{\substack{j=1\\j\neq q}}^{m} C_{jq} \sum_{l=1}^{r} \left(a_j \frac{\partial G_q^l(a_q)}{\partial a_q} \prod_{\substack{p=1\\p\neq k}}^{m} G_p^l(a_p), \phi_h(a_q) \prod_{\substack{z=1\\z\neq q}}^{m} G_z^n(a_z) \right). \tag{476}$$

This can be written compactly as

$$\sum_{l=1}^{r}\sum_{s=1}^{P} \left(\sum_{\substack{j=1\\j\neq q}}^{m} C_{jq} Y_j^{ln} L_{jq}^{ln} J_{hs} \right) \beta_{qs}^l, \tag{477}$$

where

$$Y_j^{ln} = \sum_{s,q=1}^{P} \beta_{js}^l \gamma_{jq}^n Q_{sq}, \qquad Q_{hs} = \int_{-b}^{b} \phi_h(a)\phi_s(a)da, \qquad J_{hs} = \int_{-b}^{b} \phi_h(a) \frac{\partial \phi_s(a)}{\partial a} da. \tag{478}$$

The matrix-vector form of the system (477) is

$$\left(\sum_{\substack{j=1 \\ k \neq q}}^{m} C_{jq} \left(\boldsymbol{L}_{jq} \circ \boldsymbol{Y}_j \right)^T \otimes \boldsymbol{J} \right) \boldsymbol{\beta}_q. \tag{479}$$

- Terms of type 4 ($j \neq k, q \neq k, q = j$). In this case (465) reduces to

$$\sum_{\substack{k=1 \\ k \neq q}}^{m} C_{qk} \sum_{l=1}^{r} \left(a_q \frac{\partial G_k^l(a_k)}{\partial a_k} \prod_{\substack{p=1 \\ p \neq k}}^{m} G_p^l(a_p), \phi_h(a_q) \prod_{\substack{z=1 \\ z \neq q}}^{m} G_z^n(a_z) \right). \tag{480}$$

This can be written as

$$\sum_{l=1}^{r} \sum_{s=1}^{P} \left(\sum_{\substack{k=1 \\ k \neq q}}^{m} C_{qk} E_k^{ln} L_{kq}^{ln} Q_{hs} \right) \beta_{qs}^l, \tag{481}$$

where

$$E_k^{ln} = \sum_{s,q=1}^{P} \beta_{kq}^l \gamma_{ks}^n J_{sq}. \tag{482}$$

The matrix-vector form of the system (481) is

$$\left(\sum_{\substack{k=1 \\ k \neq q}}^{m} C_{qk} \left(\boldsymbol{L}_{kq} \circ \boldsymbol{E}_k \right)^T \otimes \boldsymbol{Q} \right) \boldsymbol{\beta}_q. \tag{483}$$

- Terms of type 5 ($j \neq k, q \neq k, \quad q = j$). In this case (465) reduces to

$$\sum_{\substack{k,j=1 \\ k \neq j \neq q}}^{m} C_{jk} \sum_{l=1}^{r} \left(a_j \frac{\partial G_k^l(a_k)}{\partial a_k} \prod_{\substack{p=1 \\ p \neq k}}^{m} G_p^l(a_p), \phi_h(a_q) \prod_{\substack{z=1 \\ z \neq q}}^{m} G_z^n(a_z) \right). \tag{484}$$

This can be written as

$$\sum_{s=1}^{P} \sum_{l=1}^{r} \left(\sum_{\substack{j,k=1 \\ k \neq j \neq q}}^{m} C_{jk} Y_j^{ln} E_k^{ln} L_{jkq}^{ln} \delta_{sh} \eta_s \right) \beta_{qs}^l, \tag{485}$$

where

$$L_{jkq}^{ln} = \prod_{\substack{z=1 \\ z \neq k,j,q}}^{m} \int_{-b}^{b} G_z^l(a) G_z^n(a) da. \tag{486}$$

The matrix-vector form of the system (485) is

$$\left(\sum_{\substack{j,k=1 \\ k \neq j \neq q}}^{m} C_{jk} \left(\boldsymbol{L}_{jkq} \circ \boldsymbol{E}_k \circ \boldsymbol{Y}_j \right)^T \otimes \operatorname{diag}(\boldsymbol{\eta}) \right) \boldsymbol{\beta}_q, \tag{487}$$

At this point we are done computing all projections, and it is convenient to switch back to a notation in which the time step clearly appears. In particular, we define $\boldsymbol{\beta}_q^{(n)}$ $(q = 1, ..., m)$ to be the vectors of coefficients representing the separated series expansion of the solution functional at time $t = t_n$, i.e., $\widehat{F}([\theta], t_n)$. With this notation, we can write the alternating direction Galerkin formulation of the left hand side of (438) as $\boldsymbol{M}_q^{(n)}\boldsymbol{\beta}_q^{(n)}$, where[38]

$$\begin{aligned}\boldsymbol{M}_q^{(n)} =& \boldsymbol{L}_q^T \otimes \text{diag}(\boldsymbol{\eta}) + \frac{\Delta t}{2}\left(C_{qq}\left(\left(\boldsymbol{L}_q^{(n)}\right)^T \otimes \boldsymbol{A}\right) + \sum_{\substack{j=1\\k\neq q}}^{m} C_{jq}\left(\boldsymbol{L}_{jq}^{(n)} \circ \boldsymbol{Y}_j^{(n)}\right)^T \otimes \boldsymbol{J} + \right.\\ & \sum_{\substack{k=1\\k\neq q}}^{m} C_{kk}\left(\boldsymbol{L}_{kq}^{(n)} \circ \boldsymbol{R}_k^{(n)}\right)^T \otimes \text{diag}(\boldsymbol{\eta}) + \sum_{\substack{k=1\\k\neq q}}^{m} C_{qk}\left(\boldsymbol{L}_{kq}^{(n)} \circ \boldsymbol{E}_k^{(n)}\right)^T \otimes \boldsymbol{Q} + \\ & \left. \sum_{\substack{j,k=1\\k\neq j\neq q}}^{m} C_{jk}\left(\boldsymbol{L}_{jkq}^{(n)} \circ \boldsymbol{E}_k^{(n)} \circ \boldsymbol{Y}_j^{(n)}\right)^T \otimes \text{diag}(\boldsymbol{\eta}) \right). \end{aligned} \tag{488}$$

The superscript n in $\boldsymbol{M}_q^{(n)}$ reminds us that the matrix is calculated using $\boldsymbol{\beta}_q^{(n)}$ $(q = 1, ..., m)$, i.e., the coefficients representing the solution time t_n. Now, we take care of the right hand side of (438). The first term, i.e., $H([\theta])$, is easy to compute because we have assumed that it is separable (see Eq. (436)). Its projection onto (459) immediately yields

$$f_{qh}^n = \int_{-b}^{b} e^{-a_q^2}\phi_h(a_q)da_q \prod_{\substack{z=1\\z\neq q}}^{m}\int_{-b}^{b} e^{-a_z^2}G_z^n(a_z)da_z. \tag{489}$$

The other two terms involve the solution functional at time t_{n-1}. Such terms have exactly the same form as the ones we just calculated to assemble the matrix $\boldsymbol{M}_q^{(n)}$. The only difference is that are calculated with the coefficients $\boldsymbol{\beta}_j^{(n-1)}$ $(j = 1, ..., m)$, representing the solution at the previous time step. In summary, the alternating Galerkin formulation of (438) is

$$\boldsymbol{M}_q^{(n)}\boldsymbol{\beta}_q^{(n)} = \boldsymbol{f}_q + \boldsymbol{M}_q^{(n-1)}\boldsymbol{\beta}_q^{(n-1)} \qquad q = 1, ..., m \tag{490}$$

where $\boldsymbol{f}_q$ denotes a vector with components (489), ordered as in (464).

7.3 Summary of the Algorithm

The alternating Galerkin algorithm is summarized in Figure 25. At each time step we begin by setting the separation rank r equal to 1 and initialize $[\boldsymbol{\beta}_1, ..., \boldsymbol{\beta}_m]$ at random. Then we solve iteratively (490) for fixed separation rank until the relative residual

$$\rho = \left| \frac{\left\|\hat{\hat{F}}^{(i)}\right\|^2}{\left\|\hat{F}^{(i)}\right\|^2} - 1 \right|, \qquad \hat{F}^{(i)} = \sum_{l=1}^{r}\prod_{k=1}^{m}\hat{G}_k^l(a_k), \qquad \hat{\hat{F}}^{(i)} = \sum_{l=1}^{r}\prod_{k=1}^{m}\hat{\hat{G}}_k^l(a_k), \tag{491}$$

becomes smaller than a prescribed tolerance tol_ρ. Here $\hat{F}^{(i)}$ and $\hat{\hat{F}}^{(i)}$ denote the SSE representation of the solution at time step i before and after we update $\boldsymbol{\beta}_q$ by solving the system (490). Once the relative residual

[38] Recall that $\otimes$ and $\circ$ denote, respectively, the Kronecker and the Hadamard product between two matrices.

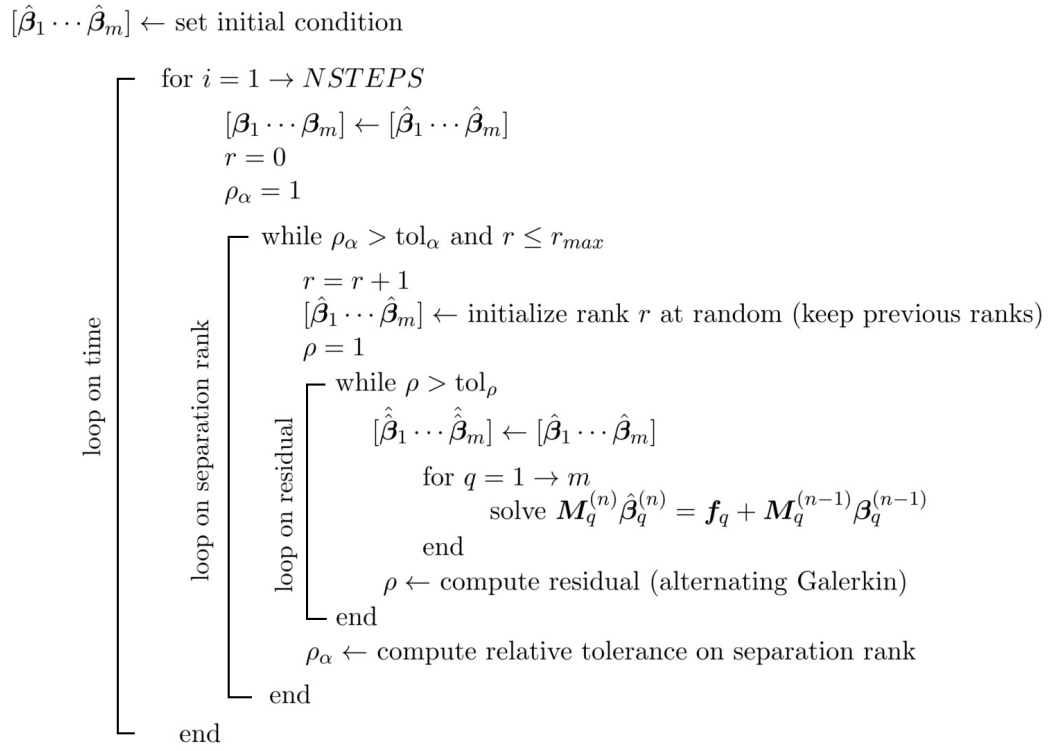
$[\hat{\boldsymbol{\beta}}_1 \cdots \hat{\boldsymbol{\beta}}_m] \leftarrow$ set initial condition
loop on time
for $i = 1 \rightarrow NSTEPS$
$[\boldsymbol{\beta}_1 \cdots \boldsymbol{\beta}_m] \leftarrow [\hat{\boldsymbol{\beta}}_1 \cdots \hat{\boldsymbol{\beta}}_m]$
$r = 0$
$\rho_\alpha = 1$
loop on separation rank
while $\rho_\alpha > \text{tol}_\alpha$ and $r \leq r_{max}$
$r = r + 1$
$[\hat{\boldsymbol{\beta}}_1 \cdots \hat{\boldsymbol{\beta}}_m] \leftarrow$ initialize rank r at random (keep previous ranks)
$\rho = 1$
loop on residual
while $\rho > \text{tol}_\rho$
$[\hat{\hat{\boldsymbol{\beta}}}_1 \cdots \hat{\hat{\boldsymbol{\beta}}}_m] \leftarrow [\hat{\boldsymbol{\beta}}_1 \cdots \hat{\boldsymbol{\beta}}_m]$
for $q = 1 \rightarrow m$
solve $\boldsymbol{M}_q^{(n)} \hat{\boldsymbol{\beta}}_q^{(n)} = \boldsymbol{f}_q + \boldsymbol{M}_q^{(n-1)} \boldsymbol{\beta}_q^{(n-1)}$
end
$\rho \leftarrow$ compute residual (alternating Galerkin)
end
$\rho_\alpha \leftarrow$ compute relative tolerance on separation rank
end
end

Figure 25: Summary of the alternating Galerkin algorithm to solve the functional equation (431).

ρ converges, we check if the ratio between the norm of the last and the first terms in the separated series expansion

$$\rho_\alpha = \frac{\alpha_r}{\alpha_1}, \qquad \alpha_i = \left\| \sum_{l=1}^{r} \prod_{k=1}^{m} \hat{\hat{G}}_k^{ri}(a_k) \right\|^2 . \tag{492}$$

is smaller than a prescribed tolerance tol_α. If not, we increase the separation rank by one and iterate again on the residual ρ, until convergence. The main difference of this algorithm with respect to separated series expansion methods [32, 28] relies on the fact that at each stage of the enrichment procedure (loop on the separation rank), we update the entire set of functions corresponding to a certain independent variable, while adaptively determining the separation rank [30]. This allows us to overcome well-known limitations of classical separated series expansion methods for hyperbolic PDEs (see [126]).

7.4 Simulation Results

We solve (431) with the alternating direction Galerkin method we described in the previous Section. We set the initial condition as

$$F_0([\theta]) = e^{-(\theta,\theta)^2}. \tag{493}$$

Moreover, we choose $b = 20$ (size of the domain in the space of Fourier coefficients $a_k = (\theta, \varphi_k)$), $P = 400$ (number of trigonometric polynomials ϕ_j we use to represent each function $G_k^l(a_k)$ in $[-b, b]$), $\text{tol}_\alpha = 10^{-12}$ (relative tolerance on the separation rank), and $\text{tol}_\rho = 10^{-6}$ (relative tolerance on the alternating

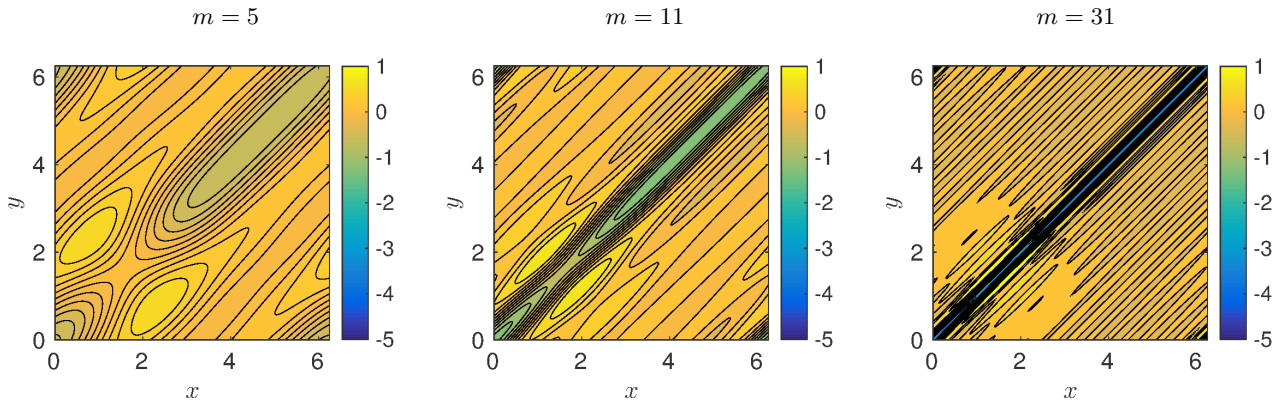

Figure 26: SSE approximation to the (singular) second-order functional derivative (494). Specifically we plot (247) evaluated at $\theta = e^{\sin(x)}/4$ for increasing values of m. It is seen that (247) converges to (494).

Galerkin iterations). As we discussed in Section 4.3.6, the initial condition (493) has a singular second-order functional derivative. In fact,

$$\frac{\delta^2 F_0[\theta]}{\delta\theta(x)\delta\theta(y)} = -2\delta(x-y) + 4\theta(x)\theta(y)e^{-(\theta,\theta)^2}. \tag{494}$$

Therefore, when we approximate F_0 it in terms of finite-dimensional separated series expansions, we will not be able to fully resolve the second-order functional derivative (no finite series expansion in terms of regular functions can). This is shown in Figure 26 where we plot the SSE approximation of (494) evaluated at $\theta = e^{\sin(x)}/4$ and for increasing values of m. It is seen that the finite dimensional representation (247) indeed converges to the Dirac delta in (494).

Fortunately, the linear equation (431) does not involve any second-order functional derivatives, and therefore we can safely study the solution functional F and its first-order functional derivative versus time. This is done in Figure 27 and Figure 28, where we show convergence in m (number of basis functions in the SSE representation) at different times. The test functions used in the evaluation of the functional derivatives do not belong to the ensemble $\{\varphi_1, .., \varphi_m\}$. To visualize the solution functional $F([\theta], t)$, we consider two different manifolds of functions, i.e., two surfaces in the test function space (351)

$$\theta(x; a, b) = \frac{1}{4}\left(ae^{\sin(2x)} + be^{\sin(20x)^6}\right), \tag{495}$$

$$\theta(x; a, b) = \frac{1}{4}a\sin(x)\log(b^2\cos(6x)^2 + 1). \tag{496}$$

In Figure 29 we plot $F([\theta(x; a, b)], t)$ versus a and b.

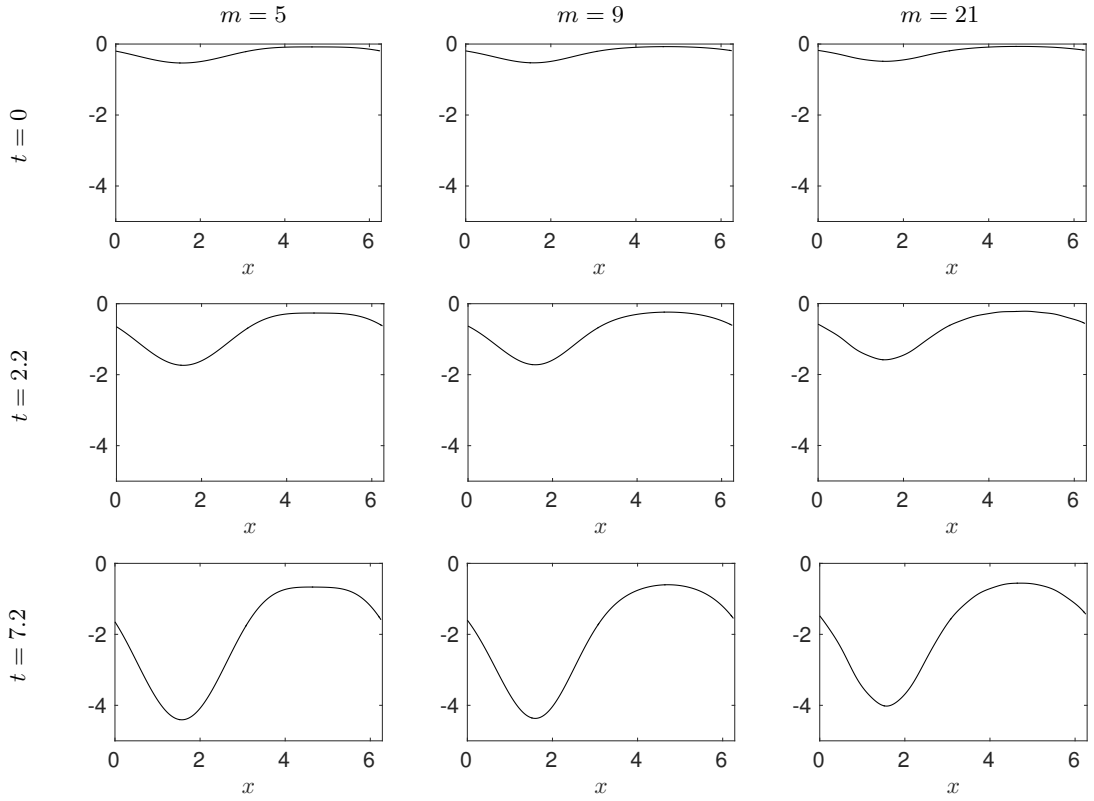

Figure 27: Solution to the functional differential equation (431). Shown are the time snapshots of the first-order functional derivative $\delta F([\theta], t)/\delta\theta(x)$ evaluated at $\theta(x) = \exp(\sin(x))/4$. It is seen that as we increase the resolution m (number of orthonormal functions $\varphi_k(x)$ used in the discretization of the functional differential equation), we convergence to a unique solution.

A Functional Fourier Transforms

Functional Fourier transforms can be defined as a continuum limit of multi-variate Fourier transforms. To introduce this concept in a simple and intuitive way, let us consider the expression of the joint probability density function of n random variables in terms of the joint characteristic function

$$p(a_1, ..., a_n) = \frac{1}{(2\pi)^{n/2}} \int_{-\infty}^{\infty} \cdots \int_{-\infty}^{\infty} e^{-i(a_1 b_1 + \cdots a_n b_n)} \phi(b_1, ..., b_n) db_1 \cdots db_n. \tag{497}$$

If we think of a_i and b_i as values of two continuous functions $a(x)$ and $b(x)$ at locations $x_i \in \mathbb{R}$, then it makes sense to consider what happens to p and ϕ as we send the number of collocation points to infinity. In this limit, the joint probability density function $p(a_1, ..., a_n)$ becomes a probability density functional $P([a(x)])$, while the joint characteristic function $\phi(b_1, ..., b_n)$ becomes a (Hopf) characteristic functional. This allows us to define the functional Fourier transform as

$$P([a(x)]) = \int e^{-i \int a(x) b(x) dx} \Phi([b(x)]) \mathcal{D}[b(x)], \tag{498}$$

where

$$\mathcal{D}[b(x)] = \lim_{n \to \infty} \frac{1}{(2\pi)^{n/2}} \prod_{i=1}^{n} db(x_i). \tag{499}$$

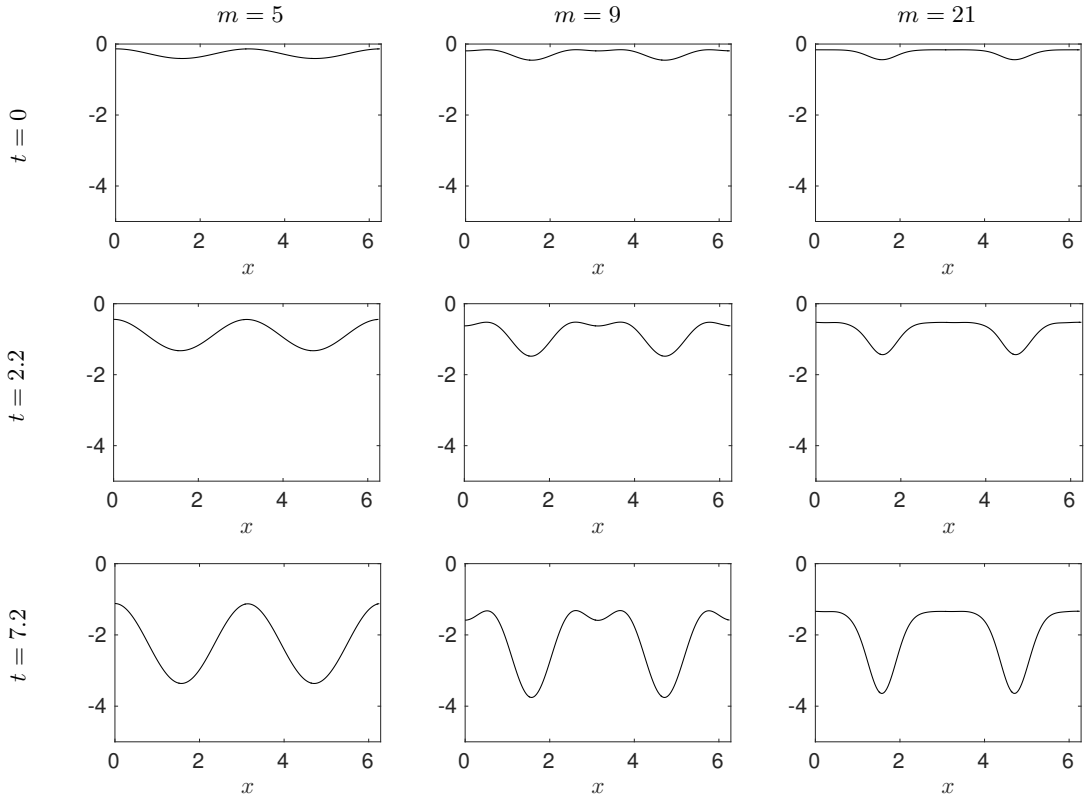

Figure 28: Same as in Figure 27 but with the test function $\theta(x) = e^{\sin(x)^6/4}$.

Equation (498) establishes the connection between the Hopf functional and the probability density functional of a random field. It also allows us to define special functionals, such as the Dirac delta functional

$$\delta[a(x)] = \int e^{-i\int a(x)b(x)dx}\mathcal{D}[b(x)]. \tag{500}$$

By using this definition, it is easy to show that the probability density functional can be expressed as an average of Dirac delta functional

$$\begin{aligned} P([a(x)]) &= \langle \delta[a(x) - u(x;\omega)]\rangle \\ &= \left\langle \int e^{-i\int a(x)b(x)dx + i\int u(x;\omega)b(x)dx}\mathcal{D}[b(x)] \right\rangle \\ &= \int e^{-i\int a(x)b(x)dx} \left\langle e^{i\int u(x;\omega)b(x)dx}\right\rangle \mathcal{D}[b(x)] \\ &= \int e^{-i\int a(x)b(x)dx}\Phi([b(x)])\mathcal{D}[b(x)]. \end{aligned}$$

B Functional Derivatives

Consider a real or a complex valued functional $F([\theta(x)])$ defined on a function space $D(F)$ (domain of the functional). We say that the functional F is differentiable at $\theta(x)$ if the limit

$$\lim_{\epsilon\to 0}\frac{F([\theta(x)+\epsilon\eta(x)]) - F([\theta(x)])}{\epsilon} \tag{501}$$

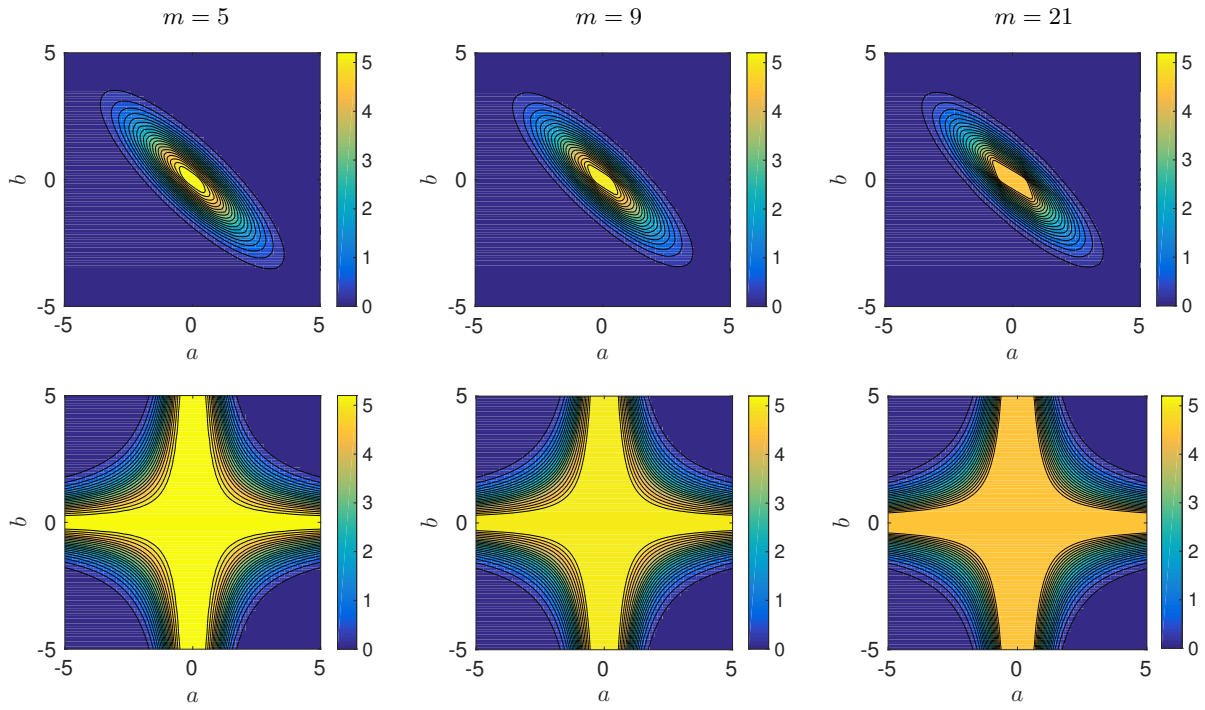

Figure 29: Functional differential equation (431). Solution functional $F([\theta], t)$ at $t = 4.7$ evaluated on two different manifolds of test functions. Specifically, we consider $\theta(x; a, b) = (a \exp(\sin(2x)) + b \exp(\sin(20x)^6))/4$ (first row) and $\theta(x; a, b) = (a \sin(x) \log(b^2 \cos(6x)^2 + 1))/4$ (second row). Shown are results for different m (number of basis functions representing the test function space (351)).

exists and it is finite. The quantity is (501) is known as *Gâteaux differential* of F in the direction of $\eta(x)$ (see, e.g., [172]). Under rather general assumptions such derivative can be represented as a linear operator [123, 172, 174] acting on $\eta(x)$. For small ϵ we have

$$F([\theta(x) + \epsilon\eta(x)]) = F([\theta(x)]) + \epsilon L([\theta(x)])\eta(x) + R_1([\epsilon\eta(x); \theta(x)]), \tag{502}$$

In this series $L([\theta(x)])$ is a linear operator that sends the function $\eta(x)$ to a real or a complex number, while R_1 represents a reminder term. It is clear that $L(\theta(x))$ involves some kind of integration with respect to x, otherwise we are not going to get a number when applied to the function $\eta(x)$. In particular, we look for a representation in the form

$$L([\theta(x)])\eta(x) = \int \frac{\delta F([\theta])}{\delta\theta(x)} \eta(x) dx, \tag{503}$$

where the kernel function $\delta F([\theta])/\delta\theta(x)$ is a functional of θ and a function of x. At this point it is convenient to establish a parallel between functionals and functions in m variables. Recall that the differential of a scalar field $f(a_1, .., a_m)$ in the direction $\widehat{n} = (n_1, ..., n_m)$ is the scalar product of the gradient ∇f and $\widehat{n}$, i.e.,

$$df_{\widehat{n}} = \nabla f \cdot \widehat{n}. \tag{504}$$

By analogy, $\delta F([\theta])/\delta\theta(x)$ in (503) can be considered as an infinite-dimensional gradient, known as *first-order functional derivative of F with respect to θ*.

The next question is: how do we compute such functional derivative? A possible way is to use the definition (501) and a compactly supported class of test functions, e.g., functions that are nonzero only in a

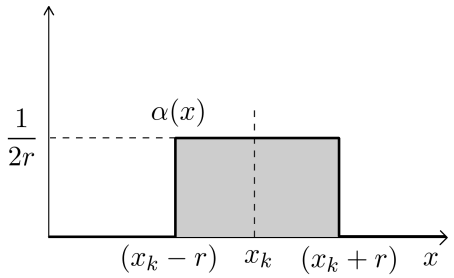

Figure 30: A possible function for the calculation of the kernel (505) at x_k. If we set $\mathcal{I}_{x_k}(r) = \{x \in \mathbb{R} : |x - x_k| \leq r\}$, then we have $\int_{\mathcal{I}_{x_k}(r)} \alpha(x)dx = 1$, independently on r.

small neighbor $\mathcal{I}_x(r)$ of radius r centered at x. Such functions could be compactly supported elements of a Dirac delta sequence (see Figure 30), or even a delta function itself. This allows us to write

$$\frac{\delta F([\theta(x)])}{\delta\theta(x)} = \lim_{\epsilon,r\to 0} \frac{F([\theta(x) + \epsilon\alpha(x)]) - F([\theta(x)])}{\epsilon \int_{\mathcal{I}_x(r)} \alpha(y)dy} \tag{505}$$

In particular, if we set $\alpha(y) = \delta(x - y)$ then the denominator in (505) simply reduces to ϵ, yielding the formula

$$\frac{\delta F([\theta])}{\delta\theta(x)} = \lim_{\epsilon\to 0} \frac{F([\theta(y) + \epsilon\delta(x - y)]) - F([\theta(y)])}{\epsilon}. \tag{506}$$

Functional derivatives of higher order can be defined in a similar manner. For example, the second order functional derivative of F is

$$\frac{\delta^2 F([\theta])}{\delta\theta(x)\delta\theta(y)} = \frac{d}{d\epsilon}\left[\frac{\delta F([\theta(z) + \epsilon\delta(z - y)])}{\delta\theta(x)}\right]_{\epsilon=0}. \tag{507}$$

Note that (507) is a function and x and y and a functional of $\theta(x)$.

An Example: Functional Derivatives of the Hopf Functional Let us consider the Hopf characteristic functional (29). The Gâteaux differential of $\Phi([\theta(x)])$ along η is

$$\begin{aligned}
\frac{d}{d\epsilon}\Phi([\theta(x) + \epsilon\eta(x)])\bigg|_{\epsilon=0} &= i\left\langle \exp\left[\int_a^b u(x;\omega)\theta(x)dx\right] \int_a^b u(x;\omega)\eta(x)dx \right\rangle \\
&= \int_a^b i\left\langle \exp\left[\int_a^b u(x;\omega)\theta(x)dx\right] u(x;\omega)\right\rangle \eta(x)dx \\
&= \int_a^b \frac{\delta\Phi([\theta])}{\delta\theta(x)}\eta(x)dx.
\end{aligned} \tag{508}$$

This implies that

$$\frac{\delta\Phi([\theta])}{\delta\theta(x)} = i\left\langle u(x;\omega)\exp\left[i\int_a^b u(x;\omega)\theta(x)dx\right]\right\rangle \tag{509}$$

is the first-order functional derivative of $\Phi([\theta])$ at $\theta(x)$. Note that (509) is itself a functional of $\theta(x)$, which depends also on x. As a result, $\delta\Phi([\theta])/\delta\theta(x)$ has two types of derivatives: an ordinary one with respect

to x, and a functional one with respect to $\theta(x)$. The latter is the the second-order functional derivative of $\Phi([\theta(x)])$. A simple calculation shows that

$$\frac{\delta^2\Phi([\theta])}{\delta\theta(x)\delta\theta(y)} = i^2\left\langle u(y;\omega)u(x;\omega)\exp\left[i\int_a^b u(x;\omega)\theta(x)dx\right]\right\rangle. \tag{510}$$

Proceeding similarly, we can obtain the expression of higher-order functional derivatives. For instance, the third-order one is explicitly given as

$$\frac{\delta^3\Phi([\theta])}{\delta\theta(x)\delta\theta(y)\delta\theta(z)} = i^3\left\langle \exp\left[i\int_a^b u(x;\omega)\theta(x)dx\right]u(y;\omega)u(x;\omega)u(z;\omega)\right\rangle. \tag{511}$$

Now, suppose we have available $\delta\Phi([\theta])/\delta\theta(x)$. Based on the definition (509), we see that

$$\langle u(x;\omega)\rangle = \frac{1}{i}\frac{\delta\Phi([0])}{\delta\theta(x)}. \tag{512}$$

Similarly, higher order moments and cumulants of the random function $u(x;\omega)$ can be obtained by computing higher order functional derivatives of $\Phi([\theta(x)])$ and $\ln\Phi([\theta(x)])$, respectively, and evaluating them at $\theta(x) = 0$. In particular, the second- and third-order correlation functions are, respectively

$$\langle u(x;\omega)u(y;\omega)\rangle = \frac{1}{i^2}\frac{\delta^2\Phi([0])}{\delta\theta(x)\delta\theta(y)}, \quad \langle u(x;\omega)u(y;\omega)u(z;\omega)\rangle = \frac{1}{i^3}\frac{\delta^3\Phi([0])}{\delta\theta(x)\delta\theta(y)\delta\theta(z)}. \tag{513}$$

C Evaluation of Functional Integrals

Functional integrals in the form[39]

$$\int_{D(F)} F([\theta])W([\theta])\mathcal{D}[\theta] \tag{514}$$

arise naturally in many branches of physics and mathematics, e.g., in quantum and statistical mechanics, field theory, quantum optics, solid state physics, and financial mathematics [88, 191, 13, 4]. Analytical results for functional integrals are available only in few exceptional cases, and therefore one usually has to resort to numerical approximation techniques [43].

Perhaps, the most classical one is Monte Carlo (MC), which gives results as an ensemble average over a large number of realizations of the test function $\theta(x)$, i.e.,

$$\int F([\theta])W[\theta]\mathcal{D}[\theta] \simeq \frac{1}{N}\sum_{k=1}^{N}\int_a^b F([\theta_k(x)])dx. \tag{515}$$

Each integral in the series corresponds to a specific *path* $\theta_k(x)$, which is drawn from the probability distribution $W([\theta])$. Monte Carlo methods have slow convergence rate and therefore they require significant computational resources to achieve good accuracy. In a renormalized perturbation theory setting [110], the functional integral can be expanded relative to a certain parameter and the terms in the series expansion have a structure determined by the order of the perturbation parameter. This yields well-know diagrammatic representations of functional (path) integrals, as a sum over all possible paths consistent with the order of the perturbation parameter [74, 88]. Alongside statistical methods and perturbation series expansions, deterministic techniques were also proposed to evaluate functional integrals. These include, path summation based on short time propagators [148], fast Fourier transforms [45], HDMR expansions [136] and functional

[39] In (514) F is a measurable functional on a complete metric space $D(F)$ and $W > 0$ is a functional integral measure.

approximation techniques [101]. An intuitive way to calculate functional integrals is to consider a finite-dimensional subset of $D_N \subset D(F)$, e.g., the linear span of the orthonormal basis $\{\varphi_1, ..., \varphi_N\}$. In this setting, $\theta(x)$ admits the representation

$$\theta(x) = \sum_{k=1}^{N} a_k \varphi_k(x), \qquad a_k = (\theta, \varphi_k)\,. \tag{516}$$

If we substitute (516) into (514) we obtain the multivariate integral

$$\int_{D_N} F\left(a_1, ..., a_N\right) W(a_1, ..., a_N) da_1 \cdots da_N. \tag{517}$$

This form includes both modal and nodal discretizations of the functional integral (514). For example, if (71) is an interpolant through N nodes then $a_j = \theta(x_j)$ and (517) becomes

$$\int_{D_N} F\left(\theta(x_1), ..., \theta(x_N)\right) W(\theta(x_1), ..., \theta(x_N)) d\theta(x_1) \cdots d\theta(x_N). \tag{518}$$

In this formulation, we obtain the functional integral (514) as the limit of an infinite number of nodes $N \to \infty$. This is the viewpoint taken in quantum mechanics and field theory to define path integrals [88, 191], i.e., integrals over suitable trajectories of functions.

C.1 Functional Integrals Involving SSE

Functional integrals involving separated series expansions can be written in the general form

$$\int F\left((\theta, \varphi_1), ..., (\theta, \varphi_m)\right) \mathcal{D}[\theta]. \tag{519}$$

An interesting question is whether such integrals can be simplified and reduced to finite-dimensional integrals over the range of the Fourier coefficients (θ, φ_j). Perhaps, the easiest way answer this question is to represent $\theta(x)$ relative to a basis $\{\xi_1(x), ..., \xi_N(x)\}$, i.e.,

$$\theta(x) = \sum_{k=1}^{N} a_k \xi_k(x). \tag{520}$$

and assume that $a_1, ..., a_N$ are in a compact subset $\Omega_1 \in \mathbb{R}^N$. A substitution of (520) into (519) yields

$$\int F\left((\theta, \varphi_1), ..., (\theta, \varphi_m)\right) \mathcal{D}[\theta] \simeq \int_{\Omega_1} F\left(\sum_{k=1}^{N} a_k \alpha_{1k}, ..., \sum_{k=1}^{N} a_k \alpha_{mk}\right) da_1 \cdots da_N, \tag{521}$$

were $\alpha_{ij} = (\varphi_i, \xi_j)$. Now, consider the change of variables

$$\begin{cases} b_1 = \displaystyle\sum_{k=1}^{N} a_k \alpha_{1k} \\ \vdots \\ b_m = \displaystyle\sum_{k=1}^{N} a_k \alpha_{mk} \\ b_{m+1} = a_{m+1} \\ \vdots \\ b_N = a_N \end{cases} \tag{522}$$

i.e., the linear transformation

$$\begin{bmatrix} b_1 \\ \vdots \\ b_m \\ b_{m+1} \\ \vdots \\ b_N \end{bmatrix} = \underbrace{\begin{bmatrix} \alpha_{11} & \alpha_{12} & \cdots & \alpha_{1N} \\ \vdots & \vdots & & \vdots \\ \alpha_{m1} & \alpha_{m2} & \cdots & \alpha_{mN} \\ 0 & 1 & \cdots & 0 \\ \vdots & \vdots & \ddots & \vdots \\ 0 & 0 & \cdots & 1 \end{bmatrix}}_{A} \begin{bmatrix} a_1 \\ \vdots \\ a_m \\ a_{m+1} \\ \vdots \\ a_N \end{bmatrix} \tag{523}$$

Substituting (522) into (521) and using the well-known theorem to change variables in multi-dimensional integrals we obtain

$$\int_{\Omega_1} F\left(\sum_{k=1}^{N} a_k\alpha_{1k}, ..., \sum_{k=1}^{N} a_k\alpha_{mk}\right) da_1 \cdots da_N = \frac{1}{\det(A)} \int_{A(\Omega_1)} F(b_1, ..., b_m) db_1 \cdots db_N. \tag{524}$$

The last integral can be rewritten as an integral in m dimensions multiplied by a weight function, i.e.,

$$\int_{A(\Omega_1)} F(b_1, ..., b_m) db_1 \cdots db_N = \int_{\Omega_2} F(b_1, ..., b_m) w(b_1, ..., b_m) db_1 \cdots db_m. \tag{525}$$

Therefore,

$$\int F\left((\theta, \varphi_1), ..., (\theta, \varphi_m)\right) \mathcal{D}[\theta] \simeq \int_{\Omega_2} F(b_1, ..., b_m) w(b_1, ..., b_m) db_1 \cdots db_m. \tag{526}$$

Example: Let us provide a simple example of equation (525). Consider the half-disk

$$A(\Omega_1) = \{(b_1, b_2) \in \mathbb{R}^2 | b_1^2 + b_2^2 \leq 1 \cap b_2 \geq 0\} \tag{527}$$

and the integral

$$\begin{aligned} \int_{A(\Omega_1)} f(b_1) db_1 db_2 &= \int_{-1}^{1} \int_{0}^{\sqrt{1-b_1^2}} f(b_1) db_1 db_2 \\ &= \int_{-1}^{1} f(b_1) \underbrace{\sqrt{1 - b_1^2}}_{w(b_1)} db_1. \end{aligned} \tag{528}$$

Remark: If the linear transformation (523) sends a hyper-rhomboid $\Omega_1 = A^{-1}([-b, b]^N)$ into the hyper-cube $[-b, b]^N$ then

$$\int_{\Omega_1} F\left(\sum_{k=1}^{N} a_k\alpha_{1k}, ..., \sum_{k=1}^{N} a_k\alpha_{mk}\right) da_1 \cdots da_N = \frac{(2b)^{N-m}}{\det(A)} \int_{[-b,b]^N} F(b_1, ..., b_m) db_1 \cdots db_m \tag{529}$$

Another way to prove (526) is to consider a discretization of the inner products (θ, φ_j), i.e., a quadrature formula in terms of weights z_k

$$(\theta, \varphi_j) = \sum_{k=1}^{N} \theta(x_k) \varphi_j(x_k) z_k. \tag{530}$$

This yields the following representation of the functional integral (519)

$$\underbrace{\int\cdots\int}_{m} F\left(\sum_{k=1}^{N}\theta(x_k)\varphi_1(x_k)z_k,...,\sum_{k=1}^{N}\theta(x_k)\varphi_m(x_k)z_k\right)d\theta(x_1)\cdots d\theta(x_N). \tag{531}$$

Next, consider the change of variables ($m < N$)

$$\begin{cases} y_1 = \displaystyle\sum_{k=1}^{N}\theta(x_k)\varphi_1(x_k)z_k \\ \vdots \\ y_m = \displaystyle\sum_{k=1}^{N}\theta(x_k)\varphi_1(x_k)z_k \\ y_{m+1} = \theta(x_{m+1}) \\ \vdots \\ y_N = \theta(x_N) \end{cases} \tag{532}$$

By inverting this transformation (in general this cannot be done analytically) we can rewrite the integral (531) as

$$\underbrace{\int\cdots\int}_{m} F\left(y_1,...,y_m\right)w(y_1,...,y_m)dy_1\cdots dy_m. \tag{533}$$

Example: Consider

$$\int_0^1\int_0^1\cos(x_1+x_2)dx_1dx_2, \tag{534}$$

the transformation

$$y_1 = x_1 + x_2 \qquad y_2 = x_2 \tag{535}$$

and the inverse

$$x_1 = y_1 - y_2 \qquad y_2 = x_2. \tag{536}$$

The Jacobian determinant of such transformation is 1 (volume preserving). The unit square $[0,1]^2$ in the (x_1,x_2) plane is sent into a rhomboid in the (y_1,y_2) plane by (535) (see Figure 31). Therefore,

$$\begin{aligned}\int_0^1\int_0^1\cos(x_1+x_2)dx_1dx_2 &= \int_0^1\cos(y_1)dy_1\int_0^{y_1}dy_2 + \int_1^2\cos(y_1)dy_1\int_{y_1-1}^1 dy_2 \\ &= \int_0^1\cos(y_1)y_1dy_1 + \int_1^2\cos(y_1)(2-y_1)dy_1 \\ &= \int_0^2\cos(y_1)\underbrace{\left(y_1I_{[0,1]} + (2-y_1)I_{[1,2]}\right)}_{w(y_1)}dy_1,\end{aligned} \tag{537}$$

where $I_{[a,b]}$ is the indicator function on $[a,b]$. This shows how to transform the two-dimensional integral (534) into the one-dimensional one (537) involving a weight function $w(y_1)$ supported over the range of (x_1+x_2) ($x_1,x_2\in[0,1]$).

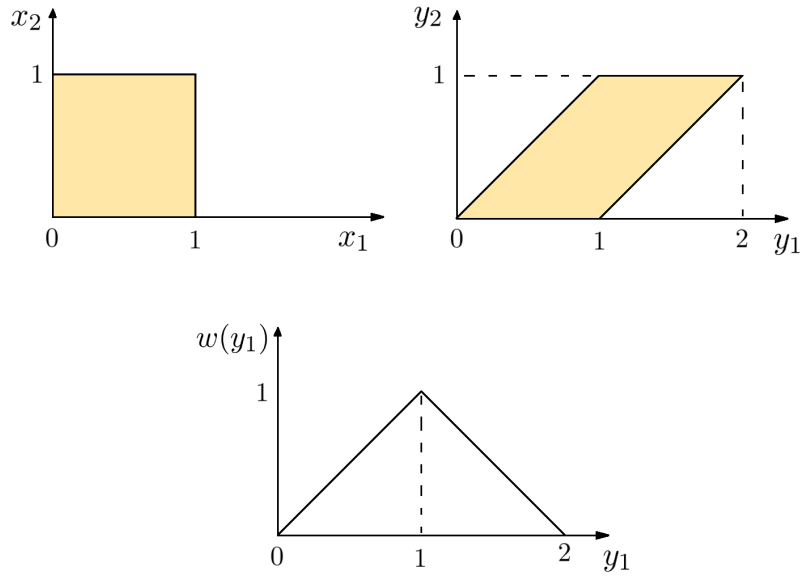

Figure 31: Transformation of the unit square under the linear map (535) and weight function $w(y_1)$ appearing in the integral (537).

References

[1] G. Ahmadi. An approximate method for solving Hopf's equation of Burgers's model of turbulence. *Appl. Sci. Res.*, 32:207–215, 1976.

[2] T. Alankus. The generating functional for the probability density functions of Navier-Stokes turbulence. *J. Stat. Phys.*, 53(5-6):1261–1271, 1988.

[3] G. Allasia and C. Bracco. Lagrange interpolation on arbitrarily distributed data in Banach spaces. *Numerical Functional Analysis and Optimization*, 32(2):111–125, 2011.

[4] D. J. Amit and V. Martín-Mayor. *Field theory, the renormalization group and critical phenomena*. World Scientific Publishing, 2005.

[5] M. Avellaneda. Statistical properties of shocks in Burgers turbulence, II: Tail probabilities for velocities, shock-strengths and rarefaction intervals. *Commun. Math. Phys.*, 169(1):45–59, 1995.

[6] N. V. Azbelev, V. P. Makasimov, and L. F. Rakhmatullina. *Introduction to the theory of functional differential equations: methods and applications*. Hindawi Publishing Corporation, first edition, 2007.

[7] J. Baldeaux and M. Gnewuch. Optimal randomized multilevel algorithms for infinite-dimensional integration on function spaces with anova-type decomposition. *SIAM J. Numer. Anal.*, 52(3):1128–1155, 2014.

[8] M. Van Barel, M. Humet, and L. Sorber. Approximating optimal point configurations for multivariate polynomial interpolation. *Electronic Transactions on Numerical Analysis*, 42:41–63, 2014.

[9] V. Barthelmann, E. Novak, and K. Ritter. High dimensional polynomial interpolation on sparse grids. *Advances in Computational Mechanics*, 12:273–288, 2000.

[10] T. W. Baumgarte and S. L. Shapiro. *Numerical Relativity: Solving Einstein's Equations on the Computer*. Cambridge, 2010.

[11] C. M. Bender, K. A. Milton, and V. M. Savage. Solution of Schwinger-Dyson equation for pt-symmetric quantum field theory. *Phys. Rev. D*, 62:085001(1–13), 2000.

[12] A. Bensoussan, G. Da Prato, M. C. Delfour, and S. K. Mitter. *Representation and control of infinite dimensional systems*. Birkhäuser, second edition, 2006.

[13] M. J. Beran. *Statistical continuum theories*. New York: Interscience Publishers, 1968.

[14] A. Bertuzzi, A. Gandolfi, and A. Germani. Causal polynomial approximation for input-output maps on Hilbert spaces. *Math. Systems Theory*, 14:339–392, 1981.

[15] A. Bertuzzi, A. Gandolfi, and A. Germani. A Weierstrass-like theorem for real, separable Hilbert spaces. *Journal of Approximation Theory*, 32:76–81, 1981.

[16] G. Beylkin, J. Garcke, and M. J. Mohlenkamp. Multivariate regression and machine learning with sums of separable functions. *SIAM J. Sci. Comput.*, 31:1840–1857, 2009.

[17] S. E. Bodner. Turbulence theory with a time-varying Wiener-Hermite basis. *Phys. Fluids*, 12(1):33–38, 1969.

[18] C. Bonatto, J. A. C. Gallas, and Y. Ueda. Chaotic phase similarities and recurrences in a damped-driven Duffing oscillator. *Phys. Rev. E*, 77:026217(1–5), 2008.

[19] L. Bos, S. De Marchi, A. Sommariva, , and M. Vianello. Computing multivariate Fekete and Leja points by numerical linear algebra. *SIAM J. Numer. Anal.*, 48(5):1984–1999, 2010.

[20] H. Broer, C. Simó, and R. Vitolo. Bifurcations and strange attractors in the Lorenz-84 climate model with seasonal forcing. *Nonlinearity*, 15:1205–1267, 2002.

[21] H. J. Bungartz and M. Griebel. Sparse grids. *Acta Numerica*, 13:147–269, 2004.

[22] R. H. Cameron and W. T. Martin. The orthogonal development of non-linear functionals in series of Fourier-Hermite functionals. *Annals of Mathematics*, 48(2):385–392, 1947.

[23] Y. Cao, Z. Chen, and M. Gunzbuger. ANOVA expansions and efficient sampling methods for parameter dependent nonlinear PDEs. *Int. J. Numer. Anal. Model.*, 6:256–273, 2009.

[24] H. A. Carteret, A. Higuchi, and A. Sudbery. Multipartite generalization of the Schmidt decomposition. *J. Math. Phys.*, 41(12):7932–7939, 2000.

[25] M. Chaika and S. I. Perlman. A Weierstrass theorem for a complex separable Hilbert space. *Journal of Approximation Theory*, 32:76–81, 1981.

[26] H. Chen, S. Chen, and R. H. Kraichnan. Probability distribution of a stochastically advected scalar field. *Phys. Rev. Lett.*, 63(24):2657–2660, 1989.

[27] W. Cheney and W. Light. *A course in approximation theory*. Brooks/Cole publishing company, 2000.

[28] F. Chinesta, R. Keunings, and A. Leygue. *The Proper Generalized Decomposition for Advanced Numerical Simulations*. Springer, 2014.

[29] A. Chkifa, A. Cohen, and C. Schwab. High-dimensional adaptive sparse polynomial interpolation and applications to parametric PDEs. *Found. Comput. Math.*, 14:601–633, 2014.

[30] H. Cho, D. Venturi, and G. E. Karniadakis. Numerical methods for high-dimensional probability density function equation. *J. Comput. Phys*, 315:817–837, 2016.

[31] P. G. Constantine. *Active subspaces: emerging ideas for dimension reduction in parameter studies*. SIAM Spotlights, 2015.

[32] T. L. D. Croft. *Proper generalized decomposition: theory and applications*. PhD thesis, School of Mathematics, Cardiff University, 2015.

[33] J. Dick and M. Gnewuch. Infinite-dimensional integration in weighted Hilbert spaces: anchored decompositions, optimal deterministic algorithms, and higher-order convergence. *Foundations Comput. Math.*, 14(5):1027–1077, 2014.

[34] J. Dick, F. Y Kuo, and I. H. Sloan. High-dimensional integration: The quasi-Monte Carlo way. *Acta Numerica*, 22:133–288, 2013.

[35] G. Dimarco and L. Pareschi. Numerical methods for kinetic equations. *Acta Numerica*, 23(4):369–520, 2014.

[36] A. Doostan and G. Iaccarino. A least-squares approximation of partial differential equations with high-dimensional random inputs. *J. Comp. Phys.*, 228(12):4332–4345, 2009.

[37] A. Doostan and H. Owhadi. A non-adapted sparse approximation of PDEs with stochastic inputs. *J. Comput. Phys.*, 230(8):3015–3034, 2011.

[38] A. Doostan, A. Validib, and G. Iaccarino. Non-intrusive low-rank separated approximation of high-dimensional stochastic models. *Comput. Methods Appl. Mech. Engrg.*, 263:42–55, 2013.

[39] C. Dopazo and E. E. O'Brien. Functional formulation of nonisothermal turbulent reactive flow. *Physics of Fluids*, 17(11):1968–1975, 1998.

[40] T. A. Driscoll and B. Fornberg. Interpolation in the limit of increasingly flat radial basis functions. *Comput. Math. Appl.*, 43:413–422, 2002.

[41] W. E, E. Ren, and E. Vanden-Eijden. Minimum action method for the study of rare events. *Comm. Pure Appl. Math.*, (57):637–656, 2004.

[42] S. F. Edwards. The statistical dynamics of homogeneous turbulence. *J. Fluid Mech.*, 18:239–273, 1964.

[43] A. D. Egorov, P. I. Sobolevsky, and L. A. Yanovich. *Functional integrals: approximate evaluation and applications*. Springer, 1993.

[44] O. G. Ernst, A. Mugler, H.-J. Starkloff, and E. Ullmann. On the convergence of generalized polynomial chaos expansions. *ESAIM: Math. Model. Numer. Anal.*, 46(2):317–339, 2012.

[45] A. Eydeland. A fast algorithm for computing integrals in function spaces: financial applications. *Computational Economics*, 7:277–285, 1994.

[46] G. L. Eyink. Action principle in nonequilibrium statistical mechanics. *Phys. Rev. E*, 54(4):955–1019, 1996.

[47] G. L. Eyink. Turbulence noise. *J. Stat. Phys.*, 83(5/6):3419–3435, 1996.

[48] R. Farwig. Rate of convergence of Shepard's global interpolation formula. *Math.Comp.*, 46:577–590, 1986.

[49] B. A. Finlayson. *The method of weighted residuals and variational principles*. Academic Press, 1972.

[50] C. Foias, O. Manley, R. Rosa, and R. Temam. *Navier-Stokes equations and turbulence*. Cambridge Univ. Press, first edition, 2008.

[51] L. Frachebourg and Ph. A. Martin. Exact statistical properties of the Burgers equation. *J. Fluid. Mech.*, 417:323–349, 2000.

[52] M. Frechét. Sur les fonctionelles continues. *Annales Scientifiques de l'Ecole Normale Superieure*, 27:193–216, 1910.

[53] R. Friedrich, A. Daitche, O. Kamps, J. Lülff, M. Voβkuhle, and M. Wilczek. The Lundgren-Monin-Novikov hierarchy: kinetic equations for turbulence. *Comptes Rendus Physique*, 13(9-10):929–953, 2012.

[54] U. Frisch. *Turbulence: the legacy of A. N. Kolmogorov*. Cambridge University Press, 1995.

[55] T. Funaki and A. Inoue. On a new derivation of the Navier-Stokes equation. *Comm. Math. Phys.*, 65:83–90, 1979.

[56] P. G. Galman and K. S. Narendra. Representations of nonlinear systems via the Stone-Weierstrass theorem. *Automatica*, 12(2):619–622, 1976.

[57] I. M. Gelfand and S. V. Formin. *Calculus of variations*. Dover publications, 2000.

[58] M. J. Giles. Probability distribution functions for Navier-Stokes turbulence. *Phys. Fluids*, 7(11):2785–2795, 1995.

[59] D. A. Gomes. A variational formulation for the Navier-Stokes equation. *Comm. Math. Phys.*, 257:227–234, 2005.

[60] E. Gourgoulhon. *3+1 Formalism in General Relativity: Bases of Numerical Relativity*. Springer, 2012.

[61] S. N. Gurbatov, S. I. Simdyankin, E. Aurell, U. Frisch, and T. Tòth. On the decay of Burgers turbulence. *J. Fluid. Mech.*, 344:339–374, 1997.

[62] J. K. Hale and S. M. Verduyn Lunel. *Introduction to functional differential equations*. Springer-Verlag, first edition, 1993.

[63] J. R. Herring. Self-consistent-field approach to nonstationary turbulence. *Phys. Fluids*, 9(11):2106–2110, 1966.

[64] J. S. Hesthaven, S. Gottlieb, and D. Gottlieb. *Spectral methods for time-dependent problems*. Cambridge Univ. Press, 2007.

[65] I. I. Hirschman and D. V. Widder. *The convolution transform*. Princeton University Press, 1955.

[66] D. Hochberg, C. Molina-París, J. Pèrez-Mrcander, and M. Visser. Effective action for stochastic partial differential equations. *Phys. Rev. E*, 60(6):6343–6360, 1999.

[67] R. Hohlfeld, J. I. F. King, T. W. Drueding, and G. V. H. Sandri. Solution of convolution integral equations by the method of differential inversion. *SIAM J. Appl. Math.*, 53(1):154–167, 1993.

[68] E. Hopf. Statistical hydromechanics and functional calculus. *J. Rat. Mech. Anal.*, 1(1):87–123, 1952.

[69] I. Hosokawa. Monin-Lundgren hierarchy versus the Hopf equation in the statistical theory of turbulence. *Phys. Rev. E*, 73:067301(1–4), 2006.

[70] I. Hosokawa and K. Yamamoto. Numerical study of the Burgers' model of turbulence based on the characteristic functional formalism. *Physics of Fluids*, 13:1683–1692, 1970.

[71] P. Howlett, C. Pierce, and A. Torokhti. On nonlinear operator approximation with preassigned accuracy. *Journal of Computational Analysis and Applications*, 5(3):273–297, 2003.

[72] K. Ishizaka. Weak*-convergence to minimum energy measure and dispersed-dot halftoning. *SIAM J. Imaging Sciences*, 7(2):1035–1079, 2014.

[73] V. I. Istrăţescu. A Weierstrass theorem for real Banach spaces. *Journal of Approximation Theory*, 19:118–122, 1977.

[74] C. Itzykson and J. B. Zuber. *Quantum field theory*. Dover, 2005. Republication of the work originally published by McGraw-Hill, Inc., NY, 1980.

[75] J. R. Jancaitis and J. Junkins. Modeling in n dimensions using a weighting function approach. *Journal of Geophysical Research*, 23(79):3361–3366, 1974.

[76] R. V. Jensen. Functional integral approach to classical statistical dynamics. *J. Stat. Phys.*, 25(2):183–210, 1981.

[77] B. Jouvet and R. Phythian. Quantum aspects of classical and statistical fields. *Phys. Rev. A*, 19:1350–1355, 1979.

[78] V. M. Kaplitskiĭ. Interpolation of nonlinear operators in weighted l_p-spaces. *Siberian Mathematical Journal*, 51(2):255–266, 2010.

[79] A. Karimi and M. R. Paul. Extensive chaos in the Lorenz-96 model. *Chaos*, 20(4):043105(1–11), 2010.

[80] G. E. Karniadakis and S. Sherwin. *Spectral/hp element methods for computational fluid dynamics*. Oxford University Press, second edition, 2005.

[81] E. F. Kashpur and V. V. Khlobystov. Interpolation of polynomial operators in a Hilbert space. *Journal of Mathematical Sciences*, 86(1):2455–2458, 1997.

[82] V. V. Khlobystov. On convergence of interpolation processes in a Hilbert space. *Cybernetics and Systems Analysis*, 36(6):936–941, 2000.

[83] V. V. Khlobystov. On the convergence of interpolation process in a Hilbert space. *Cybernetics and Systems Analysis*, 36(6):936–941, 2000.

[84] V. V. Khlobystov. On the convergence of an interpolation processes to an entire operator in a Hilbert space. *Journal of Mathematical Sciences*, 104(6):1682–1684, 2001.

[85] V. V. Khlobystov and E. F. Kashpur. On the accuracy of polynomial interpolation in Hilbert space with disturbed nodal values of the operator. *Cybernetics and Systems Analysis*, 38(1):143–147, 2002.

[86] S. Kida. Asymptotic properties of Burgers turbulence. *J. Fluid. Mech.*, 93:337–377, 1979.

[87] H. Kleinert. *Critical properties of ϕ^4 theories*. World Scientific Publishing Company, 2001.

[88] H. Kleinert. *Path integrals in quantum mechanics, statistics, polymer physics, and financial markets*. World Scientific Publishing Company, 2009.

[89] V. I. Klyatskin. *Dynamics of stochastic systems*. Elsevier Publishing Company, 2005.

[90] T. Kolda and B. W. Bader. Tensor decompositions and applications. *SIREV*, 51:455–500, 2009.

[91] P. M. Kroonenberg and J. de Leeuw. Principal component analysis of three-mode data by means of alternating least squares algorithms. *Psychometrika*, 45:69–97, 1980.

[92] R. Kubo. Generalized cumulant expansion method. *Journal of the Physical Society of Japan*, 17(7):1100–1120, 1962.

[93] F. Langouche, D. Roekaerts, and E. Tirapegui. Functional integral methods for stochastic fields. *Physica A: Statistical and Theoretical Physics*, 95:252–274, 1979.

[94] D. Lazzaro and L. B. Montefusco. Radial basis functions for the multivariate interpolation. *Journal of Computational and Applied Mathematics*, 140:521–536, 2002.

[95] C. P. Lee, W. C. Meecham, and H. D. Hogge. Application of the Wiener-Hermite expansion to turbulence of moderate reynolds number. *Phys. Fluids*, 25(8):1322–1327, 1982.

[96] S. E. Leugarans, R. A. Moyeed, and B. W. Silverman. Canonical correlation analysis when the data are curves. *J. Roy. Soc. Ser. B*, 55:725–740, 1993.

[97] R. M. Lewis and R. H. Kraichnan. A space-time functional formalism for turbulence. *Communications on Pure and Applied Mathematics*, 15:397–411, 1962.

[98] G. Li and H. Rabitz. Regularized random-sampling high dimensional model representation (RS-HDMR). *Journal of Mathematical Chemistry*, 43(3):1207–1232, 2008.

[99] G. Li, S.-W. Wang, H. Rabitz, S. Wang, and P. Jaffé. Global uncertainty assessments by high dimensional model representations (HDMR). *Chemical Engineering Science*, 57(21):4445–4460, 2002.

[100] D. Liberzon. *Calculus of Variations and Optimal Control Theory: A Concise Introduction*. Princeton University Press, 2012.

[101] Yu. Yu. Lobanov. Deterministic computation of functional integrals. *Computer Physics Communications*, 99:59–72, 1996.

[102] A. López-García and E. B. Saff. Asymptotics of greedy energy points. *Math. Comp.*, 79:2287–2316, 2010.

[103] T. S. Lundgren. Distribution functions in the statistical theory of turbulence. *Phys. Fluids*, 10(5):969–975, 1967.

[104] Y. Maday, O. Mula, A. T. Patera, and M. Yano. The generalized empirical interpolation method: stability theory on Hilbert spaces with an application to the Stokes equation. *Comput. Meth. Appl. Engng.*, (In Review):1–25, 2014.

[105] Y. Maday, O. Mula, and G. Turinici. Convergence analysis of the generalized empirical interpolation method. *SIAM J. Numer. Anal.*, (In Review):1–24, 2014.

[106] F. Magri. An operator approach to Poisson brackets. *Annals of Physics*, 99:196–228, 1976.

[107] V. L. Makarov and V. V. Khlobystov. Polynomial interpolation of operators. *Journal of Mathematical Sciences*, 84(4):1244–1289, 1997.

[108] S. De Marchi. On Leja sequences: some results and applications. *Applied Mathematics and Computation*, 58(198):785–727, 2004.

[109] P. C. Martin, E. D. Siggia, and H. A. Rose. Statistical dynamics of classical systems. *Phys. Rev. A*, 8:423–437, 1973.

[110] W. D. McComb. *The Physics of Fluid Turbulence*. Oxford University Press, 1990.

[111] W. C. Meecham and D. T. Jeng. Use of the Wiener-Hermite expansion for nearly normal turbulence. *J. Fluid Mech.*, 32(2):225–249, 1968.

[112] W. C. Meecham and A. Siegel. Wiener-Hermite expansion in model turbulence at large Reynolds numbers. *Phys. Fluids*, 7(8):1178–1190, 1964.

[113] J.-M. Miao. General expressions for the Moore-Penrose inverse of a 2×2 block matrix. *Linear Algebra and its Applications*, 151(1):1–15, 1991.

[114] M. J. Mohlencamp and L. Monzón. Trigonometric identities and sums of separable functions. *Math. Intelligencer*, 27:65–69, 2005.

[115] A. S. Monin and A. M. Yaglom. *Statistical Fluid Mechanics, Volume I: Mechanics of Turbulence*. Dover, 2007.

[116] A. S. Monin and A. M. Yaglom. *Statistical Fluid Mechanics, Volume II: Mechanics of Turbulence*. Dover, 2007.

[117] D. Montgomery. A BBGKY framework for fluid turbulence. *Phys. Fluids*, 19(6):802–810, 1976.

[118] C. S. Morawetz, J. B. Serrin, and Y. G. Sinai, editors. *Selected works of Eberhand Hopf with commentaries*. American Mathematical Society, 2002.

[119] A. S. Vasudeva Murthy. a note on the differential inversion method of Hohlfeld *et al. SIAM J. Appl. Math.*, 55(3):719–722, 1995.

[120] A. Narayan and J. Jakeman. Adaptive Leja sparse grid constructions for stochastic collocation and high-dimensional approximation. *SIAM J. Sci. Comput.*, 36(6):A2952–A2983, 2014.

[121] A. Narayan and D. Xiu. Stochastic collocation methods on unstructured grids in high-dimensions via interpolation. *SIAM J. Sci. Comput.*, 34(3):A1729–A1752, 2012.

[122] A. Narayan and D. Xiu. Constructing nested nodal sets for multivariate polynomial interpolation. *SIAM J. Sci. Comput.*, 35(5):A2293–A2315, 2013.

[123] M. Z. Nashed. Differentiability and related properties of non-linear operators: some aspects of the role of differentials in non-linear functional analysis. In L. B. Rall, editor, *Nonlinear Functional Analysis and Applications*. Academic Press, 1971.

[124] O. Nelles. *Nonlinear system identification: from classical approaches to neural networks and fuzzy models*. Springer, 2001.

[125] A. Nouy. Generalized spectral decomposition method for solving stochastic finite element equations. *Comput. Methods. Appl. Mech. Engrg.*, 197:4718–4736, 2008.

[126] A. Nouy. A priori model reduction through proper generalized decomposition for solving time-dependent partial differential equations. *Comput. Methods Appl. Mech. Engrg.*, 199:1603–1626, 2010.

[127] E. Novak and K. Ritter. High dimensional integration of smooth functions over cubes. *Numer. Math*, 75:79–97, 1996.

[128] E. Novak and K. Ritter. Simple cubature formulas with high polynomial exactness. *Constructive Approximation*, 15:499–522, 1999.

[129] E. A. Novikov. Functionals and the random-force method in turbulence. *Sov. Phys. JETP*, 20:1290–1294, 1965.

[130] H. Ogura. Orthogonal functionals of the Poisson process. *IEEE Trans. Inf. Theory*, 4:473–481, 1972.

[131] D. S. Oliver. Calculation of the inverse of the covariance. *Mathematical Geology*, 30(7):911–933, 1975.

[132] A. Olopińska. Solving Schwinger-Dyson equations by truncation in zero-dimensional scalar quantum field theory. *Phys. Rev. D*, 43(10):3561–3564, 1991.

[133] G. Palm and T. Poggio. The Volterra representation and the Wiener expansion: validity and pitfalls. *SIAM J. Appl. Math.*, 33(2):195–216, 1977.

[134] R. Phythian. The operator formalism of classical statistical dynamics. *J. Phys A: Math. Gen.*, 8(9):1423–1432, 1975.

[135] R. Phythian. The functional formalism of classical statistical dynamics. *J. Phys A: Math. Gen.*, 10(5):777–788, 1977.

[136] L. Plaskota and G. W. Wasilkowski. Tractability of infinite-dimensional integration in the worst case and randomized settings. *Journal of Complexity*, 27(6):505–518, 2011.

[137] V. N. Popov. *Functional integrals in quantum field theory and statistical physics*. D. Reider publishing company, 1983.

[138] W. A. Porter. Nonlinear systems in Hilbert space. *Int. J. Contr.*, 13:593–602, 1971.

[139] W. A. Porter. Synthesis of polynomic systems. *SIAM J. Math. Anal.*, 11(2):308–315, 1980.

[140] W. A. Porter and T. M. Clark. Causality structure and the Weierstrass theorem. *J. Math. Anal. Appl.*, 52:351–363, 1975.

[141] P. M. Prenter. A Weierstrass theorem for real, separable Hilbert spaces. *Journal of Approximation Theory*, 3:341–351, 1970.

[142] P. M. Prenter. A Weierstrass theorem for real, separable Hilbert spaces. *Journal of Approximation Theory*, 3:341–351, 1970.

[143] P. M. Prenter. Lagrange and Hermite interpolation in Banach spaces. *Journal of Approximation Theory*, 4:419–432, 1971.

[144] Zhong quing Wang and Ben yu Guo. Legendre-Gauss-Radau collocation methods for solving initial value problems for first order ordinary differential equations. *J. Sci. Comput.*, 52:226–255, 1938.

[145] H. Rabitz, Ö. F. Aliş, J. Shorter, and K. Shim. Efficient input–output model representations. *Computer Physics Communications*, 117(1-2):11–20, 1999.

[146] T. M. Rassias. *Functional equations in mathematical analysis*. Springer, 2011.

[147] T. M. Rassias. *Handbook of functional equations: stability theory*. Springer, 2014.

[148] M. Rosa-Clot and S. Taddei. Deterministic technique of path summation. *Phys. Rev. C*, 50:627–629, 1994.

[149] G. Rosen. Turbulence theory and functional integration I. *Phys. Fluids*, 3(4):519–524, 1960.

[150] G. Rosen. Functional integration theory for incompressible fluid turbulence. *Phys. Fluids*, 10(12):2614–2619, 1967.

[151] G. Rosen. Dynamics of probability distributions over classical fields. *International Journal of Theoretical Physics*, 4(3):189–195, 1971.

[152] G. Rosen. Functional calculus theory for incompressible fluid turbulence. *J. Math. Phys.*, 12(5):812–820, 1971.

[153] G. Rosen, J. A. Okolowski, and G. Eckstut. Functional integration theory for incompressible fluid turbulence II. *J. Math. Phys.*, 10(3):415–421, 1967.

[154] A. Rosteck and M. Oberlack. Lie algebra of the symmetries of the multi-point equations in statistical turbulence theory. *J. Nonlin. Math. Phys.*, 18:251–264, 2011.

[155] W. J. Rugh. *Nonlinear system theory: the Volterra/Wiener approach*. Johns Hopkins University Press, 1981.

[156] N. Sablon, F. De Proft, P. W. Ayers, and P. Geerlings. Computing second-order functional derivatives with respect to the external potential. *J. Chem. Theory Comput.*, 6:3671–3680, 2010.

[157] P. K. Sahoo and P. Kannappan. *Introduction to functional equations*. CRC Press, 2011.

[158] R. Schaback. Multivariate interpolation by polynomials and radial basis functions. *Constructive Approximation*, 21:293–317, 2005.

[159] A. Segall and T. Kailath. Orthogonal functionals of independent-increment processes. *IEEE Trans. Inf. Theory*, 22(3):287–298, 1976.

[160] Z. S. She, E. Aurell, and U. Frisch. The inviscid Burgers equation with initial data of Brownian type. *Commun. Math. Phys.*, 148:623–641, 1992.

[161] M. Shetzen. *The Volterra and Wiener theories of nonlinear systems*. Wiley, New York, 1980.

[162] I. I. Gikhman A. V. Skorokhod. *The Theory of Stochastic Processes I*. Springer, 2004.

[163] G. Song, J. Riddle, G. E. Fasshauer, and F. J. Hickernell. Multivariate interpolation with increasingly flat radial basis functions of finite smoothness. *Adv. Comput. Math.*, 36:485–501, 2012.

[164] M .M. Stanišić. *The Mathematical Theory of Turbulence*. Springer Verlag, 1985.

[165] R. L. Stratonovich. Some Markov methods in the theory of stochastic processes in nonlinear dynamical systems. In F. Moss and P. V. E. McClintock, editors, *Noise in nonlinear dynamical systems (Vol. 1)*, pages 16–68. Cambridge Univ. Press, 1989.

[166] E. Tonti. Variational formulation for nonlinear differential equations (i). *Académie royale de Belgique, boulletin de la classe des sciences, 5 Série -Tome LV*, 3:137–165, 1969.

[167] E. Tonti. Variational formulation for nonlinear differential equations (ii). *Académie royale de Belgique, boulletin de la classe des sciences, 5 Série -Tome LV*, 4:262–278, 1969.

[168] E. Tonti. Variational formulation for every nonlinear problem. *Int. J. Engng. Sci.*, 2(11/12):1343–1371, 1984.

[169] A. Torokhti and P. Howlett. *Computational methods for modelling of nonlinear systems*. Elsevier, first edition, 2007.

[170] M. Ueda. Probability-density-functional description of photoelectron statistics. *Phys. Rev. A*, 40(2):1096–1108, 1989.

[171] M. Ueda. Probability-density-functional description of quantum photodetection process. *Quantum Opt.*, 1:131–151, 1989.

[172] M. M. Vainberg. *Variational methods for the study of nonlinear operators*. Holden-Day, 1964.

[173] J. van Neerven. *Stochastic Evolution Equations*. 2008. ISEM Lecture Notes.

[174] D. Venturi. Conjugate flow action functionals. *J. Math. Phys*, 54:113502(1–19), 2013.

[175] D. Venturi, H. Cho, and G. E. Karniadakis. The Mori-Zwanzig approach to uncertainty quantification. In R. Ghanem, D. Higdon, and H. Owhadi, editors, *Handbook of uncertainty quantification*. Springer, 2016.

[176] D. Venturi and G. E. Karniadakis. New evolution equations for the joint response-excitation probability density function of stochastic solutions to first-order nonlinear PDEs. *J. Comput. Phys.*, 231:7450–7474, 2012.

[177] D. Venturi and G. E. Karniadakis. Convolutionless Nakajima-Zwanzig equations for stochastic analysis in nonlinear dynamical systems. *Proc. R. Soc. A*, 470(2166):1–20, 2014.

[178] D. Venturi, T. P. Sapsis, H. Cho, and G. E. Karniadakis. A computable evolution equation for the joint response-excitation probability density function of stochastic dynamical systems. *Proc. R. Soc. A*, 468(2139):759–783, 2012.

[179] D. Venturi, D. M. Tartakovsky, A. M. Tartakovsky, and G. E. Karniadakis. Exact PDF equations and closure approximations for advective-reactive transport. *J. Comput. Phys.*, 243:323–343, 2013.

[180] D. Venturi, X. Wan, R. Mikulevicius, B. L Rozovskii, and G. E. Karniadakis. Wick-Malliavin approximation to nonlinear stochastic partial differential equations: analysis and simulations. *Proc. R. Soc. A*, 469(2158):1–20, 2013.

[181] V. Volterra. *Theory of functionals and of integral and integro-differential equations*. Dover, 1959.

[182] M. Waclawczyk and M. Oberlack. Application of the extended Lie group analysis to the hopf functional formalism of the Burgers equation. *J. Math. Phys.*, 54:07291(119), 2013.

[183] M. Waclawczyk, N. Staffolani, M. Oberlack, A. Rosteck, M. Wilczek, and R. Friedrich. Statistical symmetries of the Lundgren-Monin-Novikov hierarchy. *Phys. Rev. E*, 90:013022(111), 2014.

[184] X. Wan and G. E. Karniadakis. Long-term behavior of polynomial chaos in stochastic flow simulations. *Comput. Methods Appl. Mech. Engrg.*, 195:5582–5596, 2006.

[185] G. W. Wasilkowski. Liberating the dimension for l_2-approximation. *Journal of Complexity*, 28:304–319, 2012.

[186] S. Weinberg. *The quantum theory of fields: volume I*. Cambridge University Press, 2002.

[187] N. Wiener. *Nonliner problems in random theory*. MIT Press, 1966.

[188] J. Wu. *Theory and applications of partial functional differential equations*. Springer, first edition, 1996.

[189] D. Xiu and G. E. Karniadakis. Modeling uncertainty in flow simulations via generalized polynomial chaos. *J. Comp. Phys.*, 187:137–167, 2003.

[190] K. Yasue. A variational principle for the Navier-Stokes equation. *Journal of Functional Analysis*, 51:133–141, 1983.

[191] J. Zinn-Justin. *Quantum field theory and critical phenomena*. Oxford Univ. Press, fourth edition, 2002.